Mechanism of HPV8-E7 mediated keratinocyte invasion

Inaugural-Dissertation

zur

Erlangung des Doktorgrades

der Mathematisch-Naturwissenschaftlichen Fakultät

der Universität zu Köln

vorgelegt von

Sandra Heuser

aus Mechernich

Köln, 2016

...to my beloved parents

Table of Contents

1. Introduction

1.1   Oncogenic Viruses

The multistep nature of human carcinogenesis is described as the accumulation of 'oncogenic hits' resulting from spontaneously or environmentally caused mutations, together with the host's genetic background and the selective pressure of the tissue microenvironment (Mesri *et al.* 2014). Different mechanistic strategies are involved in cancer development leading to genetic changes and acquired characteristics, which were summarised and defined as the 'hallmarks of cancer' (figure 1) by Hanahan and Weinberg (Hanahan and Weinberg 2000).
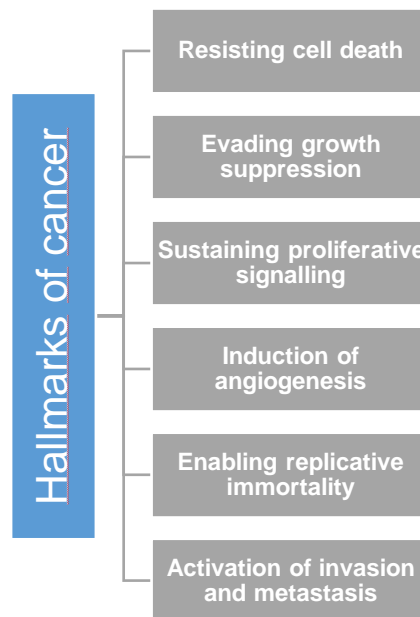
Figure 1. The hallmarks of cancer (Hanahan and Weinberg 2000). The hallmarks of cancer describe 6 characteristics occurring during the development of most cancers due to different mechanistic strategies.

In 2012, the International Agency for Research on Cancer (IARC) has classified 6 viruses as Group 1 carcinogens, described as being carcinogenic to humans, based on epidemiological and biological studies (Bouvard *et al.* 2009, Mesri *et al.* 2014). About 12 to 15% of human cancers worldwide are caused by oncogenic viruses. Historically, in 1911, the first oncogenic virus, avian Rous sarcoma virus, was identified by Peyton Rous, which was followed decades later by the identification of a series of oncogenic viruses, including cottontail rabbit papillomavirus and simian virus 40 (SV40). Due to the identification of *v-src* as the viral oncogene of the Rous sarcoma

virus, Harold Varmus and Michael Bishop confirmed the theory of virus-associated oncogenesis (Stehelin *et al.* 1976).

Table 1. Tumour viruses, associated cancers and viral oncogenes important in humans (Ajiro and Zheng 2014, Howley and Pfister 2015). The virus type is described with its abbreviation, its associated cancer and its viral oncogene. In addition, the asterisks indicate the members of the Group 1 carcinogens defined by the International Agency for Research on Cancer.

Tumour-virus	Abbreviation	Associated cancer(s)	Viral oncogenes
Human papillomavirus of genus alpha	HPV*	Cervical cancer, anal cancer, vaginal cancer, oropharyngeal cancer	E5, E6, E7
Human papillomavirus of genus beta	HPV	Skin cancer in Epidermodysplasia verruciformis patients	E2, E6, E7
Merkel cell polyomavirus	MCPyV	Merkel cell carcinoma	T antigens
Human T cell lymphotrophic virus, type-1	HTLV-1*	Adult T-cell lymphoma	Tax
Epstein-Barr virus	EBV*	Burkitt lymphoma, Hodgkin lymphoma, non-Hodgkin lymphoma, nasopharyngeal cancer, T-cell and NK lymphoma	LMP1
Kaposi's sarcoma herpes virus	KSHV*	Kaposi's sarcoma, primary effusion lymphoma	LANA, vFLIP, vCyclin, vGPCR, vIRF-1, K1
Hepatitis B virus	HBV*	Hepatocellular carcinoma	HBx
Hepatitis C virus	HCV*	Hepatocellular carcinoma	Core protein, NS3, NS4B, NS5A

The confirmation of virus-associated cancer development in humans was obtained by findings such as the identification of Epstein-Barr virus (EBV) in Burkitt lymphomas (1965), the isolation of human T-cell lymphoma virus-1 (HTLV-1) from adult T-cell lymphomas, the association of cervical cancer with high-risk human papillomaviruses (HPV) and the discovery of several other cancer-inducing viruses including Merkel cell polyomavirus (more cancer associated viruses are shown in table 1) (Mesri *et al.* 2014). All human tumour-associated viruses encode oncogenes or genes with oncogenic activities, which allow changes in the cellular machinery (compare to the 'hallmarks of cancer'). Therefore, host cell transformation and a persistent virus infection are two major events in virus-associated cancer development (Ajiro and Zheng 2014).

1.2   Discovery of Human Papillomaviruses

In the ancient Greek and Romans, skin and genital warts were already noted and genital warts were supposed to be infectious and sexually transmitted. In 1907, first cell-free transmission experiments were performed in Italy and demonstrated the infectious potential of human warts (Ciuffo 1907). The infectious origin of genital warts and laryngeal papillomatosis was confirmed in the 1920's (Syrjanen and Syrjanen 2008). First viral particles of HPV were demonstrated in electron microscopy in 1949 (Strauss *et al.* 1949). The successful transmission of the rabbit papillomavirus from wild cottontail rabbits to domestic rabbits and the observation that initial papillomas developed frequently into squamous cell carcinomas (SCCs) demonstrated the first hints for a carcinogenic potential of the virus (Rous and Kidd 1938). In 1965, first studies were able to describe the circularized, double-stranded DNA of HPV (Crawford 1965, Klug and Finch 1965). Furthermore, the group of Harald zur Hausen identified a clear heterogeneity within the group of HPV due to hybridisation studies including material from cutaneous and genital warts, as well as cervical cancer biopsies (zur Hausen *et al.* 1974). Additionally, in the 1970's experiments were performed demonstrating a relationship between papillomavirus infection and cervical cancer, which arose to the hypothesis that cervical cancer development results from HPV infection (zur Hausen 1977). In 2008, Harald zur Hausen got the Nobel prize for his discovery that high-risk HPV types are the causative agents of cervical cancer.

1.3   The Family of Papillomaviruses

Papillomaviruses (PV) infect a wide variety of animals as well as humans. Up to now, 204 types of HPV (according to papillomavirus episteme, http://pave.niaid.nih.gov) have been identified on DNA sequence analysis. Homologous nucleotide sequences of the major capsid protein gene L1 were used to design a phylogenetic tree, which characterised HPV into five different genera (alpha, beta, gamma, mu and nu). A new HPV type is defined with 10% difference in the DNA sequence of L1 compared to the closest known HPV type. A difference between 2 to 10% defines a new subtype and less than 2% a new variant (de Villiers *et al.* 2004). Furthermore, HPV can be divided into cutaneous and mucosal types, depending on their site of infection, as well as in high-risk and low-risk types, referring to their oncogenic potential. Mucosal HPV types infect the non-keratinizing epithelium mainly of the anogenital tract and the oral lining,

while cutaneous types infect the keratinizing epithelium of the skin (Gomez 2007). The best-studied group is the genus alphaHPV, infecting the mucosal epithelium, comprising the high-risk types HPV16 and HPV18, which are accepted as oncogenic types found in mucosal cancer. The cutaneous epithelium-infecting betaHPV types gained attention, due to their involvement in the development of cutaneous SCCs (see section 1.8)

1.4 Structure of Human Papillomaviruses

HPVs are small (Ø 55 nm) non-enveloped, double-stranded DNA tumour viruses with an icosahedral capsid composed of 72 capsomers. The viral genome is circularized and about 8000 bp in size with 7 - 9 overlapping open reading frames (ORFs), encoding the viral proteins from one DNA strand (Pfister and Fuchs 1994). The genome is associated with histones, forming a nucleosome-like structure (Favre *et al.* 1977, Pfister and zur Hausen 1978). The DNA strand can be divided into the coding region, including the early and the late region and the non-coding region (NCR) or upstream regulatory region (URR), which are separated by two polyadenylation sites (Pfister and Fuchs 1994, Zheng and Baker 2006). The coding region contains ORFs encoding specific viral proteins at different time points of the viral life cycle. Therefore, the respective proteins are named after their expression during the viral life cycle and are called 'early' and 'late' proteins (Gomez 2007).

The early coding region contains typically the early proteins E1, E2, E4, E5, E6 and E7, which play an important role in viral transcription, replication and transformation (figure 2). Expression of the viral early gene products determines whether the infection is active or latent or whether it leads to malignant transformation. The late region encodes the structural proteins L1 and L2 responsible for the formation of the viral capsid (Gomez 2007). The NCR is located between the ORFs of the L1 and the E6 protein and contains control elements, such as the origin of replication (*ori*) and promoters responsible for transcription of the polycistronic mRNAs (Akgül *et al.* 2003). The early promoter, located 3' from the NCR, expresses the E1, E2/E4, E5, E6 and E7 proteins from their respective mRNAs, whereas the late promoter is responsible for the transcription of the late proteins L1 and L2, but also for E1, E2 and E4 (Stubenrauch *et al.* 1992, Stubenrauch and Laimins 1999). Alternative splicing gives rise to a fusion protein E1^E4, which is involved in releasing infectious viral particles (Doorbar *et al.*

4

1991). Comparing related and more divergent PV types, the NCR shows the highest degree of variation in the viral genome (Gomez 2007).
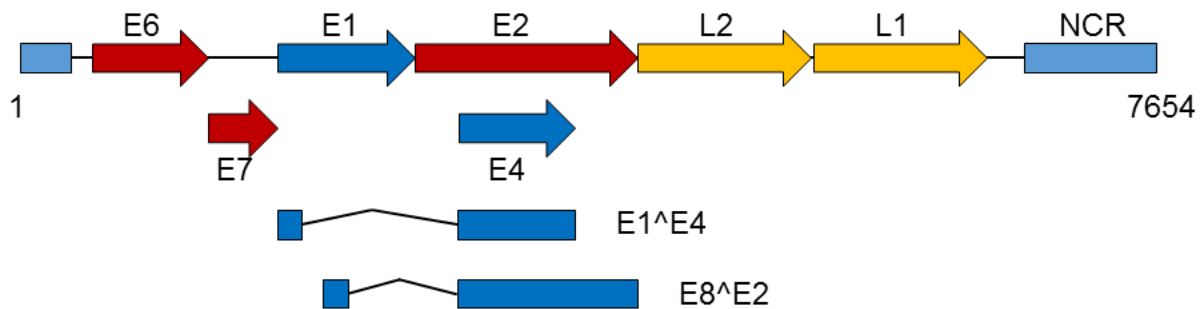
Figure 2: Schematic genome organisation of HPV8. Early and late proteins are indicated as arrows, whereby HPV8 lacks E5. The genome is presented as linearized version and has a size of 7654 bp. NCR: non-coding region.

1.5   HPV viral life cycle

Despite the heterogeneity of different HPV types, all types target keratinocytes of different epithelia, including the mucosa and skin. All these different HPV types are able to produce infectious virions by sharing specific features of reproduction. Most studies have focused on the analysis of high-risk HPV types, such as HPV16 (Doorbar 2016). Information gained from these studies can be applied, with some modifications (here indicated for alpha and betaHPV), to the other groups of HPV.

The general target of HPV is the basal layer of the stratified squamous epithelium. An initial HPV infection starts with the exposure of basal cells to infectious particles due to micro wounds. For high-risk alphaHPVs, the initial site of infection includes the cervical and anal transformation zones, whereas for betaHPVs, the hair follicles are an important site of infection (Iannacone *et al.* 2014, Quint *et al.* 2015).

Basal cells possess proliferative potential, which is necessary for the viral life cycle of HPV due to its dependence on the replication machinery of the host cell (Quint *et al.* 2015). The entry of viral particles into human keratinocytes is a multistep process starting with the attachment to heparin sulphate proteoglycans (HSPGs) either located on the surface of an epithelial cell or on the basement membrane. HSPGs interact with the L1 major capsid protein, initiating a series of conformational changes leading to cell binding and delivery of viral DNA into the cells. The most prominent HSPG in keratinocytes is syndecan-1, which functions as HPV attachment receptor (Schelhaas *et al.* 2012, Surviladze *et al.* 2015, Kines *et al.* 2016). Furthermore, laminin-5 has been

proposed to act as a transient receptor for virion binding, as it is secreted during epithelial wounding (Culp *et al.* 2006, Schelhaas *et al.* 2012). For infectious internalisation, integrin α6β4, a transmembrane glycoprotein receptor, appears to be involved as a secondary receptor. After skin injuries, keratinocytes produce more integrin α6β4, which is bound by HPV particles during wound healing and the particles are endocytosed to the microfilament network via hemidesmosomes (Evander *et al.* 1997, Culp *et al.* 2006, Raff *et al.* 2013). The viral life cycle of alphaHPV results in productive infections and neoplasia, whereby betaHPV only lead to asymptomatic infections in the general population. BetaHPVs infect long-lived, slow-cycling epidermal stem (or stem-like) cells, populating the surrounding basal layer with transiently amplifying cells containing viral episomes (Quint *et al.* 2015).
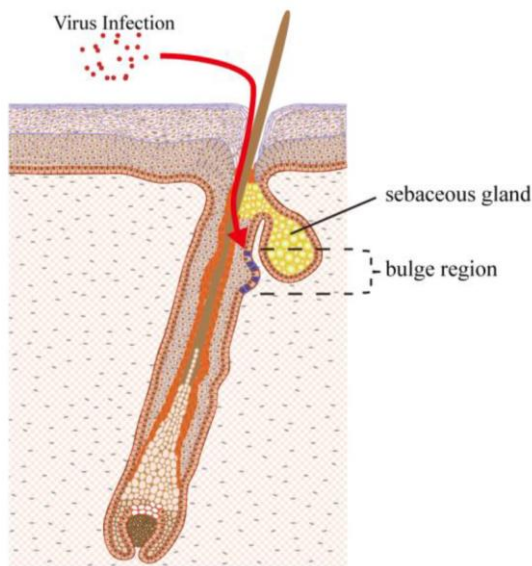
Figure 3. Infection site of betaHPV. BetaHPVs gain access to epithelial stem cells through microwounds or hair follicles. The bulge region of hair follicles contains epithelial stem cells (purple cells), which populate cutaneous epithelial sites, involved in initial betaHPV infection (Egawa *et al.* 2015).

In the basal cell layer, the viral genome is replicated and maintained as episomes at a low copy number (50 - 100 copies per cell). The early proteins E1 and E2 are expressed and bind specifically to the *ori* of replication to recruit cellular replication factors (Lazarczyk *et al.* 2009, Quint *et al.* 2015). This state is known as the amplification phase, which is followed by the maintenance phase. During cell division, viral DNA is distributed between both daughter cells, whereby one cell migrates and enters cell differentiation and one cell continues cell division in the basal cell layer providing a reservoir of viral DNA. Therefore, the maintenance phase ensures viral persistence and latent viral infection. During HPV infection, cell cycle exit is blocked and induction of S-phase is mediated by the early proteins E6 and E7 (Stubenrauch

and Laimins 1999, Moody and Laimins 2010). The E6 and E7 proteins are responsible for the re-entry of the infected cell into the cell cycle, allowing genome amplification (Quint *et al.* 2015). In high-risk alphaHPVs, E6 and E7 allow extensive cell proliferation associated with neoplasia, whereas in betaHPVs cell cycle re-entry and genome amplification is maintained without neoplasia. However, gene expression in betaHPVs can become deregulated, i.e. in association with UV irradiation and immunosuppression (Akgül *et al.* 2003, Howley and Pfister 2015, Quint *et al.* 2015). During the vegetative phase, the expression of regulatory viral proteins, including E4 and E5 (only for some genera), increases in the *stratum spinosum*. In the upper layers of the stratified epithelium, viral genome expression is accelerated resulting in the amplification of thousands of copies per cell (McBride 2008, Doorbar *et al.* 2012). After genome amplification, the expression of the capsid proteins L1 and L2 is triggered in the most upper layers of the *stratum spinosum*, whereby expression in the *stratum granulosum* leads to virion assembly and the encapsidation of viral genomic DNA. The virus particles are released by shedding off keratinocytes from the *stratum corneum* (Lazarczyk *et al.* 2009, Quint *et al.* 2015).
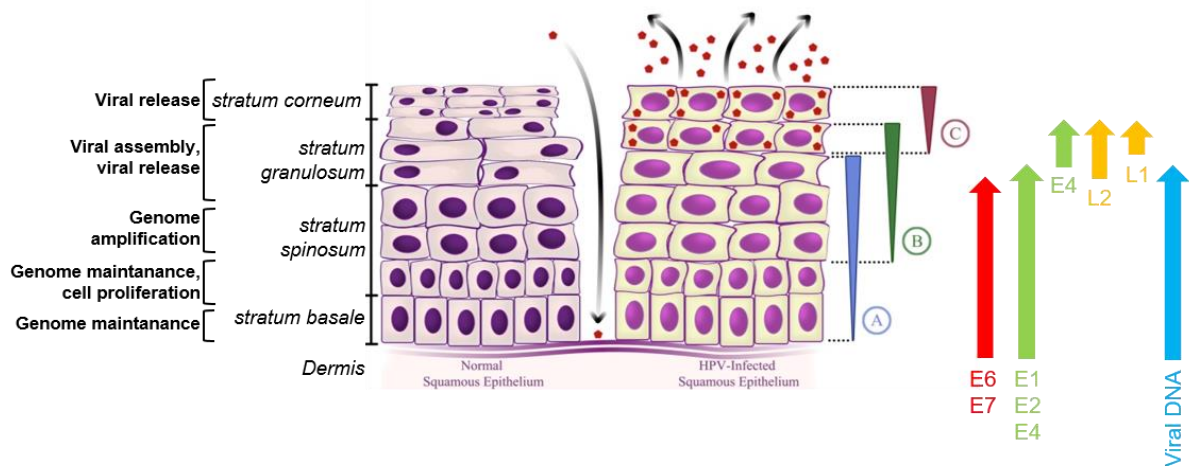
Figure 4. Life cycle of HPV. HPV infects the basal cells, where the early proteins are weakly expressed. The expression increases in the *stratum spinosum* and the vegetative viral DNA replication takes place. The expression of the structural proteins is restricted to the differentiated cells of the *stratum granulosum*, where the virus assembly takes place, the virus particles are then released with stratification. The viral proteins disturb the normal differentiation program, resulting in thickening of the suprabasal layers. (A) Early gene expression of E1, E2, E6 and E7, (B) viral genome amplification, (C) virion assembly and release (taken from Soave (2013)).

1.6 HPV in anogenital cancer

The alphaHPV types mainly infect the mucosa of the anogenital tract. A group of about 30 HPV types infect the genital tract due to sexual contact. These HPV types can be divided into low-risk and high-risk HPV types according to their association with cancer.

The low-risk HPV types, only rarely found in malignant tumours and usually causing benign anogenital warts, include HPV types 6, 11, 40, 42, 43, 44, 54, 55, 57, 61, 71, 81, 83, 84 and 89, whereas high-risk HPV types include types 16, 18, 26, 30, 31, 33, 34, 35, 39, 45, 51, 52, 56, 58, 59, 66, 67, 68, 70, 73 and 82 and cause anogenital cancer (Bouvard *et al.* 2009). The main representatives of the high-risk alphaHPV types are HPV16 and HPV18, which are most commonly associated with cervical cancer. More than 95% of cervical cancers, 50 - 90% of other anogenital cancers and 20 - 30% of oropharyngeal cancers have been associated with persistent infection and genomic integration of high-risk HPVs (Ajiro and Zheng 2014, Hübbers and Akgül 2015).

Up to 80% of sexually active men and women acquire an anogenital HPV infection during their lifetime, however, most infections are transient and cleared by the immune system after a few months. Persistent infections can lead to the development of cancer precursor lesions, named intraepithelial neoplasia, which may result in invasive carcinomas of the anogenital tract. Cervical cancer is the most common cancer induced by HPV and is the second most prevalent cancer in women worldwide (Wieland *et al.* 2014). A total of 470,000 new cases of cervical cancer are diagnosed per year, however, cervical screening has reduced the incidence of HPV-associated cancers in the developed world. In 2008, the incidence rate in Germany was 9.5 per 100,000 (Seifert and Klug 2014). In addition, persistent HPV infections are very common in immunosuppressed persons, such as HIV-positive patients (Esser *et al.* 2015). For HIV-positive women, cervical cancer is an AIDS-defining clinical condition and HIV-positive men who have sex with men (MSM) have been identified as a high-risk group to develop HPV-associated anal carcinoma (Wieland *et al.* 2014, Esser *et al.* 2015). Two prophylactic vaccines for HPV are internationally available based on virus-like particles (VLP) of L1, the major virion protein. A bivalent vaccine containing VLPs of HPV16 and HPV18 and a quadrivalent vaccine containing VLPs of HPV6, 11, 16 and 18. Both vaccines have been reported to reduce infection incidence and cervical lesions (Schiller and Muller 2015, Malik *et al.* 2016). However, to further reduce cases of HPV-associated cancer, a third nonavalent vaccine has been approved for use, which comprises the high-risk HPV types 16, 18, 31, 33, 45, 52 and 58, known to be associated with 90% of cervical cancers worldwide and the low-risk types HPV6 and 11 (Riethmuller *et al.* 2015, Van Damme *et al.* 2016).

1.7 Head and neck cancers and HPV infection

HPV infection does not only play a role in the development of genital cancers, but is also an etiological cause of some SCC of the head and neck (HNSCC). They are described as neoplasms originating from the mucosal surface of the oral cavity, oropharynx, hypopharynx, larynx and nasopharynx (Cleary *et al.* 2016). In 1983, it was suggested for the first time, that HPV is a causative agent of head and neck cancer, which was based on similar clinical features in oral and genital injuries, similarities in the epithelia and the affinity of HPV for epithelial cells (Syrjanen *et al.* 1983). Generally, every year about 270,000 cases of cancer of the oral cavity and 135,000 cases of pharyngeal cancers are diagnosed worldwide. It was shown that in 50% of HNSCC a HPV infection was present, with HPV16 being the most prevalent type (90%) (Kreimer *et al.* 2005). Most of the HPV-related HNSCC are oropharyngeal squamous cell carcinomas (OPSCC) located at the tonsils and the base of the tongue, whereas the involvement of HPV in other HNSCC is still under investigation. For oral squamous cell carcinoma (OSCC) an influence of HPV was already hypothesised in 1983, but until now it is not proved and accepted (Hübbers and Akgül 2015).

1.8 Genus beta papillomaviruses and skin cancer development

1.8.1 Non-melanoma skin cancer and cutaneous HPV

Non-melanoma skin cancer (NMSC) is the most frequent malignancy in the Caucasian population with an incidence of about 30% of all human cancers (Nindl *et al.* 2007). Most lesions are found on sun-exposed body sites mostly affecting light-skinned and sun-sensitive individuals. NMSC is comprised of basal cell carcinoma (approx. 80% of cases), SCC (approx. 20% of cases), actinic keratosis and Merkel cell carcinoma (Nindl *et al.* 2007, Kolk *et al.* 2014, Vinzon and Rösl 2015). Main risk factors for the development of NMSC are UV irradiation, skin type and pigmentation, ionising radiation, immunosuppression, chemical carcinogens and the individual age (Nindl *et al.* 2007).

Epidemiological and experimental data have advocated a potential carcinogenic role of betaHPV in the development of skin SCCs. A direct interaction of betaHPV and cancer development is accepted in immunosuppressed organ-transplant recipients (OTR) and Epidermodysplasia verruciformis (EV) patients (Patel *et al.* 2010). In 1922, EV was originally characterised by Lewandowsky and Lutz, who described a group of

patients having a predisposition to HPV infection. Two susceptibility gene loci were identified in EV patients, the first is located on chromosome 17q25 and the second has been mapped to chromosome 2p21-p24 (Ramoz *et al.* 2000, Ramoz *et al.* 2002). Recessive mutations in one of the two homologous genes *EVER1* and *EVER2,* located on chromosome 17q25, increase when homozygous the susceptibility to betaHPV infection and therefore result in an enlarged risk for cutaneous SCC (Nindl *et al.* 2007, Quint *et al.* 2015). *EVER*1/2 code for transmembrane channel-like proteins belonging to a group of iron transporters located in the endoplasmic reticulum of keratinocytes. They form complexes with zinc-transporter-1 and may thereby maintain zinc homeostasis. A deregulation of the cellular zinc balance as a result of mutated *EVER*1 and *EVER*2 genes may favour HPV infection in EV patients (Lazarczyk *et al.* 2009). Recent studies identified a new genetic aetiology in EV patients by detecting RHOH (ras homologue family member H) and MST1 (serine/threonine kinase 4) as two additional autosomal recessive defects leading to T-cell defects and increased susceptibility to persistent HPV infections (Crequer *et al.* 2012a, Crequer *et al.* 2012b). EV patients develop flat warts and macular, red, brown or achromic lesions (Majewski *et al.* 1997, Howley and Pfister 2015). In 30 - 60% of cases EV-associated lesions proceed into SCCs, 10 to 30 years after the development of benign skin lesions. The most frequent HPV types in EV patients are HPV5 and 8 found in 90% of cutaneous SCCs (Orth *et al.* 1978, Howley and Pfister 2015). Therefore, an interaction between UV irradiation and betaHPV infection is assumed in the transformation of cutaneous epithelial keratinocytes (Quint *et al.* 2015). In 2009, IARC classified HPV5 and HPV8 as 'possibly carcinogenic' in EV patients (Bouvard *et al.* 2009). In contrast to genus alphaHPV, the genome of cutaneous HPV types is not integrated into the host genome and persists extrachromosomally (Favre *et al.* 1997). However, betaHPVs seem to possess carcinogenic properties due to their interference with cell cycle regulatory pathways, as well as by their property to inhibit normal DNA repair and apoptosis pathways in UV-damaged cells (Quint *et al.* 2015).

Due to the oncogenic properties of betaHPV types, they seem to be an important factor for skin cancer development also in the general population. More than 80% of healthy individuals are positive for betaHPV DNA in skin swabs or plucked eyebrow hairs (Kohler *et al.* 2007, de Koning *et al.* 2009, Weissenborn *et al.* 2009b). The range of betaHPV types, present on different body sites can representatively be found in hair follicles of the eyebrow, as a hair follicle is considered to be the natural reservoir for

cutaneous betaHPV (Howley and Pfister 2015). In SCCs developed in the general population, the DNA of betaHPV types was detected with less than one copy per cell. However, betaHPV DNA was identified in precancerous actinic keratosis with up to 50 copies per cell, representing an influence in the early stages of skin cancer development (Weissenborn *et al.* 2005). A study analysing the intrafamilial transmission of betaHPV pointed out that family members carry a similar spectrum of betaHPV types, which can be transferred to babies already soon after birth. Nevertheless, a persistent infection with a specific HPV type in a parent does not always result in an infection of a child with the same type. Therefore, regular exposure to cutaneous HPV does not necessarily result in the establishment of a persistent infection (Weissenborn *et al.* 2009a). Natural history studies of betaHPV infections demonstrated that it should be differentiated between transiently and persistently detectable HPV types, where persistent infections are more likely to have pathological consequences (Howley and Pfister 2015).

In OTRs the frequency of SCC development is increased 65 - 250 times. OTRs frequently exhibit field cancerization of the skin from which multiple HPV-associated NMSCs develop (Nindl and Rösl 2008, Vinzon and Rösl 2015). The viral load of betaHPVs was determined in OTRs and immunocompetent patients by collecting eyebrow hairs and it spanned 7 orders of magnitude (Howley and Pfister 2015). The prevalence was highest for HPV5, HPV8 and HPV20. However, only the highest betaHPV loads in OTRs were close to those observed in EV patients (Dell'Oste *et al.* 2009). In case control studies, high betaHPV loads were associated with cutaneous SCCs (Neale *et al.* 2013).

Taken all together, a persistent presence and infection of the skin with betaHPV could facilitate the accumulation of genetic changes, over a long period, promoting the development of skin cancer especially in sun-exposed body sites.

1.8.2 Transgenic mouse models to study HPV oncogene functions

A number of transgenic mouse models have been established to analyse E6 and E7 properties of high-risk HPV16 and HPV18, however, only a few *in vivo* models have been reported for betaHPV types. In 2006, a transgenic mouse line expressing HPV20 E6 and E7 under the control of the K10-promoter in hairless SKH-hr1 mice (K10-HPV20-E6/E7) was established, but those animals did not develop spontaneous tumours within the observation period of 2 years. After 9 weeks of chronic UVB

irradiation (90 to 200 mJ/cm^2) with 3 treatments per week a slight increase in the tendency of papilloma development was observed compared to control animals. However, only 2 of 20 K10-HPV20-E6/E7 mice developed skin SCCs (Michel *et al.* 2006). A HPV38 transgenic mouse expressing the oncoproteins E6/E7 under the control of the bovine homologue of the human K10-promoter did not develop spontaneous papillomas during the observation period of 2 to 2.5 years. However, treatment according to the two-step carcinogenesis protocol with 7,12-dimethylbenzanthracene (DMBA) and 12-O-Tetradecanoylphorbol-13-acetate (TPA) led to the development of several papillomas after seven to eight weeks, where 3 of 8 animals developed SCCs (Dong *et al.* 2005). Also K14-HPV38-E6/E7 transgenic mice showed no spontaneous tumour development during their lifespan, however, they were highly susceptible to DMBA/TPA treatment. Single UV irradiation of K14-HPV38-E6/E7 transgenic mice led to accumulation of p21 and cell cycle arrest. Interestingly, chronic UV irradiation with 3 treatments per week for 20 weeks (UVB from 120 mJ/cm^2 to 450 mJ/cm^2) induced the development of actinic keratosis and SCCs in 80% of transgenic animals (Viarisio *et al.* 2011). Our group developed HPV8 transgenic mice in FVB/n background in which oncogene expression is controlled by the human keratin-14 promoter, which directs expression to the *stratum basale*, the hair follicle and to a lesser amount to the *stratum spinosum* of the epidermis. The K14-HPV8-CER mouse model expressing the complete early genome region (E1, E2/E4, E6, E7) was generated first (Schaper *et al.* 2005). A few years later, the K14-HPV8-E2 and the K14-HPV8-E6 transgenic mouse lines, were also established (Pfefferle *et al.* 2008, Marcuzzi *et al.* 2009). For the K14-HPV8-CER and K14-HPV8-E6 transgenic mouse lines, 91% of all animals spontaneously developed single or multifocal benign tumours, which showed papillomatosis, acanthosis, hyperkeratosis and varying degrees of epidermal dysplasia, whereas 6% developed SCCs. In addition, a study performed by Hufbauer and colleagues, in which a knock-down of HPV8-E6 mRNA in K14-HPV8-CER mice was induced by tattooing a HPV8-E6 specific siRNA, papilloma development was significantly reduced (Hufbauer *et al.* 2010b). Therefore, we concluded that E6 represents the main oncoprotein in murine skin, since K14-HPV8-E6 mice represent a phenocopy of the K14-HPV8-CER mice. Three epidermal specific HPV8-E2 transgenic FVB/n mouse lines were generated having different E2 mRNA levels. The rate of tumour development correlated with mRNA expression levels. Only 8% of the K14-HPV8-E2 transgenic animals with medium mRNA levels have

developed spontaneous papilloma and only 2 HPV8-E2 transgenic animals developed SCCs (Pfefferle *et al.* 2008). To test the synergistic effect of UV light, all three transgenic mouse lines were treated with UVA/B light. UV irradiation stimulated papillomatosis in HPV8-CER, -E2 and -E6 transgenic mice within 3 weeks, whereas the skin of FVB/n wild type littermates healed completely from UV-induced hyperplasia. Therefore, an early increase of viral oncogene expression seems to be important for the induction of papillomatosis (Hufbauer *et al.* 2010b). The influence of the transcription factor signal transducer and activator of transcription 3 (Stat3) was analysed in the background of the K14-HPV8-CER mouse line, by generating heterozygous $Stat3^{+/-}$ / HPV8 and homozygous $Stat3^{+/+}$ / HPV8 mice. During an observation period of 12 weeks, only 13% of heterozygous $Stat3^{+/-}$ / HPV8 transgenic mice developed tumours, whereas 54% of $Stat3^{+/+}$ / HPV8 mice showed tumour development in the same time. Therefore, Stat3 has a critical role in epithelial carcinogenesis mediated by HPV8 (De Andrea *et al.* 2010).

1.9 Early proteins

1.9.1 The E1-protein

The early protein E1, representing the only protein with enzyme activity, is encoded by the largest and most conserved ORF, ranging in size from 600 to 650 aa, dependent on the type of HPV. The E1 protein is an ATP-dependent DNA helicase, which assembles at the viral origin, unwinds DNA by binding to and stimulation of Topoisomerase I and interacts with cellular DNA replication factors (Sun *et al.* 1990, Yang *et al.* 1993, Clower *et al.* 2006). E1 interacts with cyclin E-Cdk2 kinase, a key cell cycle regulator of the S-phase, building a complex responsible for cell cycle regulation of HPV replication (Cueille *et al.* 1998). Generally, the E1 protein is required during the viral life cycle a) to increase the episomal copy number after infection of basal keratinocytes, b) to maintain a constant level of episomes in epithelial cells prior to differentiation and c) to promote viral genome amplification in the upper most epithelial layers (Bergvall *et al.* 2013).

1.9.2 The E2 protein

The E2 protein possesses transcriptional regulation function due to its interaction with the DNA helicase E1 via its N-terminal domain, facilitating its binding to the viral *ori* of replication (Sedman and Stenlund 1995, Akgül *et al.* 2003). The DNA strand is

unwound and the cellular DNA polymerase is able to contact the viral genome. Furthermore, the E2 protein is able to bind as a dimer to a 12 bp palindromic sequence (ACC(N)$_6$GGT), mostly located within the NCR of the HPV genome, via its C-terminal DNA binding/dimerization domain, thereby regulating viral transcription (Muller *et al.* 2002, Akgül *et al.* 2003).

In addition to its regulatory role at viral promoters, E2 has recently been described as a factor able to regulate also expression of cellular proteins. By binding to its recognition motif, HPV8-E2 was found to suppress the β4 integrin (Oldak *et al.* 2004) and to activate the promoter of the matrix-metalloproteinase 9 (Akgül *et al.* 2011b). HPV8-E2 is able to down-regulate epidermal AKT activity by decreasing AKT1 isoforms leading to cutaneous differentiation changes (O'Shaughnessy *et al.* 2007). HPV5-E2-specific mRNA was shown to be present in the upper layers of the epidermis of an EV-associated benign cutaneous lesion (Haller *et al.* 1995). The E1 and E2 proteins of HPV5 were identified as viral factors necessary for viral replication in complementation assays. The E8^E2C protein, representing a splice variant of the E8 and E2 ORF acts as replication repressor (Sankovski *et al.* 2014). E2 proteins are able to tether the viral genome to host mitotic chromosomes to ensure persistent and long-term maintenance of the viral genome during cell division, which is associated with complex formation of E2 with the cellular protein Brd4 (You *et al.* 2005, McBride 2013). E2 proteins of different genera are able to bind to different regions of mitotic chromosomes (Oliveira *et al.* 2006). HPV8-E2 binds most prominently to the pericentromeric regions of chromosomes overlapping the loci for ribosomal RNA genes as dimeric speckles and co-localises with the ribosomal transcription factor UBF1 and not with Brd4 (Poddar *et al.* 2009).

1.9.3 The E4 protein

The ORF of the E4 protein is located within the E2 ORF and is translated from a spliced mRNA (E1^E4), which contains the initiation codon and the first few amino acids from the E1 ORF (Chow *et al.* 1987, Doorbar 2013). The gene products of E1^E4 can be detected with the start of the vegetative viral genome amplification, giving the E4 protein an important role during the later stages of the viral life cycle. The identification of the E4 protein in lesions became an important role, as it can serve as a biomarker of active HPV infection and serves as a marker for severity in the cervix (Doorbar 2013). For betaHPV and other cutaneous HPV types, the E4 protein assembles into

distinctive cytoplasmic inclusion granules, first noticeable in the lower to mid epithelial layers. Furthermore, E1^E4 can interact with and reorganise the cytokeratin filaments within a cell (Doorbar *et al.* 1991). Generally, E4 is expressed before the late proteins L1 and L2 and is involved in cell cycle progression and exit. Therefore, it generally functions in viral release and transmission (Doorbar 2013). In skin tissues of EV patients and in intraepithelial precursor lesions of OTRs, the cytoplasmic expression of E4 could be associated with the onset of vegetative viral genome amplification by using antibodies raised against E4 of genus betaHPVs (Borgogna *et al.* 2012, Borgogna *et al.* 2014).

1.9.4 The E6 protein

The tumorigenic potential of alphaHPV types is partly dependent on the inactivation of the tumour suppressor proteins p53 and the retinoblastoma tumour suppressor protein (pRB) by E6 and E7, respectively (Münger and Howley 2002). However, recent studies demonstrated that interactions with proteins of the PDZ family are also important for immortalisation (Mantovani and Banks 2001). High-risk E6 proteins possess a PDZ binding motif at their C-terminal end, mediating its binding to the PDZ proteins hDlg1, hDgl4, hScrib or MAGI1 and MUPP1, thereby targeting them for degradation by ubiquitin ligases (Howie *et al.* 2009). HPV5 and HPV8-E6 proteins do not encode a C-terminal PDZ-binding motif, but decreased expression of the PDZ domain protein Syntenin-2 was identified in HPV8-E6 expressing keratinocytes, representing the first PDZ domain protein controlled by HPV8 at transcriptional level (Lazic *et al.* 2012).

Degradation of p53 is only achieved for high-risk HPV types. In the case of genus betaHPV, the E6 protein does not interact with E6AP and p53 is not degraded (Steger and Pfister 1992). However, HPV38 possesses transforming activity partly mediated by the accumulation of ΔNp73, an antagonist of p53/p73 functions involved in growth suppression and apoptosis, thereby targeting the same pathway as alphaHPV types (Accardi *et al.* 2006). An alternative deregulation of the cell cycle is achieved by E6 proteins, due to their ability to activate telomerase in epithelial cells. E6 binds E6AP, which is crucial for hTERT regulation by E6, thereby activating telomerase and hTERT (Liu *et al.* 2005). Bedard and colleagues demonstrated that HPV38-E6 is able to activate telomerase by increased hTERT mRNA levels and other proteins involved in HPV16 E6 mediated activation of telomerase (Bedard *et al.* 2008).

Genus betaHPV E6 proteins bind to the transcriptional co-activator mastermind-like protein (MAML1), which is a transcriptional regulator involved in cellular signalling pathways (White *et al.* 2012a). The interaction between E6 and MAML1 inhibits Notch mediated transcription, which acts as a tumour suppressor in squamous epithelial cells and plays a role in keratinocyte differentiation by regulating the cell cycle inhibitor p21 (Brimer *et al.* 2012, Meyers *et al.* 2013).

Due to the prevalence of SCC in EV patients on sun-exposed body sites, it is suggested that a betaHPV infection synergises with the carcinogenic effect of UV light. Therefore, SCC development after betaHPV infection may result from the effect of the E6 proteins on DNA repair and on UV-induced apoptosis (Jackson and Storey 2000). For several E6 proteins, including HPV5 and HPV8, a degradation of the proapoptotic protein Bak was reported (Jackson *et al.* 2000). In addition, HPV5 and HPV8-E6 proteins bind to the acetyltransferases CBP and p300 leading to delayed ATR activation. This effect leads to the accumulation of p53, reduced G1 arrest and thereby increases double-strand breaks and a delayed repair of DNA induced by UV (Howie *et al.* 2011, White *et al.* 2012a). For HPV8-E6 a specific lysine in the C-terminal part of the protein was identified, responsible for the prevention of DNA damage repair and p300 binding after UV irradiation. This study demonstrated first mechanistical *in vivo* data for the critical role of HPV8-E6 in HPV-driven skin carcinogenesis due to impaired DNA damage repair pathways (Hufbauer *et al.* 2015).

1.9.5 The E7 protein

The E7 proteins are divided into three parts: a) the conserved region (CR1), which is necessary for cellular transformation and the degradation of pRB in high-risk HPV types, b) the CR2, which contains a conserved pRB family binding site and a consensus casein kinase II (CKII) phosphorylation site and c) the C-terminal domain. This domain is involved in dimerization of E7 proteins and the association with cellular complexes and contains a zinc-binding domain out of two C-X-X-C motifs, which are separated by 29 - 30 aa (Jones and Munger 1996, Zwerschke and Jansen-Durr 2000, McLaughlin-Drubin and Münger 2009).

Generally, transforming activities of different E7 proteins can be associated with their low-risk and high-risk classification, as high-risk HPV-E7 proteins possess higher transforming and immortalisation properties compared to low-risk types (Barbosa *et al.* 1991). Furthermore, E7 interacts with pRB, which is destabilised by high-risk E7

proteins via proteasomal degradation, due to its interaction with the S4 subunit of the 26S proteasome (Dyson *et al.* 1989, Boyer *et al.* 1996). Low-risk alphaHPV and betaHPV-E7 proteins bind pRB with an approximately 10-fold lower efficiency compared to high-risk HPVs (Iftner *et al.* 1988, Sang and Barbosa 1992, Schmitt *et al.* 1994).

The Leu-X-Cys-X-Glu (LXCXE) motif present in the CR2 homology domain is the association site of the E7 protein with pRB and the related pocket proteins, p107 and p130 (White *et al.* 2012b). Under normal conditions these proteins are able to regulate G1/S-phase entry and progression due to the regulation of the transcriptional activities of E2F transcription factors. The disruption of the pRB/E2F complex is induced by cdk4/6 and cdk2 mediated phosphorylation of pRB, thereby the released E2F is able to activate the necessary gene transcription for S-phase entry and progression. During HPV infection, high-risk E7 proteins associate with E2F-bound pRB in G1, causing disruption of the repressive pRB/E2F complex ending up in uncontrolled G1 exit and S-phase entry (Dyson *et al.* 1992). HPV8-E7 binds only weakly to pRB, however, it is able to deregulate G1/S transition control (Akgül *et al.* 2007). Additional binding partners of alpha and betaHPVs are UBR4 (p600) and its binding partner KCMF1 suspected to function as E3 ubiquitin ligase (White *et al.* 2012b). Quantitative 2D differential gene expression (DiGE) gel approach combined with mass spectrometry led to the identification that actin binding/regulating proteins are modulated by HPV8-E7 expression (Akgül *et al.* 2009). In addition, cDNA microarray analysis identified lipocalin-2 to be overexpressed in HPV8-E7 positive keratinocytes, which also correlated with HPV-positivity in cutaneous SCCs (Akgül *et al.* 2011a).

HPV8-E7 is predominantly located in the nucleus, but was also found at lower levels in the cytoplasm (Sperling *et al.* 2012). This fact was verified by Onder and colleagues, who showed that HPV8-E7 is able to shuttle between the nucleus and the cytoplasm, with its predominant location in the nucleus. Within the zinc-binding domain, the HPV8-E7 protein contains a nuclear localisation signal (NLS) for import and localisation in the nucleus, as well as a nuclear export signal (NES), responsible for its transport (Onder and Moroianu 2014, Onder *et al.* 2015). The expression of HPV8-E7 in primary keratinocytes causes polyploidy, which is associated with decreased levels of pRB and p21 (Akgül *et al.* 2007). Three-dimensional organotypic skin cultures (OSC) have been used to study the effects of HPV-E7 on keratinocyte growth and differentiation. The first study on keratinocyte transforming activities of betaHPV oncoproteins in OSC was

based on a collagen type I matrix. On top of these cultures primary human keratinocytes (PHK) expressing the E6/E7 genes of betaHPV types (HPV5, 12, 15, 17, 20 and 38) and of HPV16 were seeded and differentiated. Under these conditions cell differentiation was disturbed to different degrees. Cultures expressing either oncoproteins of HPV5, 12 or 38 were less organised compared to control cultures, showing no cornified layer and only thin granular layers. In suprabasal layers degenerated changes were characterised by vacuolisation of the cytoplasm (Boxman *et al.* 2001). Using the OSC model, based on de-epidermalised human dermis, the keratinocytes of the regenerated epithelium expressing HPV8-E7 displayed hyperproliferation and were positive for both cyclin E and p16INK4a indicating that E7 is able to overcome p16INK4a induced cell cycle arrest (Westphal *et al.* 2009). In addition, and most strikingly, keratinocytes lost their normal polarity and migrated downwards. Invasion was proved by the identification of a disrupted basement membrane in areas of invading keratinocytes due to immunohistochemical staining against basement membrane (BM) components, such as collagen VII, IV and laminin-5. This coincided with the overexpression of matrix metalloproteinase-1 (MMP-1), MMP-8 and membrane type1-MMP (MT1-MMP) (Akgül *et al.* 2005, Smola-Hess *et al.* 2005). In addition, the E7 proteins of HPV5, HPV8 and HPV20 have been reported to possess an increased clonogenicity and were highly positive in tumour sphere assays, which coincided with increased stem cell-like keratinocytes possessing a higher expression of CD44 and EpCAM on their cell surface (Hufbauer *et al.* 2013).

1.10 Human skin - organisation and structural components

1.10.1 The organisation of the epidermis

The skin represents an effective barrier preventing organisms from chemical and physical damage, including UV irradiation, from invading pathogens and unregulated loss of water and solutes (Proksch *et al.* 2008). The skin is a complex structure composed of three main layers, the stratified, cellular epidermis, the underlying dermis composed of connective tissue and the subcutaneous layer (subcutis), whereas epidermis and dermis represent the main structure of human skin. The epidermis consists of stratified squamous keratinizing epithelium, containing proliferating basal and differentiated suprabasal keratinocytes. Up to 95% of the epidermis are made up of keratinocytes, whereas Merkel cells, melanocytes and Langerhans cells are also

present (Kanitakis 2002). The epidermis is relatively thin (0.1 - 0.2 mm in depth) and is attached to the underlying dermis by the BM (Watt and Fujiwara 2011).

The epidermis can be divided from top to bottom into *stratum corneum*, *stratum granulosum*, *stratum spinosum* and *stratum basale*. The *stratum basale* is made up of basal keratinocytes, which divide continually and migrate superficially forming the *stratum spinosum*. During the process of differentiation, the cells are getting highly organised, form cellular junctions between each other and secrete keratin proteins, contributing the development of an extracellular matrix (ECM). During this process, the cells finally reach the *stratum corneum* and can be shed from the surface, called keratinisation (Simpson *et al.* 2011).
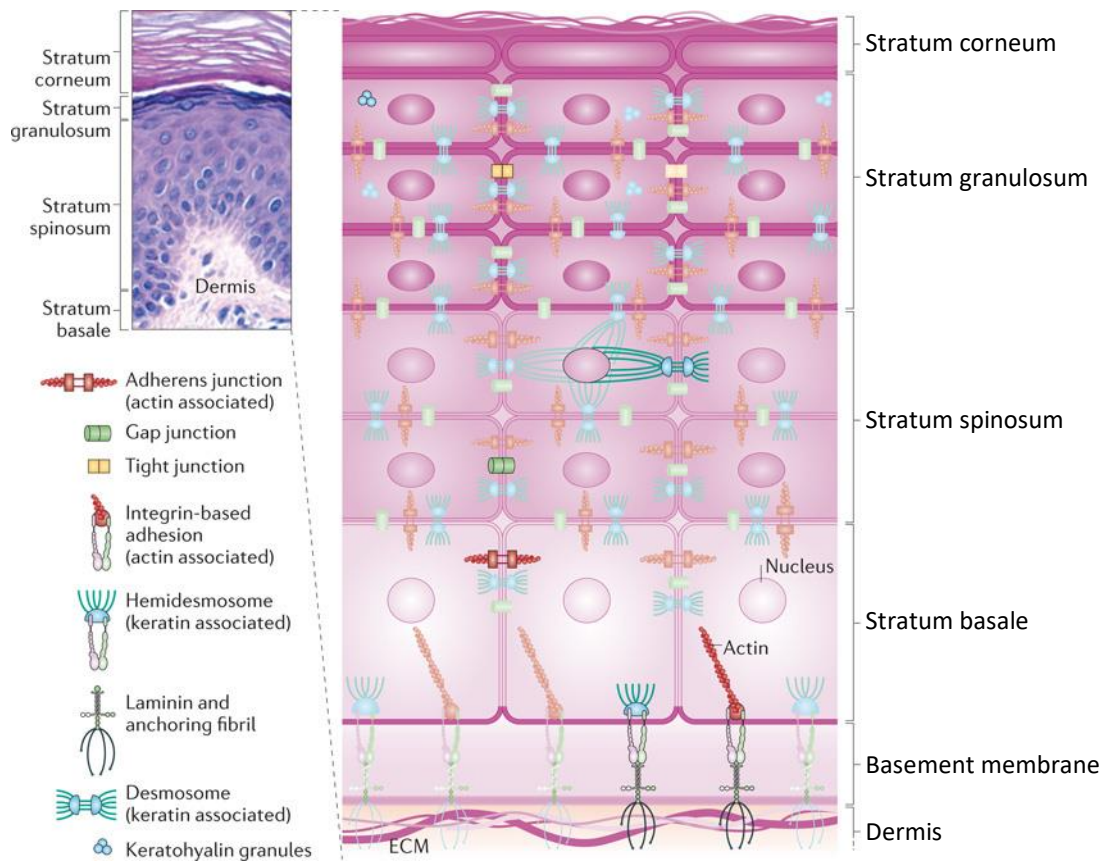
Figure 5. Schematic representation of the human skin (taken from (Simpson *et al.* 2011)). On the left the four main layers of the epidermis are visualised via haematoxylin and eosin (HE) staining of human skin, which are from top to bottom: *stratum corneum, stratum granulosum, stratum spinosum* and *stratum basale*. The *stratum basale* is the basal and proliferating cell layer of the epidermis, which stays in contact with the dermis through hemidesmosomes and integrin-based adhesions. Both interactions provide contact to the underlying extracellular matrix (ECM). During keratinocyte differentiation, each layer forms a specific architecture comprising the arrangement of the cytoskeleton as well as of cell junctions, including adherens junctions, tight junctions, desmosomes and gap junctions.

To allow tissue integrity, two types of cell adhesions are achieved, either cell-cell adhesion, a connection of the intracellular cytoskeleton between cells, or the cell-matrix adhesion, which is a connection of the cellular cytoskeleton with components of the ECM. Both connections are formed due to different types of cell adhesion molecules, including integrins and cadherins. Adherens and tight junctions are essential for the formation of adhesive contacts between two neighbouring cells. They are composed of transmembrane glycoproteins of the cadherin family, such as E-cadherin, which interact with members of the catenin family including β-catenin. Generally, adherens junctions initiate and stabilize cell-cell adhesion, regulate the actin cytoskeleton, intracellular signalling and transcription (Hartsock and Nelson 2008). Tight junctions are composed of two types of transmembrane proteins, occludins and claudins, which associate with cytoplasmic proteins, including zona occuldens-1 (ZO-1), belonging to the membrane-associated guanylate kinase homologs (MAGUK) family, which links tight junctions to the actin cytoskeleton and to adherens junctions (Simpson *et al.* 2011).

1.10.2 Extracellular matrix

The ECM of the dermis regulates and maintains tissue homeostasis and stabilizes the structural integrity of the skin. The ECM forms a complex network of macromolecules with specific biochemical and biomechanical properties regulating different cellular processes (Pickup *et al.* 2014). It is predominantly composed of fibrillar collagens, the BM and elastin fibres, which can be remodelled due to the degradation of structural proteins. Degradation is regulated by proteins of the family of MMPs, which are also essential to epidermal differentiation. An upregulation of MMPs is known to facilitate cancer development (Philips *et al.* 2011). The deposition of a specialised layer of ECM between the epidermis and the underlying dermis forms the BM. This amorphous, dense, sheet-like structure is composed of about 50 proteins, mainly collagen IV, laminin, HSPG, nidogen/entactin and minor constituents including Fibulins, which are able to interact with each other (Breitkreutz *et al.* 2013). However, collagen IV comprises about 50% of the BM and resembles a kind of scaffolding network (Kalluri 2003). The maintenance of the normal structure of the BM is an important factor, whereby BM disruption is associated with different stages of invasive carcinoma (Barsky *et al.* 1983, Watt and Fujiwara 2011).

1.11 Mechanisms of keratinocyte invasion

The process of cancer progression involves the ability of cancer cells to leave the primary tumour, moving through the ECM and invade the surrounding tissue to settle and grow at another body site. This process contains a complex series of cell-biological events and is called the 'invasion-metastasis cascade' (Guan 2015, Aneta *et al.* 2016). During tumour cell migration into the surrounding tissue several mechanisms of normal cell migration are activated to change the cellular shape, to create conditions allowing movement and to reorganise the surrounding tissues. Two patterns of invasive growth can be distinguished, collective (group) cell migration and single cell migration, which is dependent on the tissue microenvironment and on molecular changes of the cells (Krakhmal *et al.* 2015). In addition, tumour cell invasion is associated with changes in cell metabolism, characterised by switching from oxidative metabolism to aerobic glycolysis (Krakhmal *et al.* 2015, Liberti and Locasale 2016).
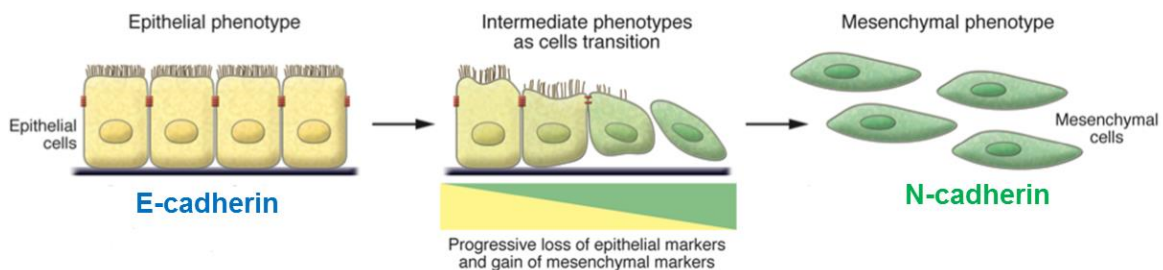
Figure 6. Schematic representation of epithelial-mesenchymal transition (Kalluri and Weinberg 2009). EMT describes a process in which polarised epithelial cells are converted into motile mesenchymal cells. The involved cells pass through several changes, which can be detected by epithelial and mesenchymal cell markers. A key molecular event of EMT is the downregulation of E-cadherin which coincides with an upregulation of N-cadherin, describes as a 'cadherin switch'.

To shed off from the primary tumour, cells detach from the ECM resisting to anoikis and thereby activating a complex cell-biological program, described as epithelial-mesenchymal transition (EMT) (Guan 2015). EMT describes the transformation of highly differentiated, polarised and organised epithelial cells into undifferentiated, mesenchymal-like cells possessing migratory and invasive properties (figure 6) (Profumo and Gandellini 2013). However, cells may show some epithelial and some mesenchymal characteristics, which is described as partial EMT (Lamouille *et al.* 2014). Cadherin-mediated cell-cell adhesion is a highly dynamic process, which enables the reorganisation and movement of cells. A loss of cell-cell adhesions is associated with epithelial derived tumours, therefore EMT is associated with a down-

regulation of E-cadherin. Furthermore, this downregulation coincides with an upregulation of N-cadherin, promoting cell motility and invasion. This phenomenon is representative for EMT and is also known as 'cadherin switch' (Lamouille *et al.* 2014). A decrease of E-cadherin causes an incorrect localisation of the adherens junction core proteins, α- and β-catenin, and the tight junction protein ZO-1 (Hartsock and Nelson 2008).

Cell adhesion to the ECM is achieved by the interaction with integrins. Integrins are a family of transmembrane glycoprotein receptors consisting of α and β subunits. At least 19 α and 8 β subunits build 24 different non-covalently bound integrin heterodimers. They are composed of a large extracellular binding domain, a single-membrane-spanning transmembrane domain and a short intracellular cytoplasmic tail, forming links to cytoskeletal elements (Watt and Fujiwara 2011). Integrins are able to bind to ECM proteins including collagens, fibronectin and laminin and they play an important role in actin cytoskeleton assembly, as well as in cell adhesion and migration. Cell adhesion to the ECM is achieved by binding of the integrin extracellular domain to the ECM molecule, leading to the interaction of the intracellular domain with the cytoskeleton through intracellular structures called focal adhesions (Janes and Watt 2006). The most prevalent integrins in the epidermis are integrin α2β1, a collagen receptor, integrin α3β1, predominantly a laminin-5 receptor and integrin α6β4, a laminin receptor. In addition, integrin αvβ5, a vitronectin receptor, is expressed at lower levels, whereas integrin α5β1 (fibronectin receptor) and αvβ6 (fibronectin and tenascin receptor) are induced in cell culture and wound healing (Watt 2002). Different studies showed that deregulation of integrin subunits are important during cancer development and metastasis processes (Pawelek and Chakraborty 2008). Integrins are also able to activate the synthesis of cyclins, inositol lipids, focal adhesion kinase (FAK) and MAPK, as well as MMPs (Brooks *et al.* 1996, Schlaepfer *et al.* 1998).

A complete EMT implies several distinct molecular processes, including the activation of transcription factors, the expression of specific cell-surface proteins, the reorganisation and expression of cytoskeletal proteins and the production of ECM-degrading enzymes, which ends with the degradation of the underlying ECM and the migration/invasion of keratinocytes (Kalluri and Weinberg 2009).

1.12 Aim of the study

As described above, my group could show that HPV8-E7 induces keratinocyte invasion in *in vitro* OSC, which were composed of de-epidermalised human dermis as matrix (Akgül *et al.* 2005). No invasive phenotype was observed for different betaHPV oncoproteins in OSCs composed of a 100% collagen type I matrix (Boxman *et al.* 2001). Both systems differed in the composition of the ECM and the presence of the epithelial basement membrane, which is only present on the de-epidermalised dermis at start of the experiment. Interestingly, OSCs based on a mixture of 50% collagen type I and 50% Matrigel (a gelatinous mixture of ECM proteins) triggered strong invasion of HPV8-E7 positive keratinocytes (figure 7, Akgül, personal communication). We therefore hypothesised that components of the ECM are critical for the induction of the invasive behaviour of HPV8-E7 positive keratinocytes. To answer this hypothesis, we first generated the K14-HPV8-E7 transgenic mouse model to proof the oncogenic potential of HPV8-E7 also *in vivo* in the murine skin. In addition, we analysed the effect of different ECM proteins and downstream pathways on the invasive capacity of HPV8-E7-positive cells. This work therefore provides further experimental evidence of an association between betaHPV infection and the development of cutaneous SCC.
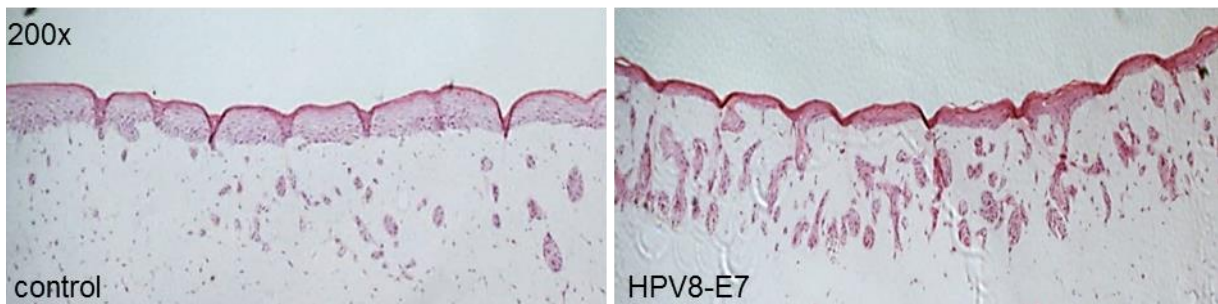
Figure 7. Invading HPV8-E7-positive cells in 50% collagen I and 50% Matrigel OSCs. Representative HE staining of OSCs established with keratinocytes expressing HPV8-E7 or empty vector pLXSN. The epithelium regenerated onto a matrix composed of 50% collagen I and 50% Matrigel showed increased invasive capacity of HPV8-E7 cells. In addition, invasion of empty vector cells was also triggered due to matrix composition (provided by Dr B. Akgül, magnification 200x).

2. Material

2.1   Equipment

Agfa CP1000	Agfa, Mortsel, Belgium
Bioruptor ® PLUS	Diagenode, Liege, Belgium
Bioruptor® Water cooler	Diagenode, Liege, Belgium
Eppendorf Centrifuge 5417	Eppendorf, Hamburg, Germany
Eppendorf Thermostat 5320	Eppendorf, Hamburg; Germany
GelDoc Universal Hood	BioRad Life Science Research, Hercules, USA
Glomax ® Luminometer	Promega, Madison, USA
Heraeus Megafuge 1.0R	Heraeus Instruments, Hanau, Germany
Heraeus Multifuge L-R	Heraeus Instruments, Hanau, Germany
Hettich Universal 320	Hettich, Tuttlingen, Germany
Labovert FS	Leica, Wetzlar, Germany
Lightcycler ®	Roche Applied Sciences, Mannheim, Germany
NanoDrop®ND-1000 UV/VIS spectralphotometer	PEQLAB, Erlangen, Germany
PowerPac 300	BioRad Life Science Research, Hercules, USA
Protean II xi	BioRad Life Science Research, Hercules, USA
Stericult 200 Incubator	Labotect, Göttingen, Germany
T3 Thermocycler	Biometra, Göttingen, Germany
Ultrapure water Milli-QPlusPF	Millipore, Eschborn, Germany
Vortex VF2	Janke&Kunkel, Staufen, Germany

2.2   Chemicals and Reagents

All chemicals used in this study were purchased from Applichem (Darmstadt, Germany), Invitrogen (Karlsruhe, Germany), Merck (Darmstadt, Germany), Roth (Karlsruhe, Germany) and Sigma-Aldrich (Steinheim, Germany) and complied the reagent grade 'p.a.'.

Agarose	Sigma-Aldrich, Steinheim, Germany
Ampicillin	Sigma-Aldrich, Steinheim, Germany
β-Mercaptoethanol	AppliChem, Darmstadt, Germany
Bradford-Solution	BioRad, München, Germany

Chloroform	Sigma-Aldrich, Steinheim, Germany
Coomassie Blue	AppliChem, Darmstadt, Germany
DMSO (Dimethylsulfoxide)	AppliChem, Darmstadt, Germany
Ethanol	Roth, Karlsruhe, Germany
Ethidium bromide	AppliChem, Darmstadt, Germany
Fetal Calf Serum (FCS)	Invitrogen, Karlsruhe, Germany
Formaldehyde	Merck AG, Darmstadt, Germany
Glucose	AppliChem, Darmstadt, Germany
Glycogen	AppliChem, Darmstadt , Germany
Glycerol	AppliChem, Darmstadt, Germany
Isopropanol	Roth, Karlsruhe, Germany
LB-Agar	AppliChem, Darmstadt, Germany
LB-Broth	Invitrogen, Karlsruhe, Germany
NP-40	Sigma-Aldrich, Steinheim, Germany
Phenol-Chloroform	Sigma-Aldrich, Steinheim, Germany
Ponceau-Red	AppliChem, Darmstadt, Germany
RNAlater	Qiagen, Hilden, Germany
RNase free water	Qiagen, Hilden, Germany
TEMED (N,N,N`,N`Tetramethylendiamin)	AppliChem, Darmstadt, Germany
Tween 20	Serva, Heidelberg, Germany

Plastic ware was purchased from Eppendorf (Hamburg, Germany), Falcon BD (Heidelberg, Germany), Sarstedt (Nümbrecht, Germany) and TPP (Trasadingen, Switzerland). BD BioCoat Laminin, Fibronektin, Collagen IV (Ø 10 cm) were ordered from BD Biosciences (Heidelberg, Germany).

2.3   Kits

BM *Chemiluminescence Western Blotting* Kit	Roche Diagnostics, Mannheim, Germany
DC^{TM} Protein Assay Kit II	BioRad Life Science Research, Hercules, USA
Dual-Luciferase ® Reporter Assay System	Promega, Madison, USA
DyeEx 2.0 Spin Kit	Qiagen, Hilden, Germany
GeneJET™ PCR Cloning Kit	Fermentas, St. Leon-Rot
QIAquick Gel Extraction Kit	Qiagen, Hilden, Germany
QIAquick PCR Purification Kit	Qiagen, Hilden, Germany
QIAamp DNA Mini and Maxi Kit	Qiagen, Hilden, Germany
QIAprep Spin/QIAprep 8 Miniprep Kit	Qiagen, Hilden, Germany
QIAquick *PCR Purification* Kit	Qiagen, Hilden, Germany
Quick Change® II XL Site-Directed Mutagenesis Kit	Agilent Technologies, Boeblingen, Germany

Seahorse XF MitoStress Kit — Seahorse Biosciences, Copenhagen, Denmark

Sequencemix Big Dye ® Terminator — Applied Biosystems, Foster City, USA

PierceTM BCA Protein Assay Kit — ThermoFisher, Waltham, USA

2.4 Bacterial strain

Epicurian coli ® XL1-Blue

genotype: *recA1, end A1, gyr96, thi-1, hsdR17, supE44, relA1, lac*[F'*proAB lacqZ_AM15* Tn*10*(Tet')] (Stratagene, La Jolla, USA)

2.5 Eukaryotic cells

C33a (ATCC: HTB-31)

HPV-negative cell line derived from a cervical cancer (Auersperg 1969).

N/TERT

The immortalised cell line N/TERT was established from primary human foreskin keratinocytes due to overexpression of the telomerase gene (Dickson *et al.* 2000).

Primary human keratinocytes (PHK)

PHK were isolated from human foreskin tissue provided by Dr Ali Tok, Department of Dermatology, University Hospital Cologne.

PT67

A fibroblast cell line derived from NIH3T3 cells used for the production of infectious, non-replicative retroviruses. PT67 cells contain the *gag-, pol-* and *env-*genes of the Moloney-Murine-Leucemia-virus as stable integrated parts of their genome. The *env-*gene derived from type10A1 and encodes two surface proteins, which are able to bind the amphotropic cellular receptors RAM1 and GALV (Miller and Chen 1996). A transfection of those cells with an expression vector containing the retroviral packaging signal $\psi+$ together with the coding gene of interest and a selection marker, infectious, non-replicative viruses can be produced (Retro-X^{TM} System, Clontech Palo Alto).

RTS3b

HPV-negative keratinocyte cell line, established out of a skin carcinoma of a kidney transplant recipient (Purdie *et al.* 1993).

2.6 Nucleic Acids

2.6.1 Synthetic oligonucleotides

The HPLC-purified oligonucleotides were ordered from Sigma-Aldrich (Steinheim).

Oligonucleotides for quantitative real-time PCR

Name	Sequence 5' → 3'
βCatenin (human)	f: GCTTTCAGTTGAAGCTGACCA
	r: CAAGTCCAAGATCAGCAGTCTC
E-cadherin (human)	f: GAACGCATTGCCACATACAC
	r: AGCACCTTCCATGACAGACC
Fibronectin (human)	f: GAACTATGATGCCGACCAGAA
	r: GGTTGTGCAGATTTCCTCGT
GAPDH (human)	f: CTGACTTCAACAGCGACACC
	r: TGCTGTAGCCAAATTCGTTGT
HPRT1 (human)	f: TGACACTGGCAAAACAATGCA
	r: GGTCCTTTTCACCAGCAAGCT
HPRT1 (murine)	f: CCTAAGATGAGCGCAAGTTGAA
	r: CCACAGGACTAGAACACCTGCTAA
HPV8-E7	f: CCTGAAGTGTTACCAGTTGACCTGC
	r: CAGTTGCGTTGACAAAAAGACG
Integrin α2 (human)	f: AACTCTTTGGATTTGCGTGTG
	r: TGGCAGTCTCAGAATAGGCTTC
Integrin α3 (human)	f: ACTGTGAAGGCACGAGTGTG
	r: TGCTGGTTCGGAGGAATAG
Integrin α5 (human)	f: CAACATCTGTGTGCCTGACC
	r: CCAGGTACACATGGTTCTGC
Integrin α6 (human)	f: GCTGGTTATAATCCTTCAATATCAATTGT
	r: TTGGGCTCAGAACCTTGGTTT
Integrin αv (human)	f: GTTACTGAGAATGGGTCAAG
	r: CCAGGCCTTGAGGAACTGTG
Integrin β1 (human)	f: CAAAGGAACAGCAGAGAAGC
	r: ATTGAGTAAGACAGGTCCATAAGG
Integrin β4 (human)	f: CTGTGTGCACGAGGGACATT
	r: AAGGCTGACTCGGTGGAGAA
Integrin β5	f: GTGAAAGATGACCAGGAG

(human)	r: GTTGAAGGTGAAGTCCAC
Integrin β6 (human)	f: CATTGAGTGCCACCTGTCAG
	r: GACACCAGTAGCTTCCAGATG
N-Cadherin (human)	f: AGTATCCGGTCCGATCTGC
	r: CTGTGGGGTCATTGTCAGC
PIP5K1γ (human)	f: AAGGAGGCCGAGTTCCTG
	r: CGGGTTCTGGTTGAGGTTC
Snail (human)	r: CTGTGGGGTCATTGTCAGC
	r: CATCTGAGTGGGTCTGGAGG
Slug (human)	f: TGGTTGCTTCAAGGACACAT
	r: GCAAATGCTCTGTTGCAGTG
Twist (human)	f: GTCCGCAGTCTTACGAGGAG
	r: CCAGCTTGAGGGTCTGAATC
Vinculin (human)	f: GATGAAGCTCGCAAATGGTC
	r: TCTGCCTCAGCTACAACACCT
ZO-1 (human)	f: GAAGGAGTTGAGCAGGAAATCTA
	r: AGGACTCAGCAGTGTTTCACC

Oligonucleotides for DNA sequencing

Name	Sequence 5' → 3'	Position
pJETseq	GGAGCAGGTTCCATTCATTG	387-406 in pJET1/blunt

Oligonucleotides for reverse transcription

Name	Sequence 5' → 3'
Oligo-dT23-Primer	$(T)_{23}V$
Random Nonamers	$(N)_9$

Oligonucleotides for site-directed mutagenesis

Name	Sequence 5' → 3'
HPV8-E7-L23A	f: GAGATACAACCTGAAGTGGCACCAGTTGACCTGCTTTG
HPV8-E7-L23A	r: CAAAGCAGGTCAACTGGTGCCACTTCAGGTTGTATCTC
pFN(0.2 kb)LUC-Sp1mut	f: GGGGTGGTTCGGTTCGGGGACAGCCC
pFN(0.2 kb)LUC-Sp1mut	r: GGGCTGTCCCCGAACCGAACCACCCC

siRNAs for knock-down experiments

The HPLC purified siRNA duplex were ordered from Qiagen (Hilden) with the following sense and antisense sequences.

Name	Sequence 5' to 3'
β-catenin sense	CGGGAUGUUCACAACCGAATT
β-catenin antisense	UUCGGUUGUGAACAUCCCGAG
ZO-1 sense	AGUAUCUGAUAAUGAAGAATT
ZO-1 antisense	UUCUUCAUUAUCAGAUACUGG
Integrin a3 sense	CCAUCAACAUGGAGAACAATT
Integrin a3 antisense	UUGUUCUCCAUGUUGAUGGTG

2.6.2 Cloning vectors

pJET1.2/Blunt

PCR products were ligated into pJET/Blunt vector (GeneJET™ PCR Cloning Kit, Fermentas, St. Leon-Rot) to prepare serial dilutions of PCR standards to generate a standard curve for qRT-PCR experiments. All introduced gene fragments are listed in section 2.7.1.

2.6.3 Eukaryotic expression vectors

pCMV2-FLAG

This cloning vector (4.7 kb) contains a multiple cloning site, the CMV promoter and the SV40 origin of replication. In addition, this vector expressed a FLAG-tag N-terminal of the protein of interest.

pLXSN

The pLXSN vector is a retroviral expression vector (5.9 kb) which can be transfected into a packaging cell line. These cells secrete recombinant retroviruses into the supernatant, which can be used to transduce cells. The gene of interest is expressed under the control of the 5'-LTR promoter. Contains neomycin resistance gene (Clontech, Heidelberg).

2.6.4 Reporter constructs

pFN(1.2 kb) LUC

This fibronectin promoter construct contains approximately 1.2 kb of the 5' flanking region of the human fibronectin gene, originating from the human fibrosarcoma cell line HT-1080. This construct contains 69 bp of exon 1, a CAAT site located at -150 bp and the sequence ATATAA at -25 bp from the transcription start site. The fibronectin promoter was cloned into the *Sma*I site of the pGL3 basic luciferase reporter vector. This fibronectin promoter, as well as the deletional mutants, were kindly provided by the group of Jesse Roman (Michaelson *et al.* 2002).

pFN(0.5 kb) LUC

The full length pFN(1.2 kb) LUC was digested with *Pvu*II and *Hin*dIII. The resulting fibronectin promoter fragment extended to -510 bp and was religated into the pGL3 basic luciferase reporter construct.

pFN(0.2 kb)LUC

To create the pFN(0.2 kb) LUC construct, the pFN(0.5 kb) LUC was digested with *Sac*I and *Aat*II, blunt ended and religated into the pGL3 basic luciferase reporter construct.

pFN(0.2 kb)LUC-Sp1mut

To create the pFN(0.2 kb)LUC-Sp1mut, the pFN(0.2kb)LUC construct was mutated at the Sp1 binding site by site-directed mutagenesis (present work).

TOP-flash, FOP-flash

This reporter construct contains two sets (with the second set in the reverse orientation) of three copies of the TCF binding site followed by the minimal HSV-tk promoter and luciferase reporter coding sequence, whereby FOP-flash contains mutated TCF binding sites (provided by Dr David Prowse, University of Hertfordshire, Hatfield, Hertfordshire, UK).

pGL4.74[hRluc/TK]

The pGL4.74[hRluc/TK] (4.2 kb) reporter construct encodes the luciferase reporter gene *hRluc* (*Renilla reniformis*) under the control of an HSV-TK promoter (Promega).

2.6.5 Recombinant plasmids

K14-HPV8-E7

The K14-HPV8-E7 vector is based on the pGEM-3Z backbone, containing the K14 promoter (2007bp, nucleotide 281-2288), the second intron of the rabbit β-globin gene (639bp, nucleotides 557 - 1196), the T7 primer, the K14-polyA signal (485 bp, nucleotides 4746 - 5231) and the SP6-primer. The HPV8-E7 gene (312 bp) was inserted between the T7 promoter and the polyA signal (kindly provided by Dr G. P. Marcuzzi, University of Cologne).

pLXSN-8E7

A retroviral expression vector based on pLXSN containing the ORF of HPV8-E7 (nucleotides 623 - 986) of the pVE34 vector (Steger *et al.* 1990), which was cloned into the *Eco*RI and *Bam*HI restriction sites of the pLXSN vector.

pLXSN-8E7-L23A

The retroviral vector pLXSN-8E7 was used for site-directed mutagenesis to introduce an amino acid exchange at position L23 to A (present work).

pCMV-8E7-FLAG

The early gene of HPV8-E7 was amplified via PCR and introduced into the pCMV2-FLAG vector via the *Bam*HI restriction site (present work).

pCMV-8E7-L23A-FLAG
This vector is based on the pCMV-8E7-FLAG vector and an amino acid exchange was introduced via site-directed mutagenesis at position L23 to A (present work).

pVE34
The complete HPV8 sequence (nucleotides 1 - 5111) was cloned into pUC9 vector via *Bam*HI (Steger *et al.* (1990).

pVE34-L23A
A site-directed mutagenesis was performed to introduce an amino acid exchange in the HPV8-E7 sequence at position L23 to A in the background of the pVE34 vector (present work).

2.6.6 DNA markers and loading dyes

6x DNA Loading Dye	Fermentas, St. Leon-Rot, Germany
GeneRuler™ 1kb ladder	Fermentas, St. Leon-Rot, Germany

2.6.7 Miscellaneous nucleic acids

Adenosine 5'-triphosphate	Fermentas, St. Leon-Rot, Germany
Deoxyribonucleotide triphosphates (dNTPs)	Fermentas, St. Leon-Rot, Germany

2.7 Transfection Reagents

FuGene	Promega, Madison, USA
Lipofectamine RNAiMAX	Invitrogen, Karlsruhe, Germany
Transfast	Promega, Madison, USA

2.8 RNA preparation

Omniscript RT Kit	Qiagen, Hilden, Germany
QIAshredder	Qiagen, Hilden, Germany
RiboLock™ RNase Inhibitor	Fermentas, St. Leon-Roth, Germany
RNase-free DNase Set	Qiagen, Hilden, Germany

2.9 Proteins

2.9.1 Enzymes

Restriction enzymes were purchased from New England BioLabs (Frankfurt am Main, Germany) and Fermentas (St. Leon-Rot).

Platinum® *Taq* DNA Polymerase	Invitrogen, Karlsruhe, Germany
Proteinase K	Qiagen, Hilden, Germany
T4-DNA Ligase	Fermentas

2.9.2 Antibodies

Antibody	Company	Order Number	Application
α-ATP5B (rabbit)	Sigma-Aldrich	HPA001520	WB: 1:1000 IHC: 1:100
α-β-Catenin (mouse)	BD Biosciences	610153	WB: 1:1500 IHC: 1:200
α-CD44 (mouse)	BD Biosciences	555479	FACS: 1:100
α-Collagen IV (rabbit)	kindly provided by Dr Gerhard Sengle, Department for Biochemistry, University of Cologne.		IHC: 1:200
α-E-cadherin (mouse)	BD Biosciences	610181	IHC: 1:200
α-EpCAM-PE (mouse)	Miltenyi Biotec	130-091-253	FACS: 1:100
α-Fibulin-2 (rabbit)	Santa Cruz	sc-30176	IHC: 1:400
α-Fibulin-2 (rabbit)	kindly provided by Dr Gerhard Sengle, Department for Biochemistry, University of Cologne.		WB: 1:2000
α-Fibronectin (rabbit)	Sigma-Aldrich	F3648;	WB: 1:10,000
α-Fibronectin EDA (mouse)	Sigma-Aldrich	FN-3E2	WB: 1:2000
α-FLAG (mouse)	Sigma-Aldrich	F4042	WB: 1:2000 ICC: 1:1000
α-GAPDH (mouse)	Abcam	ab9484	WB: 1:750
α-Integrin α2-FITC (mouse)	Abcam	ab87027	FACS: 1:100
α-Integrin α3 (rabbit)	Millipore	Ab1920	WB: 1:2000 IHC: 1:400
α-Integrin α3-FITC (mouse)	Miltenyi Biotec	130-081-201	FACS: 1:100
α-Integrin α5-PE (mouse)	Miltenyi Biotec	130-097-225	FACS: 1:100
α-Integrin α6-PE (mouse)	Miltenyi Biotec	130-097-246	FACS: 1:100
α-Pancytokeratin (rabbit)	Santa Cruz	sc-15367	IHC: 1:100
α-PIP2 (mouse)	Santa Cruz	sc-53412	IHC: 1:250
α-PTRF (rabbit)	Abcam	ab48824	WB: 1:2000 ICC: 1:250
α-pRB (rabbit)	SantaCruz	sc-50	WB: 1:1000
α-Tubulin (rat)	Abcam	ab6160	WB: 1:10,000
α-ZO-1 (rabbit)	Zymed Laboratories/ ThermoFisher	61-7300	WB: 1:2000 IHC: 1:400

WB: Western blot, IHC: Immunohistochemistry, ICC: Immunocytochemistry, FACS: Fluorescence-activated cell sorting

2.10 Staining reagents

AEC	DCS, Hamburg, Germany
DAPI	Merck, Darmstadt, Germany
MitoTracker ® Green FM	ThermoFisher, Waltham, USA
Hematoxylin solution	Sigma-Aldrich, Steinheim
Kaiser's glycerol gelatine	Merck, Darmstadt, Germany
Liquid DAB Concentrated Substrate Pack	Vector Laboratories, Burlingame, USA
VECTASTAIN Elite ABC Kit (Universal)	Vector Laboratories, Burlingame, USA
VECTASTAIN Elite ABC Kit (Goat IgG)	Vector Laboratories, Burlingame, USA

2.11 Buffers and solutions

For the preparation of the listed buffers and solutions, ddH_2O was used. In the case of a special pH it was adjusted with concentrated HCl, if not stated differently. If a solution was autoclaved this was done at 120°C and 2 bar for 21 min.

10x Citrate buffer	100 mM Citrate, pH 5.8
Coomassie Staining Solution	50% Methanol, 10% acetic acid, 0.05% Coomassie brilliant blue
De-Staining Solution	5% Methanol, 7 % acetic acid
Ethidiumbromide Bath	0.5 µg ml^{-1} ethidiumbromide
2x HBS	280 mM NaCl, 10 mM KCl, 1.5 mM Na_2HPO_4 x 12 H_2O, 50 mM HEPES, pH 7.05 (adjusted with NaOH), sterile filtered
LSDB (low-salt-dilution-buffer)	20% glycerine, 50 mM Tris HCl pH 7.9, 0.1 % NP40, 100 mM, 200 mM, 500 mM or 1M KCl Prior use protease inhibitors were added to LSDB
Lysis buffer I	0.2 M NaOH, 1% SDS
Lysis buffer II	100 mM NaCl, 10 mM EDTA, 0.2% SDS, 200 µg ml^{-1} Proteinase K
5% dry-milk/TBST	5% (w/v) dry milk, in TBST
Neutralisation buffer	3 M KAc, pH 4.8
1x PBS	137 mM NaCl, 2.7 mM KCl, 4.3 mM Na_2HPO_4, 1.4 mM KH_2PO_4
Resuspension buffer	50 mM Glucose, 25 mM Tris, 10 mM EDTA, pH 6.8
RIPA Buffer	50 mM Tris-HCl, pH 7.4, 1% NP-40, 0.5% Na-deoxycholate, 0.1% SDS, 150 mM NaCl, 2 mM EDTA, 50 mM NaF
SDS Electrophoresis Buffer	25 mM Tris-Base, 192 mM glycine, 0.1% SDS
Separation gel 6 - 15%	6-15% Acrylamide, 0.2-0.4% Bisacrylamide, 25% Tris HCl/SDS, pH 8.8, 0.3% Ammoniumpersulfate, 0.1% TEMED
Stacking gel 3,9%	3.9% Acrylamide, 0.1% Bisacrylamide, 25% Tris HCl/SDS, pH 6.8, 0.3% Ammoniumpersulfate, 0.1% TEMED

Stripping Buffer	10% SDS, 62.5 mM Tris HCl, 100 mM β-mercaptoethanol
50x TAE-Puffer	2 M Tris-Acetate, 50 mM EDTA, pH 8.0 (adjusted with NaOH)
TBST	10 mM Tris HCl, pH 8.0, 150 mM NaCl, 0.05% (v/v) Tween 20
TE Buffer (pH 7.9)	10 mM Tris HCl, 1 mM EDTA, pH 7.9
4x Tris HCl/SDS, pH 8.8	1.5 M Tris-Base, 0.4% SDS, pH 8.8
4x Tris HCl/SDS, pH 6.8	0.5 M Tris-Base, 0.4% SDS, pH 6.8
Tris/EDTA buffer	10 mM Tris Base, 1 mM EDTA solution, 0.05% Tween 20, pH 9.0
1x Western blot transfer buffer	25 mM Tris Base, 192 mM Glycine, 20% (v/v) methanol

2.12 Media

2.12.1   Media for cultivation of bacteria

All media were sterilised by incubating at 2 bar, 120°C for 21 min in an autoclave.

LB-Broth-Base (Luria-Burtani-Medium, pH 7.2) AppliChem, Darmstadt, Germany
   1 % (w/v) tryptone, 1% (w/v) sodium chloride, 0.5% (w/v) yeast extract.
   Medium was cooled down to 50°C before ampicillin was added in a final concentration of 100 µg ml^{-1} (optional).

LB-Agar (Luria-Burtani-Agar, pH 7.2) AppliChem, Darmstadt, Germany
   1% (w/v) tryptone, 1% (w/v) sodium chloride, 0.5% (w/v) yeast extract, 1.5% Bacto Agar.
   Agar was cooled down to 50°C before ampicillin was added in a final concentration of 100 µg ml^{-1} (optional) and poured into petri dishes.

SOC Medium
   2% (w/v) tryptone, 0.5% (w/v) yeast extract, 0.05% (w/v) sodium chloride, 20 mM glucose

Ampicillin AppliChem, Darmstadt, Germany
   Stock solution: 100 mg ml^{-1} in H$_2$O, sterile filtered
   Endconcentration: 100 µg ml^{-1}

2.12.2   Media for cultivation of eukaryotic cells

Cell type	Media
C33a	DMEM
N/TERT	KGM-Gold or RM+
PHK	KGM-Gold
PT67	DMEM
RTS3b	RM+

RM+ Medium (DMEM+DMEM/Nut Mix F12) Invitrogen, Karlsruhe, Germany
  DMEM 45% DMEM/Nut Mix F12 (1:1) Glutamax 45%,

FCS	10%
Penicillin	100 units ml^{-1}
Streptomycin	100 µg ml^{-1}
hydrocortisone	0.4 µg ml^{-1},
choleratoxin	10^{-10} M,
transferrin	5 µg ml^{-1},
triiodothyronine	2×10^{-11} M,
adenine	1.8×10^{-4} M,
insulin	5 µg ml^{-1},
epidermal growth factor	10 ng ml^{-1}

Dulbecco´s modified Eagle´s medium (DMEM) Invitrogen, Karlsruhe, Germany
  with Glutamax^{TM}, 4500 mg l^{-1} glucose without sodium pyruvate

FCS	10%	Invitrogen, Karlsruhe, Germany
Penicillin	100 units ml^{-1}	Invitrogen, Karlsruhe, Germany
Streptomycin	100 µg ml^{-1}	Invitrogen, Karlsruhe, Germany

Assay medium

XF Base Medium		Seahorse Biosciences, Copenhagen, Denmark

Freezing medium

DMSO	10%	Invitrogen, Karlsruhe, Germany
FCS	90%	Invitrogen, Karlsruhe, Germany

Transport medium

DMEM		Invitrogen, Karlsruhe, Germany
FCS	10%	Invitrogen, Karlsruhe, Germany
Penicillin	600 U ml^{-1}	Invitrogen, Karlsruhe, Germany
Streptomycin	600 µg ml^{-1}	Invitrogen, Karlsruhe, Germany
Gentamycin	250 µg ml^{-1}	Invitrogen, Karlsruhe, Germany
Fungizone	2.5 µg ml^{-1}	Invitrogen, Karlsruhe, Germany

KGM-GOLD Bullet Kit	Lonza, Basel, Switzerland
Trypsin 0.05%	Invitrogen, Karlsruhe, Germany
Trypsin/EDTA	Lonza, Basel, Switzerland
Trypsin Neutralisation Solution TNS	Lonza, Basel, Switzerland

2.12.3 Antibiotics for cell culture

G418-Sulfat Roth, Karlsruhe, Germany
An aminoglycoside antibiotic that blocks polypeptide synthesis by inhibiting the elongation step in both prokaryotic and eukaryotic cells. Resistance to G418 is conferred by the neomycin gene.

2.13 Mice

Line	Description	Reference
FVB/n wt	wildtype mice	Charles River, Sulzfeld, Germany
K14-HPV8-E7	FVB/n mice expressing the HPV8-E7 oncoprotein under the control of the human keratin-14 promoter.	present work

The generation of and the study with transgenic mice, as well as the UV irradiation protocols were approved by the governmental animal care office North-Rhine-Westphalia (protocol no. 87–51.04.2010.A203) and were in accordance with the German Animal Welfare Act as well as the German Regulation for the protection of animals used for experimental purposes.

2.14 Miscellaneous

2.14.1 Patient material

Donated skin, composed of epidermis and dermis, for the preparation of organotypic skin cultures was sourced from the European Skin Bank, Beverwijk, Netherlands.

2.14.2 Organotypic skin cultures

Organotypic skin cultures established with primary keratinocytes expressing E7 of HPV1, HPV5, HPV8, HPV20 or HPV38 (Westphal *et al.* 2009), as well as cultures expressing HPV8-E2, E6 or E7 (Akgül *et al.* 2005, Leverrier *et al.* 2007, Akgül *et al.* 2011b) were kindly provided by Dr B. Akgül (Institute of Virology, University Hospital Cologne)

2.14.3 EV skin lesions

Nine different EV lesions with betaHPV typing and pathology results were kindly provided by Prof S. Majewski (Department of Dermatology, University of Warsaw, Poland). The study was approved by the local ethics committee at the Medical University of Warsaw.

Patient	BetaHPV type	pathology
EV-Pa1	HPV5,8,20,23,36,50	SCC
	HPV5,8,20,23,36,50	cytopathic effect
EV-Pa2	HPV5,36	SCC
	HPV5,36	SCC / Bowen's disease
EV-Pa3	HPV5,8,9,24	Bowen's disease
EV-Pa4	HPV5,8,20,23,36,50	cytopathic effect
	HPV5,8,20,23,36,50	Bowen's disease
	HPV5,8,20,23,36,50	Bowen's disease / SCC
	HPV5,8,20,23,36,50	SCC

3. Methods

3.1 Experimental work in mice

3.1.1 Generation of K14-HPV8-E7 transgenic mice

The HPV8-E7 gene was amplified by PCR and inserted into the *Bam*HI site of the K14CreERtam plasmid under the control of the human keratin-14 promoter (Vasioukhin *et al.* 1999). The *Bam*HI site is located between the sequence of the second intron of the rabbit β-globin gene and the K14 polyadenylation sequence. The recombinant vectors K14-HPV8-E7 were digested with *Hind*III and *Sac*I flanking the K14 expression cassette. The appropriate fragment was purified via agarose gel electrophoresis and membrane filtration. The linearized transgene was microinjected into the pro-nucleus of fertilised FVB/n oocytes, which were implanted into pseudopregnant surrogate mothers according to the protocol described by Hammes and Schedl (2000) to produce putative founder mice expressing the HPV8-E7 transgene (Hammes 2000). Genomic DNA was isolated from tail biopsies of 3 week-old mice with the "QIAamp DNA Mini Kit" (Qiagen) and "Proteinase K" (Qiagen) according to the manufacturer´s protocol to test for the presence of the transgene by PCR. To verify the presence of the HPV8-E7 transgene in any offspring tail biopsies were used to isolate genomic DNA used for PCR. The generation of the K14-HPV8-E7 founder mouse was performed by the animal facility of the Centrum for Molecular Medicine Cologne (CMMC).

3.1.2 UV-irradiation of mouse skin

Before any treatment, mice were anesthetized with Ketamine-hydrochloride (Sigma-Aldrich) and Xylazine-hydrochloride (Sigma-Aldrich) and shaved with an electric shaver (Wella). Skin UV radiation was performed by a UV device (UV801, Waldmann). Dorsal caudal UV-irradiation was performed at an age of 5 - 25 weeks. Mice were either irradiated once or repeatedly with 10 J/cm^2 UVA and 1 J/cm^2 UVB on a 4 cm^2 sized area, while the rest was covered with a UV-impermeable sheet (Marcuzzi *et al.* 2009). Skin samples were taken 3, 5 or 7 weeks after the last UV irradiation. Mouse skin samples were taken by punch biopsies (4 mm diameter, Pfm medical Ag, Cologne, Germany) or by scissors. For RNA analysis samples were stored at -20°C in RNALater (Qiagen) according to the manufacturer's protocol. For IHC experiments mouse skin

samples were formalin-fixed and embedded in paraffin. Samples were cut in 3 - 4 µm sections at the Institute of Experimental Medicine of the University Hospital of Cologne.

3.1.3 Long-term observation

For long-term observation, groups of 2 - 4 animals of FVB/n and K14-HPV8-E7[he] were kept in individually ventilated cages over an observation period of up to 28 weeks. Mice were inspected every 3 days to monitor the development of skin tumours. All skin alterations were examined histologically on HE stained paraffin sections for detailed diagnosis. The formation of skin alterations was monitored over time and the percentages of animals bearing skin changes were plotted as a Kaplan-Meier graph (GraphPad Software Inc., San Diego, USA).

3.2   Bacterial culture

3.2.1 Transformation of competent bacteria

Plasmid DNA has been amplified in bacteria followed by purification. Therefore, DNA (ca. 100 ng) was added to either 50 µl of competent bacteria and incubated on ice for 30 min. Then the bacteria-DNA mixture was subjected to a heat step at 42°C for 45 s and shifted back on ice for 3 min. 100 µl SOC medium was added followed by an incubation for 1 h at 37°C under agitation. 50 µl bacteria were plated onto ampicillin (100 µg ml^{-1}) LB-agar plates and incubated over night at 37°C.

3.2.2 Cultivation of bacteria for plasmid isolation

All plasmids used in this project contained an ampicillin resistance gene, therefore transformed bacteria could be selected by the addition of 100 µg ml^{-1} ampicillin to the LB-medium and agar plates. For analytic plasmid isolation, 5 ml LB-ampicillin-medium in a 13 ml PE-tube (Sarstedt) was inoculated with one colony of the transformed bacteria picked from the LB-agar plates and incubated under rotation overnight at 37°C. For preparative plasmid isolation, 200 ml LB-medium in a 1 l Erlenmeyer flask were inoculated with 1 ml of a fresh overnight culture and kept at 37°C under agitation overnight. For storage, 1 ml of a bacterial culture was mixed with 500 µl glycerol and stored at -80°C.

3.3   Cell culture

All cell lines listed here were adherent cell lines, cultivated at 37°C, 6% CO_2 and 80 - 90% humidity with DMEM, RM+ or KGM-Gold medium. All operations with these cell lines were done under a laminar flow.

3.3.1 Cultivation of cell lines

Cells were passaged when they reached a density of 60 - 90%. After a washing step with PBS, 3 ml Trypsin/EDTA was added for 3 to 6 min at 37°C. As soon as the cells detached from the bottom of the flask they were resuspended in 7 ml fresh medium or 3 ml neutralisation solution and seeded at the desired density in a new tissue culture flask. When needed, N/TERTs and PHKs were also cultured on coated cell-culture flasks (either coated with fibronectin, collagen IV or laminin, BD Biosciences) for 4 days. Cell culture supernatants and cells extracts were generated and stored at -80°C for further experiments.

3.3.2 Freezing of cell lines

For long term storage cells were grown in 150 cm^2 tissue culture flask until they reached a density of about 60 - 90%. Then the cells were washed with PBS and detached with 3 ml Trypsin/EDTA and mixed with 9 ml of the appropriate cell culture medium or 3 ml of neutralisation medium. After centrifugation at 300 x g for 5 min the pellet was resuspended in freezing medium, aliquoted into 1.5 ml in freezing vials and stored at -80°C. To adjust constant cell numbers per aliquot cells were counted by using the TC 10 automated cell counter (BioRad) and the corresponding counting slides (BioRad).

3.3.3 Transfection of cells

(a) Calciumphosphate transfection

The day before transfection cells were counted and seeded at a density of 1.5 x 10^5 cells / 6 well, 1 x 10^6 cells / 6 cm Ø-dish and 1.5 x 10^6 cells / 10 cm Ø-dish, respectively and incubated overnight at 37°C. The following day, the cells were washed with PBS and fresh medium was added 1 - 2 h prior transfection. For 1 ml of cell culture medium, 100 µL transfection solution was used containing the DNA in 2x HBS buffer, 5% 2 M $CaCl_2$. After adding 50 µl 2 M $CaCl_2$, the mixture was vortexed immediately for 15 s and incubated at room temperature (rt) for 15 min, to allow formation of a precipitate.

The mixture was added drop wise to the cell culture medium, carefully agitated and the cells were incubated at 37°C. At the next day, the cells were washed with PBS to remove the precipitate and new medium was added. Cells were harvested 24 - 48h later.

(b) Transfast

For the transfection of PHK, cells were seeded to a density of 30%. The appropriate amount of DNA (2 µg for 6 wells) was added to 1 ml of serum-free medium. Two microliters of the Transfast reagent (Promega) was added and the mixture was incubated for 15 min at rt. The medium was removed from the cells and the DNA-medium-Transfast mixture was added to the cells. Cells were incubated at 37°C overnight. 24 h post-transfection the medium was changed, 48 h after transfection cells were used for further experiments.

(c) Transfection of PT67 cells with FuGene

For the transfection of PT67 cells 770 µl medium without additives was mixed with 30 µl FuGene reagent (Promega) in a 1.5 ml tube and incubated for 5 min at rt. Then the mixture was added to a second 1.5 ml tube containing 10 µg DNA and further incubated for 15 min at rt. Then, FuGene-DNA mixture was added to the cells and incubated overnight at 37°C.

(d) Lipofectamine RNAimax

SiRNA transfections were performed with "Lipofectamine RNAimax" (Invitrogen). For this purpose, 8×10^4 cells were seeded in a 6 well and incubated overnight at 37°C. The following day cells were washed once with PBS and fresh medium without antibiotics was added. 5 to 30 picomole siRNA were added to 250 µl medium without additives and 2 µl "Lipofectamine RNAimax" were added to another 250 µl medium without additives. After vortexing both tubes, the diluted "Lipofectamine RNAimax" was added to the diluted siRNA and incubated for 20 min at rt. The siRNA-Lipofectamine RNAimax complexes were then added to the cells.

3.3.4 Production of recombinant retrovirus supernatants

For the production of recombinant retroviruses, the Retro X-System (Clontech, Palo Alto, USA) was used. At first retroviral vectors were transfected into PT67 cells, which are able to produce infectious but replication-deficient retroviruses. Those retroviruses are able to infect different types of primary mammal cells to introduce an external gene into the mammalian genome. After integration of this external gene into the host

genome a stable expression is ensured. After transfection of PT67 cells, a selection with G418 (500 ng ml^{-1}) in pLXSN-based vectors in 75 cm^2 culture flasks was performed for 14 days and the remaining positive clones were used for expansion. For retroviral supernatants, cells were grown in 150 cm^2 cell culture flasks at a density of 80%, the medium was changed and 16 ml fresh DMEM medium was added. These cells were cultured at 32°C and 10% CO_2 for 24h or 48h and supernatants were aliquoted and stored at -80°C.

3.3.5 Creation of the stable-transfected PHK-pLXSN, PHK-pLXSN-8E7, PHK-pLXSN-8E7-L23A, N/TERT-pLXSN, N/TERT-pLXSN-8E7 and N/TERT-pLXSN-8E7-L23A

One day before transduction 2 x 10^5 PHK and N/TERT cells were seeded in a cell culture dish (6 cm). The next day cells were incubated with 2 ml DMEM without additives but with 5 µg ml^{-1} polybrene (Sigma) for 10 min at 37°C. Four ml retroviral supernatant pLXSN, pLXSN-8E7 and pLXSN-8E7-L23A with 5 µg ml^{-1} polybrene (Sigma) was added to the cell culture dish. The cells were centrifuged at 300 x g for 1 h at rt, washed twice with PBS and finally incubated with 4 ml normal cultivation media for 48h at 37°C. Since pLXSN encodes the neomycin resistance gene, selection of transduced cells was performed by adding G418 (Roth) to the media in a final concentration of 500 µg ml^{-1}. As selection control, PHK and N/TERT cells without transduction were also incubated with media containing G418 (Roth) in a final concentration of 500 µg ml^{-1}. After 48h cells reached a confluence of about 80% and were splitted in a 75 cm^2 tissue flask. Usually after one week, selection media was exchanged to normal culture media when all control cells were killed. Transcription of stably transduced DNA was verified by qRT-PCR.

3.3.6 Isolation of PHK from human foreskin

Mitomycine treatment of 3T3 fibroblasts: 3T3 fibroblasts were adjusted to a cell density of 1 x 10^6 cells per millilitre and 4 µg ml^{-1} mitomycine (Sigma) was added. Cells were transferred to a falcon tube and incubated in a rotor for 2h at rt. Afterwards cells were centrifuged at 300 x g for 5 min and were either used directly or were frozen with a cell density of 2 x 10^6 cells in freezing medium.

Isolation of keratinocytes: Foreskins arriving in transport media were washed two times with PBS and transferred into a 10 cm cell culture flask. The skin was minced with the aid of scalpels, resuspended in 4 ml of 0.25% trypsin and transferred into a

falcon. The minced skin was incubated at 37°C for 2 h. The trypsin was neutralised by DMEM/FCS media every 30 min and replaced by fresh 4 ml 0.25 % trypsin. The DMEM/trypsin/cell mixture was filtrated using a 70 µm Nylon filter (BD Biosciences) and centrifuged at 300 x g for 5 min. The cell pellet was resuspended in RM+ media and seeded with a density of 2 x 10^6 cells per 150 cm^2 cell culture flask together with 2 x 10^6 mitomycine treated 3T3 fibroblasts. First keratinocyte 'islands' can be seen after 5 - 7 days. The keratinocytes were cultivated until they reach a density of 70%. Then, residual fibroblasts were removed due to trypsin treatment for 2 min. Keratinocytes could be detached from the flask in a second and longer trypsin treatment round. The isolated PHK were separated into aliquots containing 5 x 10^5 cells in CryoSFM (PromoCell) freezing medium. When cells were thawed, culturing was performed in KGM-Gold media.

3.3.7 Organotypic skin cultures

Human donor skin, stored in glycerol, composed of epidermis and dermis was washed two times in PBS and incubated in PBS containing 600 U ml^{-1} Penicillin, 600 µg ml^{-1} Streptomycin, 250 µg ml^{-1} Gentamycin, 2.5 µg ml^{-1} Fungizone for 10 days at 37°C (Todd *et al.* 1993). After incubation, the epidermis was removed and the dermis washed twice in PBS. Then the dermis was cut in 1.5 x 1.5 cm squares, put into a 6 well upside down (up: *stratum reticulare*) and a ring of stainless steel (Ø 1.2 cm) was placed in the middle of the dermis. Human primary fibroblasts were harvested, counted and 5 x 10^5 cells were resuspended in 1 ml keratinocyte media. One millilitre of this solution was added per stainless steel ring and keratinocytes media was additionally added into the 6 well. This set-up was incubated overnight at 37°C with 10% CO_2. On the next day, media and steel ring were removed. The dermis was turned and the ring was placed on the upper site of the dermis. Keratinocytes cultured in KGM-Gold media were harvested, counted and a cell suspension containing 4 x 10^5 cells ml^{-1} was prepared. One millilitre of cell suspension was added to the steel ring, the 6 well was filled with keratinocyte media and this set-up was incubated at 37°C and 10% CO_2 for one day. After the incubation period the steel ring was removed and the dermis was placed on a metal grid. The 6 well was filled with keratinocyte media until the bottom of the dermis was wetted. Every 2 days the medium was changed. Cultures were fixed in 4% formalin at day 14 and embedded in paraffin. The sections were stained with HE for histological examinations.

3.3.8 Transient replication assay

This method is modified from the experimental procedure performed by Ustav and Stenlund (1991). RTS3b cells were transfected with 12 µg of pVE34 and pVE34L23A vector. 72 h post-transfection cells were harvested by removing the cell media and washing the cells twice with PBS. Cells were removed with cell scraper, resuspended in 2 ml PBS and centrifuged at 3000 x g. For extraction of episomal DNA the cell pellet was resuspended in 200 µl 'resuspension buffer' (50 mM glucose, 25 mM Tris, 10 mM EDTA, pH 8.6) and lysed in 400 µl freshly prepared 'lysis buffer I' (0.2 M NaOH, 1% SDS) for 3 min at rt. 300 µl 'neutralisation buffer' (3 M KAc, pH 4.8) was added to the cell lysate and incubated on ice for 10 min. To remove cell fragments, the raw extract was centrifuged at 20,000 x g for 5 min. The supernatant was mixed in a new reaction tube with 540 µl isopropyl alcohol and again centrifuged at 20,000 x g for 15 min. For the removal of protein residues, the pellet was resuspended in 200 µl 'lysis buffer II' (100 mM NaCl; 10 mM EDTA; 0,2% SDS; 200 µg ml^{-1} Proteinase K) and incubated at 37°C for 1 h. After that a phenol extraction and ethanol precipitation was performed. The DNA pellet was resuspended in 20 µl RNaseA solution (0.0625 mg ml^{-1}) and 10 µl of this solution were used for a restriction digest with the restriction endonuclease DpnI. This enzyme cuts DNA, which is methylated at the adenosine of the 5'-GATC-3' motif. The transfected DNA originates and was isolated from $dam+$-bacteria and is therefore methylated at this 5'-GATC-3' motif. Therefore, after DpnI digestion only newly replicated, non-methylated DNA remained.

3.3.9 Seahorse XF MitoStress Test

Measurement of intact cellular respiration was performed using the Seahorse XF96 analyser (Seahorse Bioscience). N/TERT-8E7 and control cells (grown in RM+) were seeded into a Seahorse XF96 cell culture microplate at a cell density of 25,000 cells per 96-well 16h prior measurement. Directly prior to the respiration assay, cells were rinsed and cultured in assay medium supplemented with 5 mM glucose, 10 mM sodium pyruvate (Sigma-Aldrich) and 2 mM glutamate according to the manufacturer's protocol. Cells were incubated at 37°C in a CO_2-free incubator for 1h prior to measurement. Oxygen consumption rate (OCR), extracellular consumption rate (ECAR) and proton production rate were measured under basal conditions and in the presence of oligomycin, a complex V inhibitor (1 µg ml^{-1}), the complex III inhibitor antimycin A (0.5 µM), the complex I inhibitor rotenone (0.5 µM) and the mitochondrial

uncoupler carbonyl-cyanide-p-trifluoromethoxyphenylhydrazone (FCCP) (1.5 μM, Sigma-Aldrich) to assess maximal oxidative capacity. After respiration assay, media was aspirated, wells were washed once with PBS and total protein concentration was determined by using the DC^{TM} Protein Assay Kit II (BioRad). N/TERT-8E7 and control cells were measured in triplicate, normalised to total protein content and parameters were assessed subsequent to the subtraction of non-mitochondrial respiration from each value by the aid of the Seahorse Report Generator. The spare respiratory capacity is defined as the difference between maximal and basal respiration.

3.3.10   Transient reporter gene assays

For transient reporter gene assays, keratinocytes were transiently transfected in duplicate in 6 well dishes using the corresponding transfection reagent with 1 μg of luciferase reporter construct (TOP-flash, FOP-flash, pFN(1.2 kb)LUC, pFN(0.5 kb)LUC, pFN(0.2 kb)LUC, pFN(0.2 kb)LUC-SP1mut) and 0.25 to 1 μg of pLXSN or pLXSN-8E7 together with 0.25 μg reporter plasmid coding for renilla luciferase. The assays were performed using the Dual-Luciferase® Reporter Assay System (Promega) according to the manufacturer's protocol. Luciferase assays were measured 48 h post-transfection and normalised to renilla values. For TOP-flash/FOP-flash activation, transfected RTS3b cells were stimulated with Wnt3a (50 ng ml^{-1}, dissolved in PBS, R&D Systems) 6h prior harvesting. Luciferase activity was measured using the Glomax® Luminometer (Promega).

3.4 RNA methods

3.4.1 Total RNA Isolation

Total RNA isolation from cells or mouse skin was done by using the 'RNeasy Mini Kit' (Qiagen) combined with the 'QIAShredder' (Qiagen) system.

From cells: Cells were plated in 6 wells for RNA isolation. At the desired density and time point the medium was aspirated and cells were either pelleted and stored at -80°C until use or directly taken up in RLT buffer. For cell lysis, resuspended cells were pipetted directly into a QIAshredder. The following steps were performed according to the manufacturer's protocol. DNA digestion was performed on column using 'RNase-Free DNase Set' (Qiagen).

From mouse tissue: For RNA isolation from mouse skin, biopsy samples were stored in RNALater (Qiagen) and transferred into a tube containing a steel ball and RLT buffer

from the 'RNeasy Mini Kit' (Qiagen). Skin biopsies were homogenized in a swing mill (Mixer Mill 301, Retsch, Haan) at 30 Hz for 3 min. For full homogenization of the mouse skin, tubes were turned around and shaken for another 3 min at 30 Hz. When using "miRNeasy Mini Kit" (Qiagen) DNA digestion was performed on column using RNase-Free DNase Set (Qiagen). RNA was dissolved in 30 - 50 µl RNase-free H_2O.

RNA concentration and degree of purity was determined spectrophotometrically at a wavelength of 260 nm and 280 nm using a NanoDrop®ND-1000 UV/Vis spectral photometer (PEQLAB).

3.4.2 Reverse transcription of mRNAs

Total RNA was isolated as described in 3.5.1 and DNA was digested during isolation. One microgram of DNA-free RNA was reverse transcribed using "Omniscript RT Kit" (Qiagen) in a total volume of 20 µl with 10 µM random nonamers (TIB MOLBIOL), 1 µM oligo-dT$_{23}$-primer (Sigma-Aldrich) and 10 units RiboLock^{TM} RNase Inhibitor (Fermentas). The reaction was carried out at 37°C for 1h, afterwards reverse transcriptase was inactivated at 95°C for 10 min.

3.5 DNA methods

3.5.1 DNA standard methods

The methods mentioned below were performed according to the protocols from Sambrook (1989).

- DNA digestion by restriction nucleases
- Dephosphorylation of 5'-end DNA fragments by alkaline phosphatase
- Ligation of DNA by T4-Ligase
- Determination of DNA concentration via NanoDrop®
- Agarose gel electrophoresis

3.5.2 Plasmid preparation

Plasmid isolation for analytic and preparative was done using the 'Plasmid Maxi Kit' from Qiagen according to the manufacturer's protocol. This kit is based on the extraction method from Birnboim and Doly (1979) and the property of DNA to bind on anion exchange columns.

3.5.3 Isolation of DNA from agarose gels

Following electrophoretic separation, the desired DNA band was cut out from the agarose gel with a scalpel under long-wave UV (365 nm). DNA was isolated from agarose gel with "QIAEX II Gel Extraction Kit" (Qiagen) as described in the manufacturer's protocol.

3.5.4 Polymerase chain reaction (PCR)

Amplification of defined DNA fragments was done by the PCR described by Mullis and Faloona (1987). The reaction was performed using 50 - 100 ng DNA as template in a total volume of 20 µl containing 1 unit *Taq* DNA Polymerase and the associated buffer with $(NH_4)_2SO_4$ (Fermentas), 1 mM $MgCl_2$, 5% DMSO (Applichem) 0.5 µM forward and backward primer each and 0.2 mM deoxynucleotide triphosphates each (Fermentas).

PCR conditions			
	1x	94°C	3 min
	30x	94°C	30 s
		T_{ann}	30 s
		72°C	60 s
	1x	72°C	5 min
	1x	4°C	∞

3.5.5 Quantitative real-time polymerase chain reaction (qRT-PCR)

The mRNA levels were quantified via qRT-PCR using the LightCycler System (Roche Diagnostics, Mannheim, Germany). Five microliters of a 1:50 dilution of cDNA (prepared as described 3.4.2) were used in a total volume of 20 µl containing: 1.25 units Platinum *Taq* Polymerase, 4 mM MgCl2, 1.6 µl of a 1:1000 dilution of SybrGreen I (Sigma-Aldrich), 5% DMSO (Applichem), 0.5 µM each of forward and reverse primer, 500 ng $µl^{-1}$ non-acetylated bovine serum albumin (Fermentas) and 0.2 mM dNTPs each (Fermentas). Sample measurement was performed in duplicate together with a cDNA or plasmid dilution series. The fluorescence was detected once per cycle at the end of the elongation period.

PCR conditions			
	1x	95°C	1 min
	40x	95°C (20°C/s)	1 s
		T_{ann} (20°C/s)	5 s
		72°C (20°C/s)	5 s

Therefore, a melting curve protocol was carried out including 15 s at 95°C, 20 s at 70°C (20°C/s) and 1 s at 95°C (0.2°C/s). Fluorescence measurement was continuously done during heating to 95°C. At the end, the samples were cooled down to 40°C for 10 s. All mRNA levels were normalised to the mRNA levels of HPRT1 or GAPDH.

3.5.6 Site-directed mutagenesis

For the introduction of amino acid changes in a protein sequence, mutation was performed using the 'Quick Change® II XL Site-Directed Mutagenesis Kit' (Agilent Technologies). For the mutation of HPV8-E7wt into HPV8E7-L23A in pLXSN-8E7, pCMV2-FLAG-8E7 and pVE34-L23A the specific primers were used (see section 2.6.1). The protein-encoding plasmids and the corresponding complementary oligonucleotides were used in a PCR reaction containing 25 - 50 ng µl^{-1}plasmid DNA, forward and reverse primer (125 ng µl^{-1}), 10 mM dNTPs, QuikSolution and 2.5 U µl^{-1} *PfuUltra* HF DNA-Polymerase. A PCR was performed with the following conditions:

1x	95°C	1 min
⌈	95°C	50 s
18x ⟨	60°C	50 s
⌊	68°C	1 min/kb
Final step	68°C	7 min

PCR conditions were adapted to the size of the plasmid. To destroy the non-mutated plasmid DNA, the sample of the PCR reaction was then incubated with 1 µl *Dpn*I at 37°C for 30 min. 5 µl of this mixture were transformed with 50 µl competent *E.coli* XL1-bacteria. The new constructs were verified by sequencing analysis.

3.5.7 DNA Sequencing

The method used for DNA sequencing was based on the principle of the chain-termination-sequencing from Sanger and colleagues (1977). For DNA sequencing 3 to 10 pmol of the primer, 200 - 500 ng plasmid DNA and 2 µl BigDye were mixed in a total volume of 5 µl and a PCR with the following conditions was performed.

PCR conditions			
	1x	94°C	10 s
	⌈	94°C	10 s
	30x ⟨	60°C	10 s
	⌊	60°C	3 min
	1x	4°C	∞

The analysis of the sequence was done with the DNA Sequencer ABI 3130XL (Applied Biosystems, Genetic Analyzer, Darmstadt, Germany) and the evaluation was done using SeqMan Pro® Lasergene (DNAstar).

3.6   Protein methods

3.6.1 Protein Isolation

Cells were pelleted and stored at -80 °C until use. The thawed cell pellet was resuspended in either 100 - 400 µl RIPA buffer or 100 - 400 µl LSDB containing 1 mM PMSF, 1 mM OV, 50 mM NaF, 1 mM DTT and 1x cOmplete^{TM} protease inhibitor cocktail (Roche) and incubated on ice for 30 min. Then the cells were sonificated and centrifuged at 15,000 x g, at 4°C for 15 min. Supernatants were pipetted in new tubes and were ready for use. Protein concentrations were determined via PierceTM BCA Protein Assay Kit (ThermoFisher) according to the manufacturer's protocol.

3.6.2 Western Blot Analysis

For Western blot analysis protein extracts were separated with SDS-PAGE. The SDS-gel was transferred to a nitrocellulose membrane (Protan BA85 Nitrocellulose), which was set between two Whatman paper and flanked by two sponges. The set-up was blotted at a voltage of 30 V overnight. To prevent unspecific binding of antibodies, the membrane was incubated with 25 mL of blocking solution for 1h. Then, the membrane was carefully overlaid with 4 mL containing the diluted 1st antibody in 5% dry milk in TBST for 2h at rt or overnight at 4°C. After three washing steps (5 min each) with TBST the membrane was incubated with 4 ml containing the 2nd antibody in the appropriate dilution for 1h at rt. After 3 x 5 min washing with TBST, the membrane was overlaid with 1 ml of BM Chemiluminescence blotting substrate for 2 min. The solution was carefully removed and the chemiluminescence signals were either detected upon exposure to an ECL-hyperfeature (Amersham, Freiburg, Germany) or with the GelDoc system from BioRad (Hercules, USA). Protein bands were quantified using ImageJ.

3.6.3 Co-Immunoprecipitation (Co-IP)

For each sample 10 µl of α-FLAG M2 affinity resin (Sigma) was equilibrated with 0.1 M LSDB buffer (1 mM DTT, 1 mM PMSF) and centrifuged at 7000 rpm for 2 min at 4°C. The beads were resuspended in 85 µl 0.1 M LSDB (1 mM DTT, 1 mM PMSF) and transferred into a new tube. 300 to 500 µg of whole protein lysate containing FLAG-fusion proteins were added to the beads and filled up to a volume of 1 ml with LSDB (1 mM DTT, 1 mM PMSF). The mixture was incubated for 3h at 4°C in a rotor and afterwards centrifuged at 7000 x g for 5 min at 4°C. The supernatant was removed and the sample was washed five times with 1 ml of 0.1 M LSDB (1 mM DTT, 1 mM PMSF).

After the last washing step, the beads were resuspended in 30 µl of 0.1 M LSDB buffer, 10 µl of 4x SDS loading puffer was added and the sample was incubated at 95°C for 5 min. After centrifugation at 7000 x g for 5 min, the supernatant was transferred and separated onto a SDS-PAGE.

3.6.4 Immunocytochemistry (ICC)

Cells were seeded onto glass slides and incubated overnight, reaching a cell density of 30%. Then, the cells were washed two times with PBS and fixed with 4% Paraformaldehyde for 10 min. Afterwards the cells were washed with PBS. Permeabilisation of cells was performed with 0.1% Triton-X100 (diluted in PBS) and afterwards washed with PBS. Cells were blocked with 10% FCS in PBS for 30 min and incubated overnight with the first antibody diluted in PBS at 4°C. Again cells were washed with PBS and the second antibody was applied, diluted in PBS for 1h at rt. After washing, cells were counterstained with DAPI and embedded with Immunomount (ThermoScientific) on a slide. In case of mitochondrial staining, cells were incubated with a final concentration of 10 mM MitoTracker (ThermoFisher) in serum-free media for 30 min at 37°C prior fixation.

3.6.5 Immunohistochemistry (IHC)

Deparaffinization of 4 µm thick tissue sections was done by incubation in Xylol two times for 5 min. Samples were hydrated through a descending alcohol series (100%, 90%, 70%; 5 min each) and endogenous peroxidases were inactivated by incubation in 3% H_2O_2 in Methanol for 20 min. Antigen unmasking was performed by either a) by boiling the tissue sections in citrate buffer in a pressure cooker for 4 min in a microwave b) by boiling in Tris/EDTA puffer in a pressure cooker for 4 min in a microwave c) with protease treatment (5 mg/ml) for 10 min at 37°C or with d) trypsin treatment (0.05%) for 10 min at 37°C. Further incubation steps were performed in a humid chamber to prevent dehydration. VECTASTAIN Elite ABC Kit: Blocking of unspecific antigen sites was done with 50% horse serum or 50% rabbit serum in PBS for 60 min. Incubation of primary antibody (see section 2.9.2) was done in 2% horse or rabbit serum overnight at 4°C, followed by three washes with PBS. Detection of primary antibody was done with the "VECTASTAIN Elite ABC Kit (Universal) or (Goat IgG)" (Vector Laboratories, Burlingame, USA), which was used as described in the manufacturer's protocol. Either DAB staining with the "Liquid DAB Concentrated Substrate Pack" (BioGenex, San

Ramon, USA) or AEC staining using the 'AEC-2-Components kit' (DCS, Hamburg, Germany) was performed. Sections were counterstained with haematoxylin and dehydrated with an ascending alcohol series (70%, 90%, 100%; 3 min each). After a final incubation in Xylol for 5 min, sections were embedded with mounting medium "DePeX" (Serva Electrophoresis, Heidelberg).

3.6.6 Immunofluorescence staining

Deparaffinization of 4 µm thick tissue sections and antigen unmasking was performed as described in section 3.6.5. The tissue was blocked with 20% FCS in PBS for 30 min. The primary antibody was incubated in 2% FCS in PBS overnight. After PBS washing, the secondary antibody was applied for 1 h at rt. Tissue was counterstained with DAPI after washing and embedded with Immunomount (ThermoScientific).

3.7   Statistical analysis

All experiments were repeated at least three times. qRT-PCR data were expressed as mean±SD. Immunoblots and images of immunohistochemical analysis are from a representative experiment, which was qualitatively similar in the replicate experiments. Statistical significance was determined with an unpaired 2-tailed Student's t-test. The asterisks shown in the figures indicate significant differences between experimental groups (*$p<0.05$, **$p<0.01$, ***$p<0.001$, see figure legends).

4. Results

4.1 Oncogenic potential of HPV8-E7 in the skin of transgenic mice

4.1.1 Tumour development in K14-HPV8-E7 transgenic mice

To characterise the tumorigenic potential of HPV8-E7 *in vivo*, a transgenic mouse line was generated expressing the viral gene under the control of the human keratin-14 promoter, which allows its expression in all proliferation competent keratinocytes. The HPV8-E7 (8E7) ORF was introduced into the K14-CreERtam plasmid (Vasioukhin *et al.* 1999) and the recombinant expression cassette (figure 8 A) was microinjected into the pronucleus of fertilized mouse oocytes of the FVB/n background. These oocytes were implanted into pseudopregnant surrogate mothers to produce putative founder mice. Transgene-positive offspring was identified by PCR, resulting originally in two 8E7 positive founder mice (M41 and M46) (figure 8 A). However, only the M46 survived and was used to establish the K14-HPV8-E7 hemizygous (he) and later the homozygous (ho) mouse line. The 8E7 mRNA expression in both lines was determined by qRT-PCR in untreated back skin. To investigate whether 8E7 expression leads to spontaneous tumour development, a group of K14-HPV8-E7 mice of different litters was observed within an observation period of 28 months (figure 8 B). In this group, 6 of 14 (43%) mice developed spontaneous tumours, forming an eversion of the skin, mostly located between the head and front legs or in the neck. Previous work from our department demonstrated that UVB irradiation activates the K14 promoter thereby increasing HPV8 oncogene expression in the skin (Hufbauer *et al.* 2010a). As no papillomatosis was observed after a single UVA/B treatment, but historically did so in our K14-HPV8-CER, -E6 and -E2 mice (Schaper *et al.* 2005, Pfefferle *et al.* 2008, Marcuzzi *et al.* 2009), we changed the irradiation protocol and treated the K14-HPV8-E7 mice chronically with 6 doses of UVA/B separated by 3 weeks each. The treated skin was taken 3 weeks after the last exposure and expression levels were determined by qRT-PCR (figure 8 C).
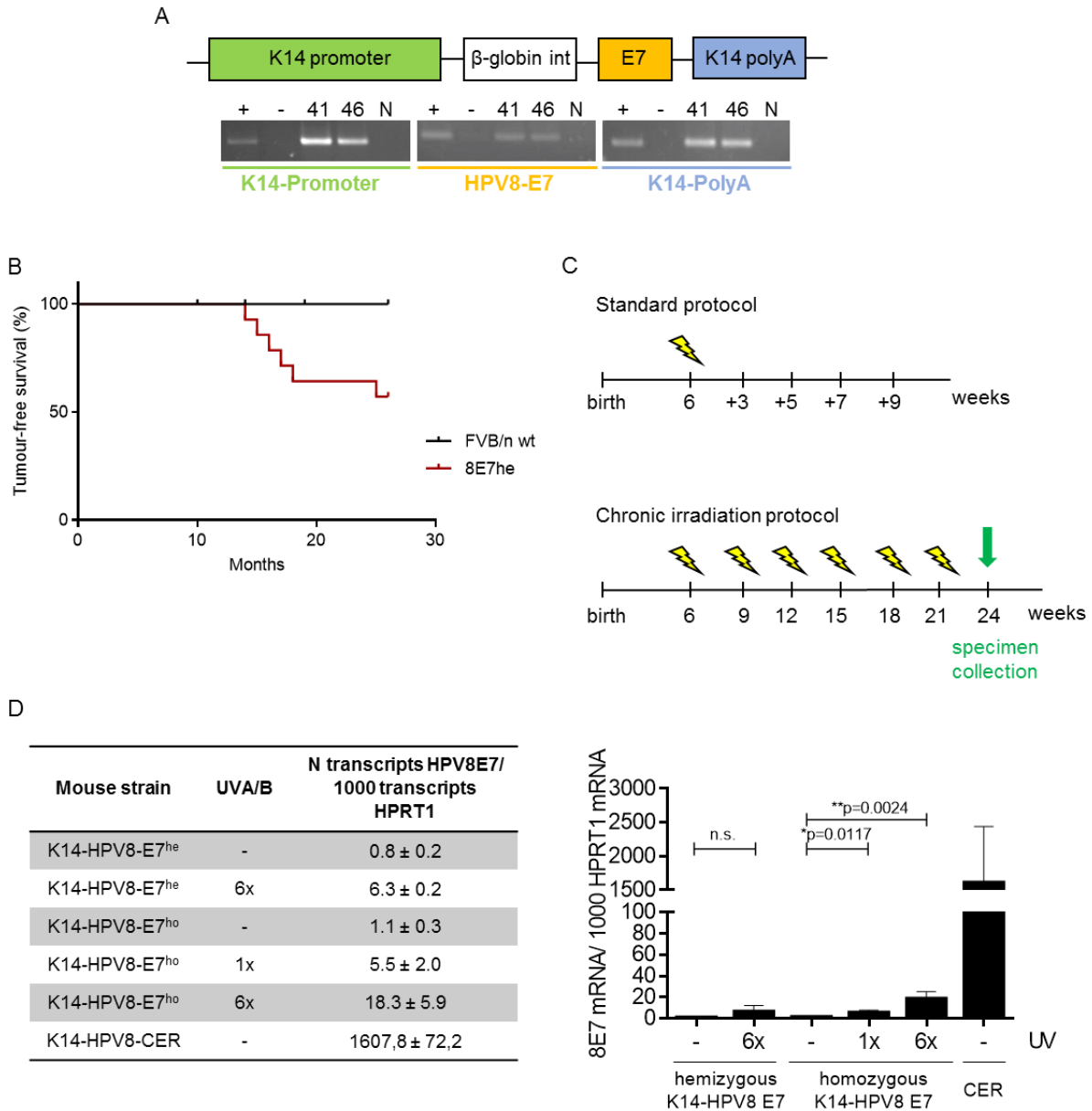
Figure 8. Different 8E7 expression levels in K14-HPV8-E7 transgenic mice. (A) Schematic representation of the K14-HPV8-E7 construct. The 8E7 ORF was inserted into the *Bam*HI restriction site of the K14CreERtam plasmid located between the sequence of the second intron of the rabbit β-globin gene and the K14-polyadenylation site. The recombinant plasmid K14-HPV8-E7 was digested with *Sac*I and *Hin*dIII and the transgene-containing fragment was used to generate transgenic founder mice. K14-HPV8-E7 founder mice (M41 and M46) were analysed for the presence of the transgene DNA by testing for the K14-Promoter, 8E7 and K14-polyA sequences. (+) positive control, (-) negative control, (41, 46) transgene positive mice, (-M) transgene negative mouse. (B) A group of 14 K14-HPV8-E7[he] mice of different litter were observed over a period of 28 months. The spontaneous tumour development is represented as a Kaplan-Meier curve, in which tumour-free survival was determined. 100% of FVB/n wt represents no tumour development. 40% of K14-HPV8-E7[he] mice developed spontaneous tumours after 18 ± 3.6 months. (C) Mice were irradiated either once at an age of 6 weeks and samples were taken after 3, 5, 7 and 9 weeks. Or mice were treated chronically, 6 doses of UV irradiation separated by 3 weeks, starting at an age of 6 weeks. Samples were taken 3 weeks after the last treatment. (D) qRT-PCR determined 8E7 transcripts per 1000 transcripts of HPRT1 in K14-HPV8-E7[he] and K14-HPV8-E7[ho] transgenic mice comparing untreated and UVA/B treated skin, as well as transcript levels in untreated hemizygous K14-HPV8-CER transgenic mice.

The skin of untreated hemizygous mice (K14-HPV8-E7^{he}) showed 0.8 transcripts of 8E7/1000 transcripts of HPRT1 and chronic treatment led to an 8-fold increase in 8E7 expression levels (6.3 transcripts 8E7/1000 HPRT1 transcripts) (figure 8 D). Homozygous mice (K14-HPV8-E7^{ho}) treated only once with UVA/B showed 5-fold increased 8E7 expression (5.5 transcripts 8E7/1000 transcripts HPRT1) as compared to untreated animals (1.1 transcripts 8E7/1000 transcripts HPRT1, figure 8 D). For chronically irradiated animals the number of transcripts was increased to 18.3/1000 transcripts of HPRT1, however, this value was about 90 times less compared to the 8E7 expression levels in untreated skin of K14-HPV8-CER transgenic mice.
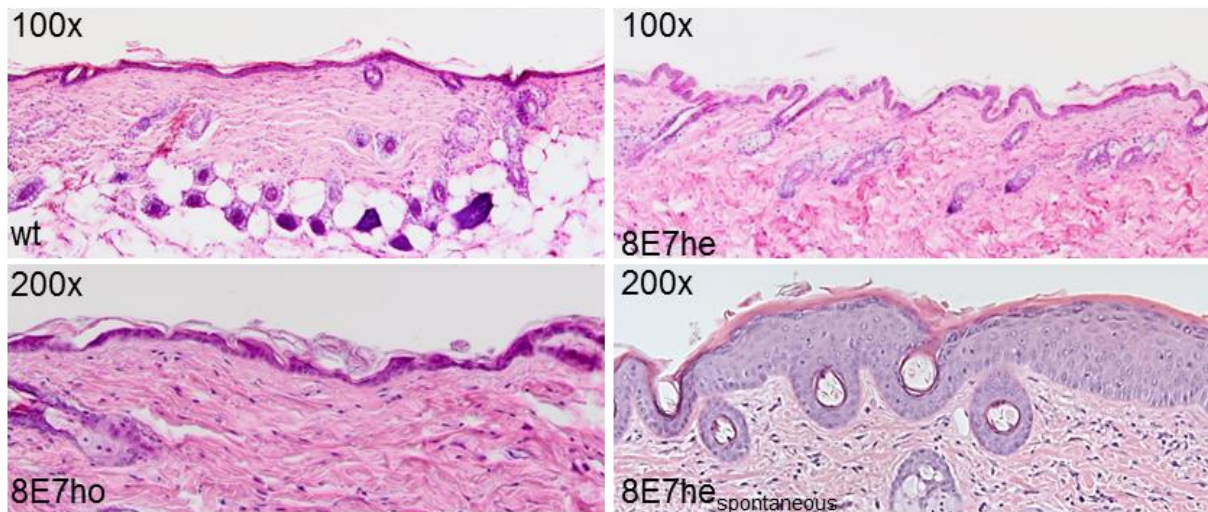
Figure 9. Untreated skin of FVB/n wt, K14-HPV8-E7^{he}, K14-HPV8-E7^{ho} and spontaneous tumour of K14-HPV8-E7^{he} transgenic mice. Skin samples were taken at an age of 9 weeks. The untreated skin of K14-HPV8-E7^{he} and K14-HPV8-E7^{ho} transgenic mice did not show any significant differences compared to skin of FVB/n wt mice. Representative spontaneous tumour of K14-HPV8-E7^{he} mouse taken at an age of 20 months (magnification 100x, 200x).

4.1.2 HPV8-E7 induces keratinocyte invasion in transgenic skin

The skin of untreated K14-HPV8-E7^{he} (n=5) and K14-HPV8-E7^{ho} (n=5) mice does not show any prominent differences compared to the skin of FVB/n wt mice (5/5) (figure 9). Spontaneous tumours of K14-HPV8-E7^{he} show mild skin hyperplasia at an age of 18 ± 3.6 months (figure 9). A single UVA/B irradiation cycle of K14-HPV8-E7^{he} (n=4) and K14-HPV8-E7^{ho} (n=4) skin led to the development of skin hyperplasia within the interfollicular epidermis after 3 weeks. Additionally, epidermal cysts, which originate from the root sheets of the hair follicles were formed. However, these alterations weakened back and regressed 5 - 7 weeks after treatment (figure 10). Chronically treated FVB/n wt mouse skin (5/5) healed from UV-induced hyperplasia three weeks after the last treatment. In chronically UV treated K14-HPV8-E7^{he} mice (8/10) mild

hyperplasia developed, which was clearly demarcated from the underlying dermis without any signs of malignancy. The skin of chronically irradiated K14-HPV8-E7[ho] developed flat or polypus skin tumours (15/20), which showed strong hyperplasia and intra-epidermal atypical keratinocytes (figure 12). Downward migrating cells showed nuclear hyperchromatism and pleomorphism with dyskeratosis (5/15). Those cells were stained positive with a pan-cytokeratin antibody (recognising an internal region of keratin-10) and confirmed that disordered squamous cells originated from the overlying epidermal sheets (figure 12). Furthermore, areas with a carcinoma *in situ* showed irregular sheets or islands of atypical squamous cells that invade the subjacent dermis (figure 12). In these areas the basement membrane was locally disrupted or completely absent as evidenced by collagen IV staining shown in figure 13. Taken together, these data demonstrated that although transgene expression was found to be relatively low, we could determine an oncogenic potential of 8E7 *in vivo*.
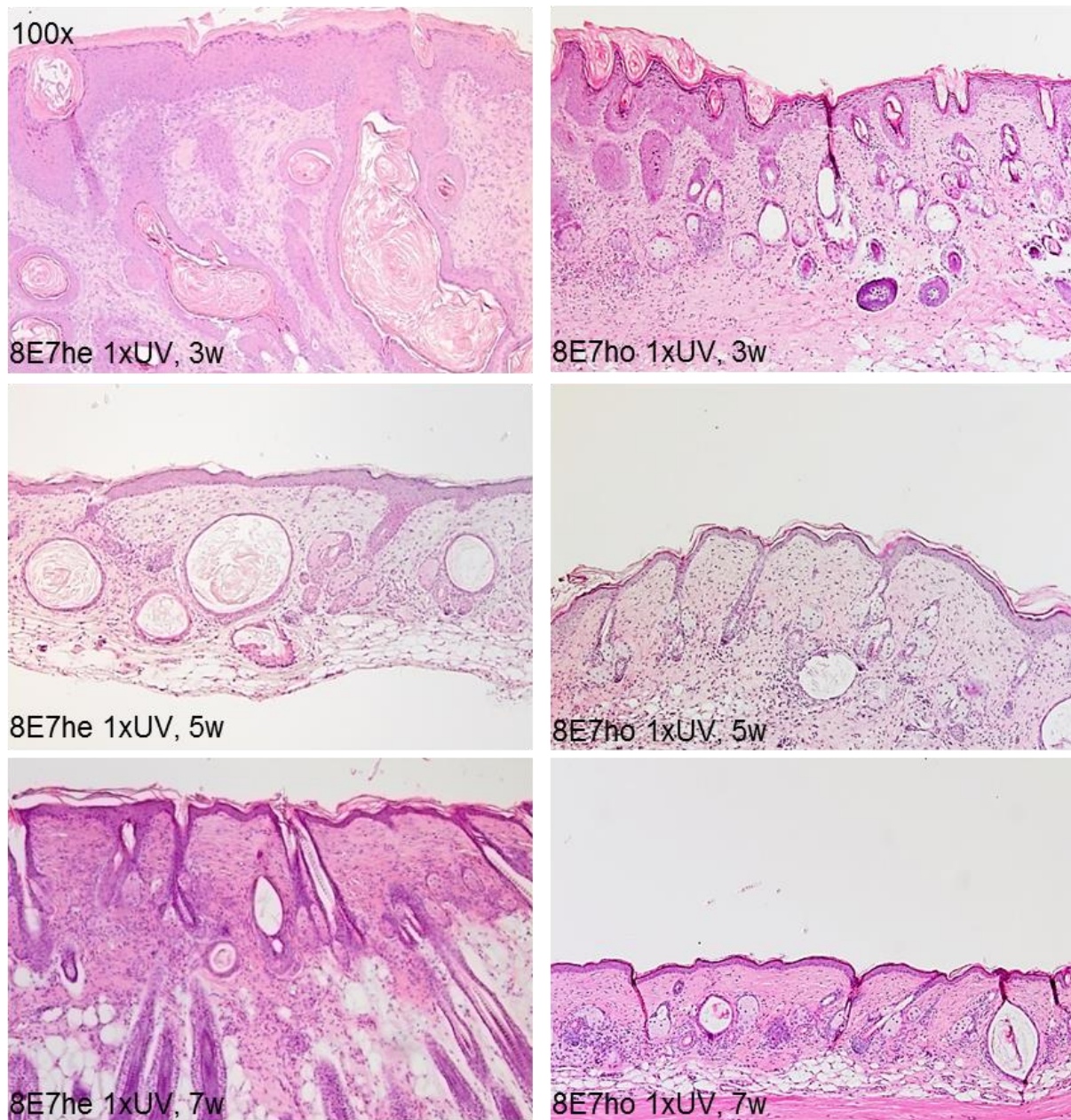
Figure 10. HE staining of 1x UVA/B treated K14-HPV8-E7he and K14-HPV8-E7ho transgenic mice. Mice were treated once with UVA/B with an age of 6 weeks and skin samples were taken 3, 5 and 7 weeks after treatment. On the left site, HE staining of 1x UV treated K14-HPV8-E7he mice are shown, on the right, HE staining of the skin of 1x UVA/B treated K14-HPV8-E7ho mice are presented. Mice developed skin hyperplasia within the interfollicular epidermis 3 weeks after treatment, which regressed after 5 - 7 weeks (magnification 100x).
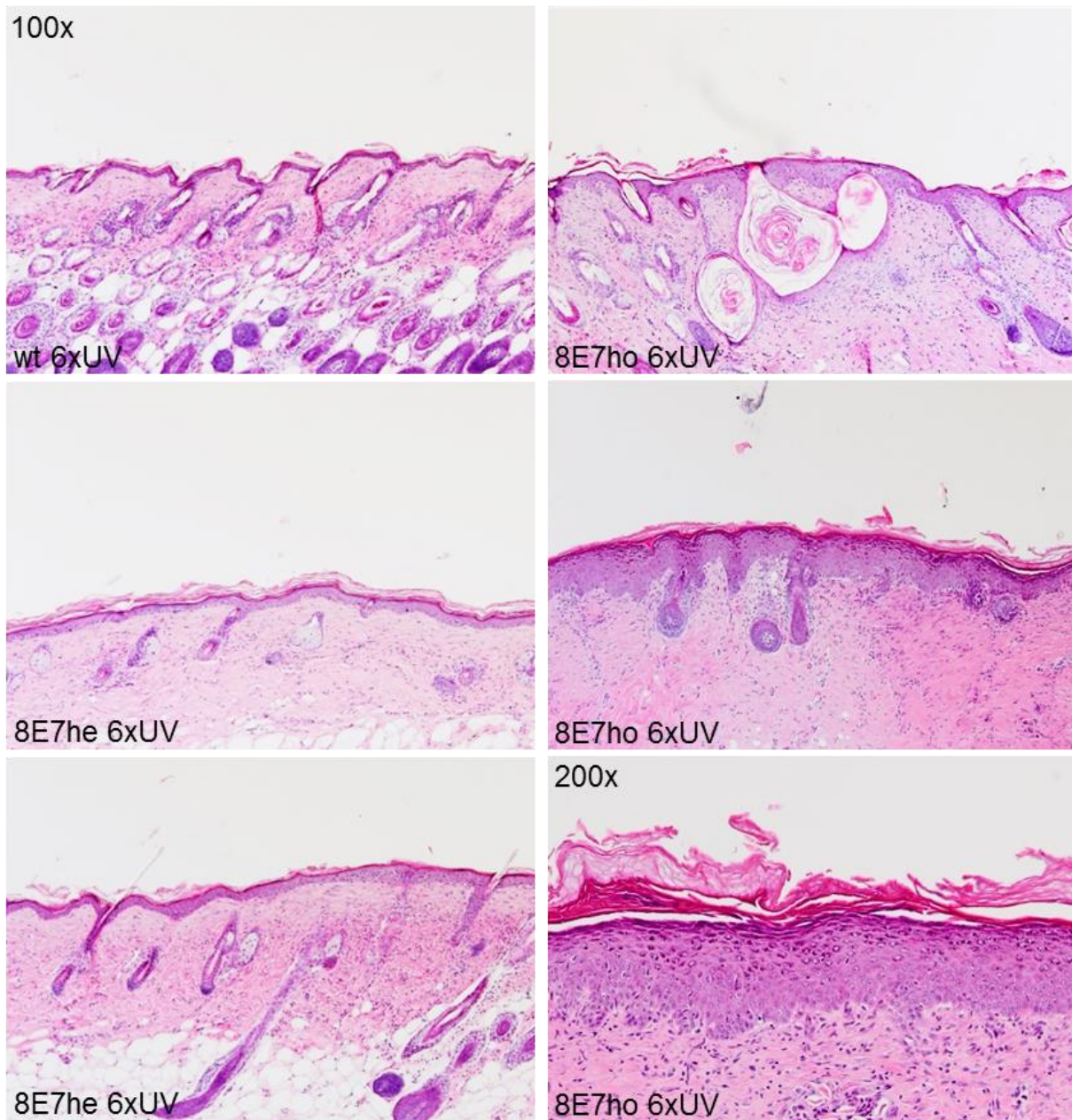
Figure 11. HE staining of chronically UVA/B irradiated skin of K14-HPV8-E7^{he} and K14-HPV8-E7^{ho} transgenic mice. Mice were treated with UVA/B chronically every 3 weeks starting at age of 6 weeks. Skin samples were taken after 6 rounds of irradiation and 3 weeks after the last treatment. Representative images for each group are presented (magnification 100x, 200x).
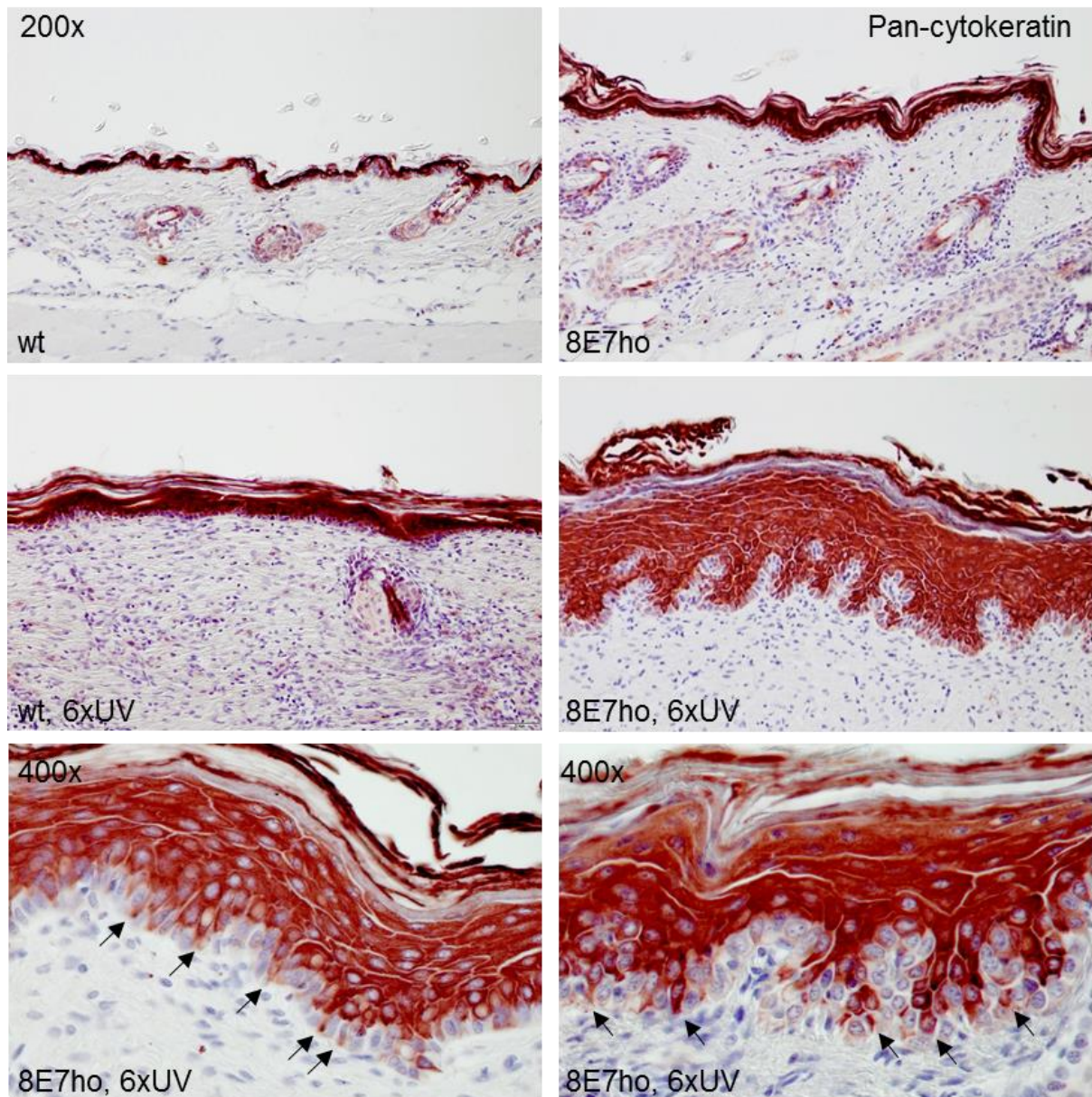
Figure 12. Carcinoma *in situ* formation in skin of chronically irradiated K14-HPV8-E7ho transgenic mice. Representative images of pan-cytokeratin staining of untreated and chronically irradiated skin of FVB/n wt and K14-HPV8-E7ho mice are shown. Atypical downward migration of cells in chronically irradiated skin of K14-HPV8-E7ho is indicated by black arrows (magnification 200x, 400x).
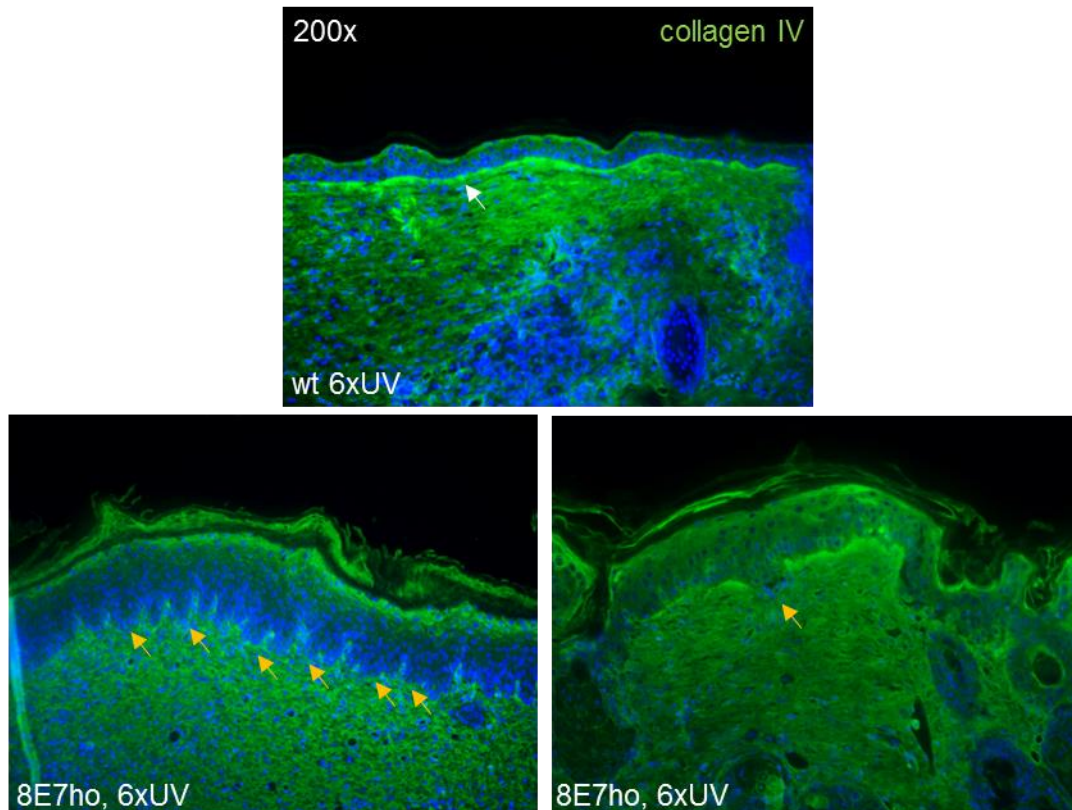
Figure 13. Degradation of the basement membrane at skin areas with carcinoma *in situ* formation. Representative immunofluorescence staining for collagen IV on skin of chronically irradiated FVB/n wt and K14-HPV8-E7ho mice tissue with carcinoma *in situ*. The BM is indicated by a white arrow in the FVB/n wt section. The absence and disruption of BM is indicated by orange arrows in the sections of K14-HPV8-E7ho mice (magnification 200x).

4.2 Deregulation of cell-cell junctions in HPV8-E7 positive skin models

Invasive growth is a main characteristic of tumour progression, which occurs either as single cell or collective cell movement, allowing cancer cells to invade through the ECM and thus spread to adjacent tissues. Common pathological consequences of invading cells are changes in cell-cell contacts and the remodelling of cell-matrix adhesions (Aneta *et al.* 2016).

4.2.1 HPV8-E7 mediates overexpression of β-catenin in OSCs

A reorganisation of cell-cell adhesion complexes by changing β-catenin expression or localisation plays an important role in EMT. To analyse a specific role of β-catenin in HPV8-E7-mediated changes of adherens junctions, β-catenin expression and localisation were analysed in de-epidermalised OSCs expressing 8E7 and compared to empty vector or E2 or E6 positive cultures. The empty vector (pLXSN) control showed a β-catenin staining restricted to the granular layer of the regenerated

epithelium (figure 14 A). In HPV8-E2 and HPV8-E6 OSCs the staining of the granular layer was absent. Interestingly, the regenerated epithelium of 8E7 OSCs showed a strong overexpression of β-catenin, by diffuse cytoplasmic staining in the suprabasal layers and strong membrane-tethered staining in the upper squamous layers (figure 14 A). Due to strong overexpression of β-catenin in OSCs expressing 8E7, in a next step β-catenin expression levels were determined in OSCs repopulated with keratinocytes expressing E7 of HPV1 (µHPV) and HPV5, HPV8, HPV20 and HPV38 (βHPV) (figure 14 B). OSCs repopulated with keratinocytes expressing the empty retroviral vector pLXSN were used as controls where expression was restricted to the upper layer of the regenerated epithelium. The β-catenin localisation and staining intensity in OSCs expressing HPV1-E7 and HPV38-E7 was not affected, compared to the control. HPV20-E7 expression led to a reduction of β-catenin expression. However, β-catenin staining was repeatedly strong in 8E7 expressing OSCs, as shown in figure 14 B. This culture showed a diffuse cytoplasmic staining in the lower suprabasal layers and membrane-tethered staining in the upper squamous layers. Strong membrane-tethered β-catenin staining was also found in OSCs repopulated with HPV5-E7 positive keratinocytes, comparable to the staining intensity of HPV8-E7.

A

B
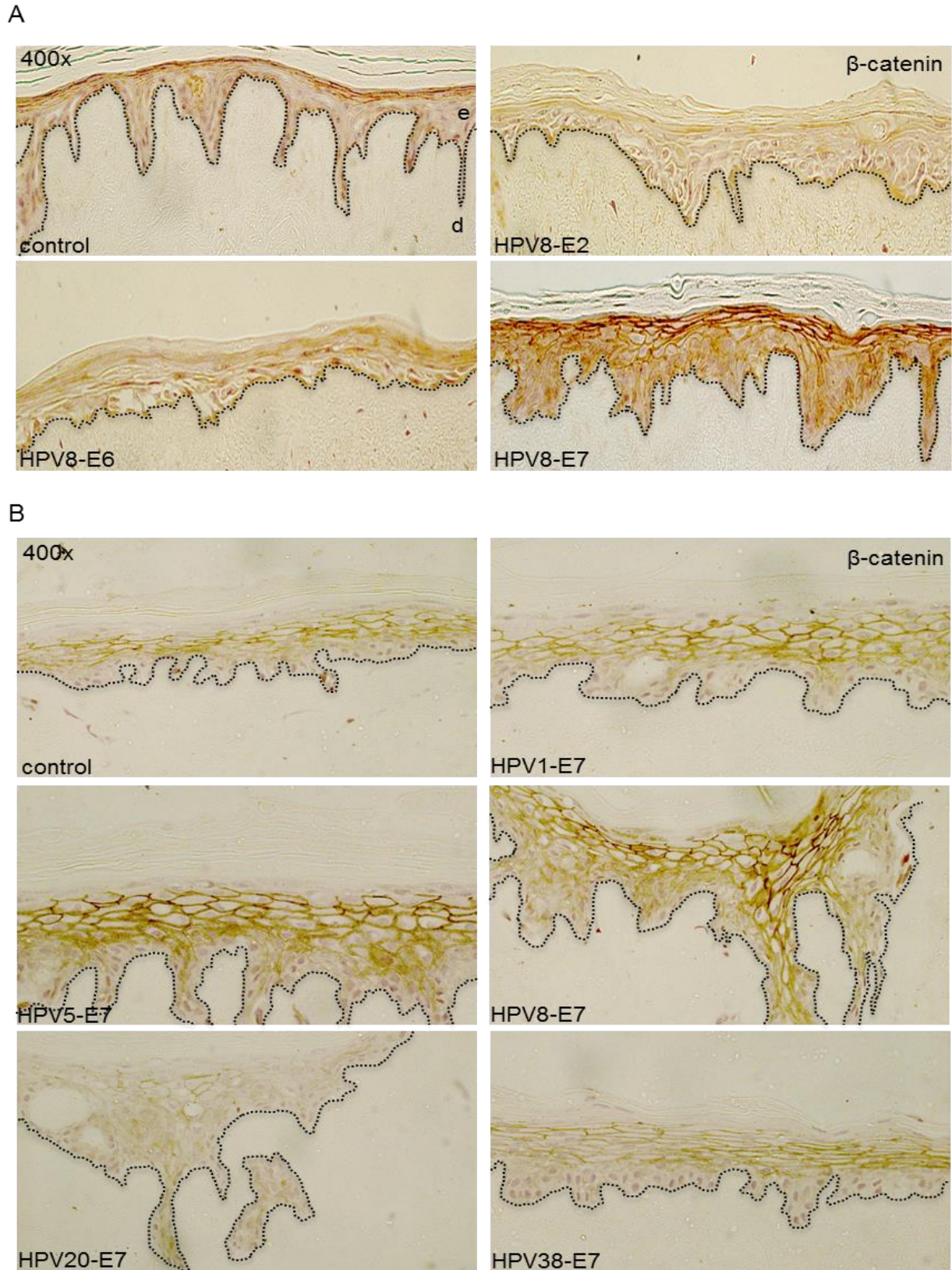
Figure 14. HPV5-E7 and HPV8-E7 increase β-catenin expression levels. (A) Representative stainings of total β-catenin expression in OSCs established with HPV8 early proteins E2, E6, E7 or empty vector control. Increased β-catenin expression was determined for OSCs expressing 8E7. (B) Representative immunohistochemical staining of OSCs expressing either empty vector or either E7 of HPV1, HPV5, HPV8, HPV20 or HPV38 against total β-catenin. Increased β-catenin expression was observed for HPV5-E7 and HPV8-E7. Tissues were counterstained with haematoxylin. Dashed lines represent the basement membrane zone, e: regenerated epithelium, d: dermis (magnification 400x).
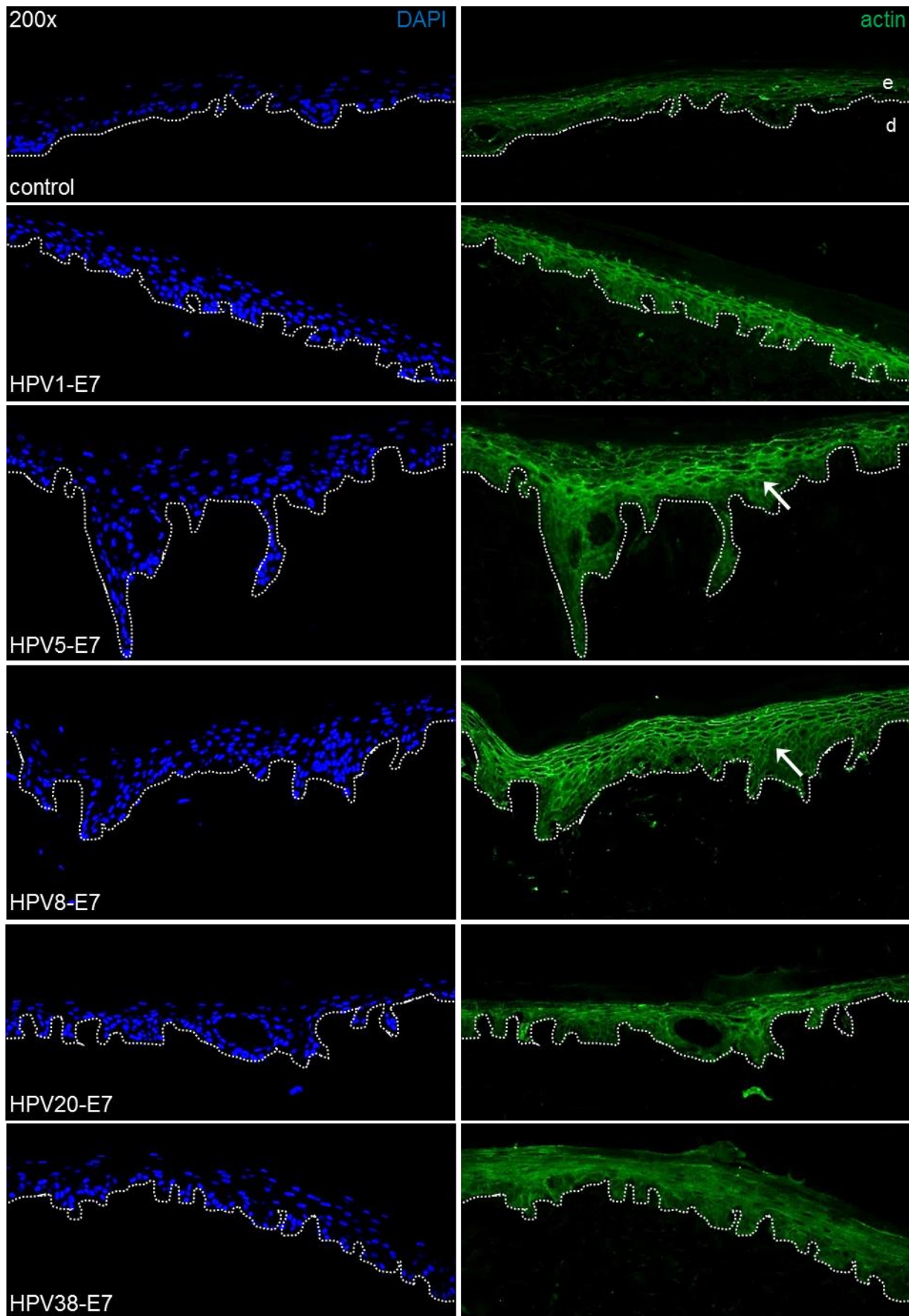
Figure 15. Elevated levels of actin in HPV5-E7 and HPV8-E7 expressing OSCs. Representative images of actin staining. Actin was fluorescently stained on OSCs established with either HPV1, 5, 8, 20 or 38 E7 expressing keratinocytes. Elevated levels of actin were detected in the upper squamous

cell layers of the regenerated epithelium of OSCs established with either HPV5-E7 and HPV8-E7 (indicated by white arrows). Counterstaining was performed with DAPI. Dashed lines represent the basement membrane zone, e: regenerated epithelium, d: dermis (magnification 200x).

To analyse the influence of overexpressed β-catenin on the actin cytoskeleton, OSCs expressing different E7 proteins, were fluorescently stained against actin (figure 15). Only OSCs expressing HPV5-E7 and HPV8-E7 showed enhanced membrane-tethered actin levels in the upper squamous cell layers. This strong staining was not detectable in the other OSCs expressing either empty vector control or E7 of HPV1, 20 and 38. Therefore, a direct role of HPV5-E7 and HPV8-E7 on β-catenin and actin localisation and expression was determined in differentiating keratinocytes.

4.2.2   Overexpressed β-catenin is not active in the Wnt signalling pathway

Beside its role at adherens junctions, non-phosphorylated β-catenin can act as transcription factor within the canonical Wnt pathway, through translocation from the cell membrane to the nucleus, where it can activate promoters containing T-cell factor (TCF) responsive elements (Staal *et al.* 2002). Ligation of Wnt proteins to their respective dimeric cell surface receptors activates Wnt signalling and stabilises β-catenin (Komiya and Habas 2008). To further analyse whether β-catenin is transcriptionally active due to its translocation into the nucleus, immunohistochemical staining of OSCs against non-phosphorylated β-catenin was performed by staining with the αABC β-catenin antibody, as shown in figure 16. The staining pattern of non-phosphorylated β-catenin overlapped the pattern of total β-catenin, being membranous and suprabasal in control and 8E7 expressing OSCs. As no active nuclear β-catenin was detected, it was suggested that β-catenin does not act within the canonical Wnt pathway in regenerated epithelium of OSCs repopulated with 8E7-positive keratinocytes.
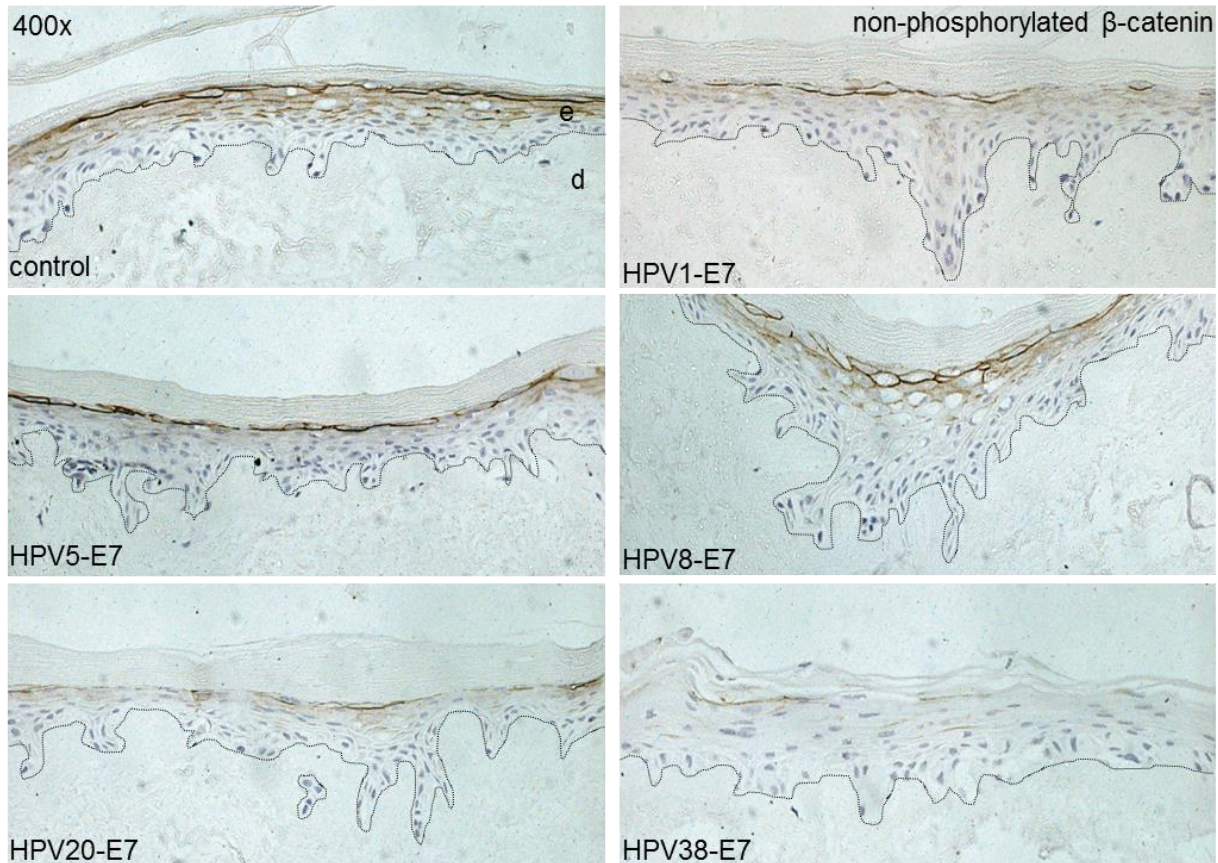
Figure 16. No nuclear translocation of β-catenin. Representative images of non-phosphorylated β-catenin in OSCs expressing either E7 of HPV1, HPV5, HPV8, HPV20 or HPV38. Membranous, suprabasal staining of non-phosphorylated β-catenin. Tissue was counterstained with haematoxylin. Dashed lines represent the basement membrane zone, e: regenerated epithelium, d: dermis (magnification 400x).

To further confirm that accumulated β-catenin is not active within the Wnt pathway, PHK were transfected with expression vectors for 8E7 together with either the β-catenin responsive TCF reporter plasmid (TOP-flash) or its negative control plasmid (FOP-flash). TOP-flash is a TCF reporter plasmid, which contains two sets (with the second set in the reverse orientation) of 3 copies of wt TCF binding sites driven by the thymidine kinase minimal promoter and upstream of a luciferase reporter gene, whereas FOP-flash contains mutated TCF binding sites. No significant difference in TOP-flash and FOP-flash luciferase activity was measured after 48h, which was confirmed in RTS3b cells (figure 17 A). The mRNA expression levels of the Wnt/β-catenin target genes c-myc and CD44, measured via qRT-PCR, were not changed in RTS3b cells transfected with 8E7, as demonstrated in figure 17 B. To verify the functionality of the Wnt signalling pathway in RTS3b cells, the activity of the TOP-flash and FOP-flash plasmids was evaluated after incubation of the cells with Wnt3a for 6h (Maubant *et al.* 2015). The promoter activity of the TOP-flash construct was significantly stimulated after Wnt3a treatment (**p=0.0045), whereas FOP-flash

showed no increased activity (figure 17 C). Additionally, protein expression of the β-catenin target c-myc was increased after Wnt3a treatment (figure 17 D). Taken together, these data indicate that the canonical Wnt/β-catenin signalling pathway is not affected in HPV8-E7 positive keratinocytes.
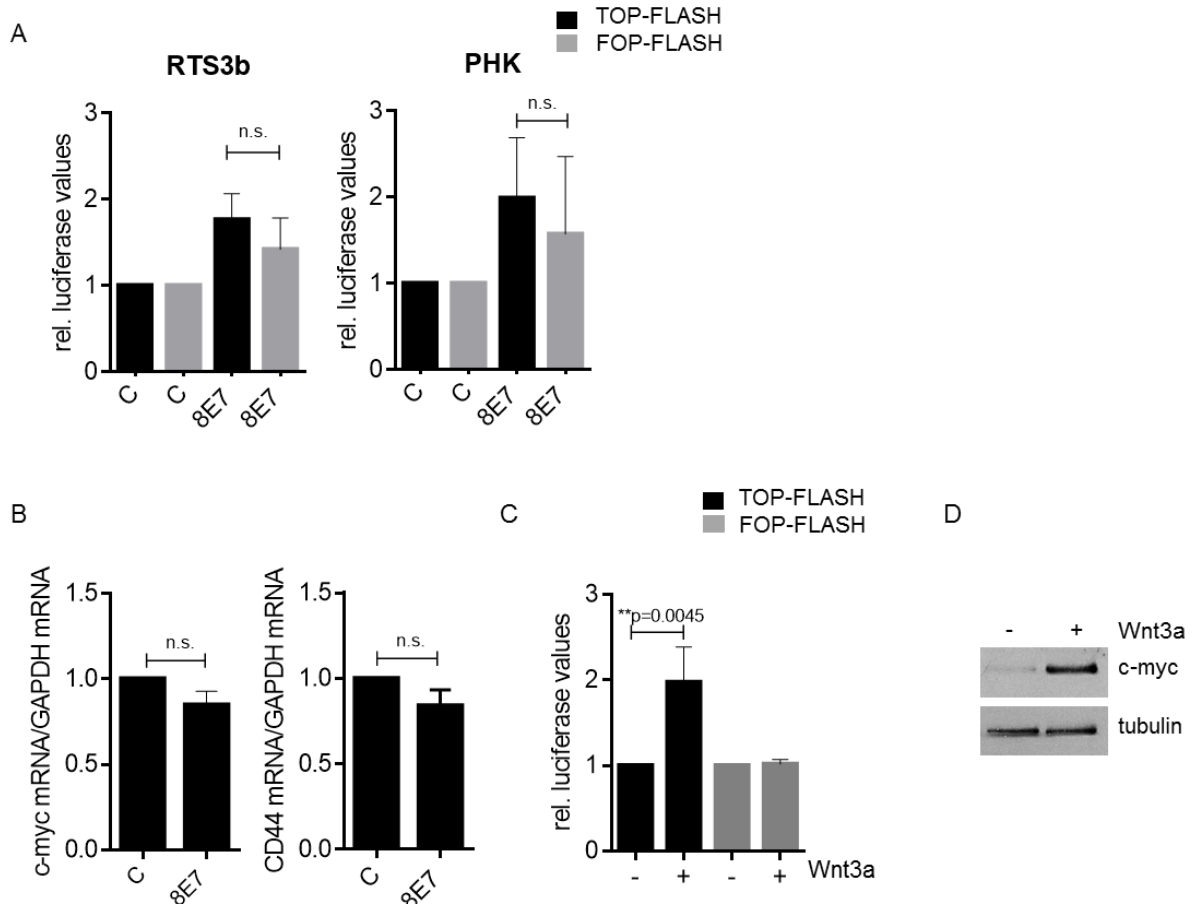
Figure 17. The canonical Wnt pathway is not activated by overexpressed β-catenin in HPV8-E7 expressing keratinocytes. (A) RTS3b cells and PHK were transfected with luciferase constructs, TOP-flash or FOP-flash, together with 8E7 expression vectors. Luciferase activity was normalised to protein levels, whereby luciferase activity of control cells was set as 1. No significant difference between TOP-flash and FOP-flash luciferase activity was determined. (B) mRNA expression levels of c-myc and CD44 were determined by qRT-PCR in 8E7 positive cells. No altered gene expression could be induced by 8E7. mRNA expression levels of target genes were normalised to transcript levels of GAPDH. mRNA expression levels in control cells were set as 1. (C) The stimulation of β-catenin/TCF signalling by Wnt3a was tested in RTS3b cells due to the transfection of either TOP-flash or FOP-flash and a Wnt3a treatment for 6h prior harvesting. Luciferase activity of control cells was set as 1. A significant stimulation was determined in TOP-flash (**p=0.0045) transfected cells. (D) Increased protein level of the β-catenin target gene c-myc was determined in Western blot analysis after Wnt3a treatment. Tubulin was used as loading control.

4.2.3 HPV5-E7 and HPV8-E7 increase expression levels of the junctional protein ZO-1

Having identified a strong upregulation of β-catenin at the cell membrane, we next tested whether the expression pattern of ZO-1 bridging between the tight junctions and the actin cytoskeleton was also changed. Therefore, HPV-E7 expressing OSCs were

stained immunohistochemically against ZO-1. In OSCs expressing HPV1-E7, HPV20-E7 and HPV38-E7, as well as in the control culture, ZO-1 expression was found in the uppermost layer of the regenerated epithelium. In contrast, HPV5-E7 and HPV8-E7 positive OSCs showed strong expression of ZO-1 throughout the regenerated epithelium (figure 18).
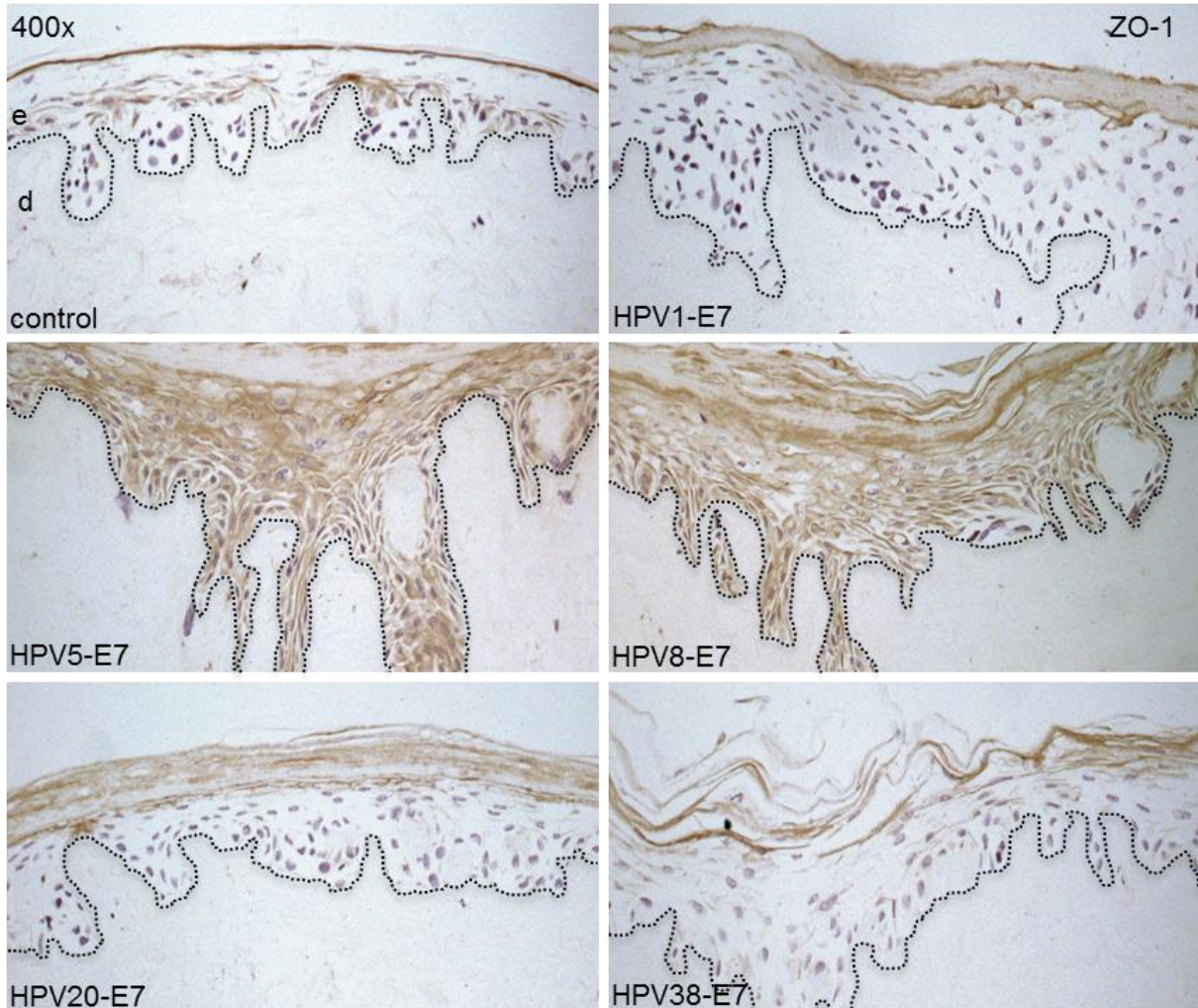
Figure 18. Increased expression of ZO-1 induced by HPV5-E7 and HPV8-E7. Representative IHC against ZO-1 expression in OSCs expressing either empty vector control or E7 of HPV1, HPV5, HPV8, HPV20 or HPV38. Strong expression of ZO-1 was determined in OSCs established with HPV5-E7 and HPV8-E7. Tissues were counterstained with haematoxylin. Dashed line shows basement membrane zone, e: regenerated epithelium, d: dermis (magnification 400x).

To confirm increased expression of β-catenin and ZO-1 triggered by 8E7, mRNA expression levels were determined via qRT-PCR in N/TERT keratinocytes grown in KGM-Gold medium. A significant increase in mRNA levels could be found for both junctional proteins. β-catenin and ZO-1 were increased about 1.5 times (**p=0.004) and 2.5 times (***<0.001) in 8E7 positive keratinocytes, respectively (figure 19 A). Under differentiating conditions, induced by the exposure to high extracellular calcium, β-catenin and ZO-1 expression was elevated in 8E7-positive keratinocytes (Akgül,

66

personal communication). Next, it was tested whether the knockdown of β-catenin and ZO-1 has an effect on proliferation or differentiation of 8E7 expressing keratinocytes. Western blot analysis confirmed the knockdown efficiency of the target-specific siRNAs used. As presented in figure 19 B, knockdown of β-catenin or ZO-1 did not affect the expression levels of the proliferating cell nuclear antigen (PCNA, a marker for cell proliferation) compared to cells transfected with a control siRNA (si-scramble). However, Western blot analysis of the epidermal differentiation marker loricrin showed a strong downregulation in empty vector and 8E7 expressing N/TERTs after knockdown of β-catenin and ZO-1, respectively (figure 19 B).
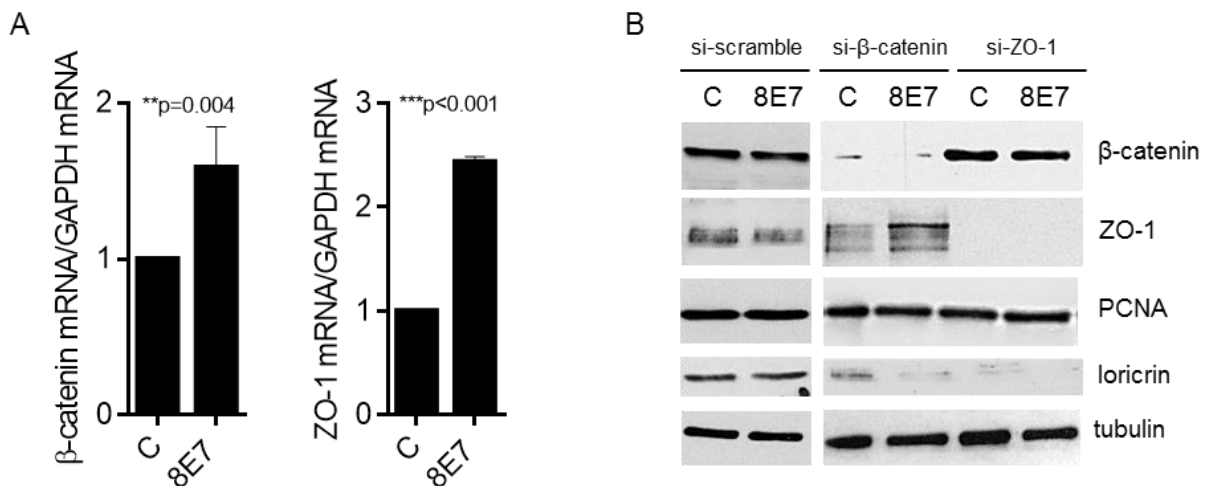
Figure 19. Increased expression of the junctional proteins β-catenin and ZO-1 in N/TERT-8E7 cells. (A) qRT-PCR measurement determined elevated mRNA expression levels of β-catenin (**p=0.004) and ZO-1 (***p<0.001) in N/TERT-8E7 cells compared to their control. (B) Control (si-scramble) and β-catenin and ZO-1 knockdown cells were analysed for changed proliferation and differentiation profiles by immunoblotting for PCNA and loricrin, respectively. Tubulin was used as loading control.

4.2.4   Overexpression of β-catenin and ZO-1 in HPV8 transgenic mice and in skin of EV patients

To confirm the increased expression of β-catenin and ZO-1 *in vivo*, skin of K14-HPV8-CER and wt mice was immunohistochemically stained against both factors. Skin of K14-HPV8-CER mice was strongly stained for total β-catenin and ZO-1 (figure 20 A). The skin of FVB/n wt animals showed only weak to moderate staining in the interfollicular epidermis for β-catenin and ZO-1. In addition, β-catenin and ZO-1 expression levels were also determined in lesional skin of EV patients, which were positive for HPV5 or HPV8. Normal human skin was stained against β-catenin and showed regular membrane-tethered expression, however, in skin of EV patients the expression was elevated at the most superficial cell layers (figure 20 B). The

expression pattern of β-catenin in EV skin was similar to the staining of OSCs established with HPV5 and HPV8-E7 expressing keratinocytes. The staining against ZO-1 showed only a light expression in normal human skin, whereas elevated levels were detected in skin of EV patients. Therefore, increased levels of β-catenin and ZO-1 could also be confirmed in murine and human HPV-positive skin.

A
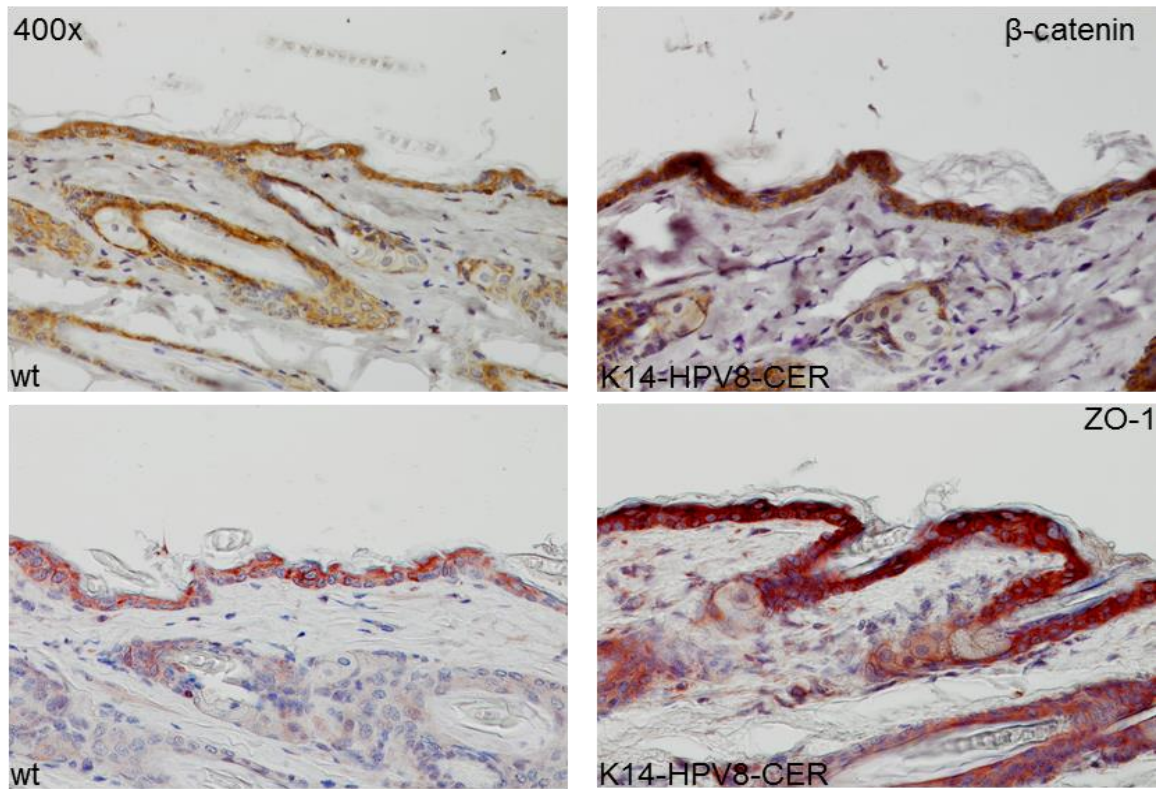
B
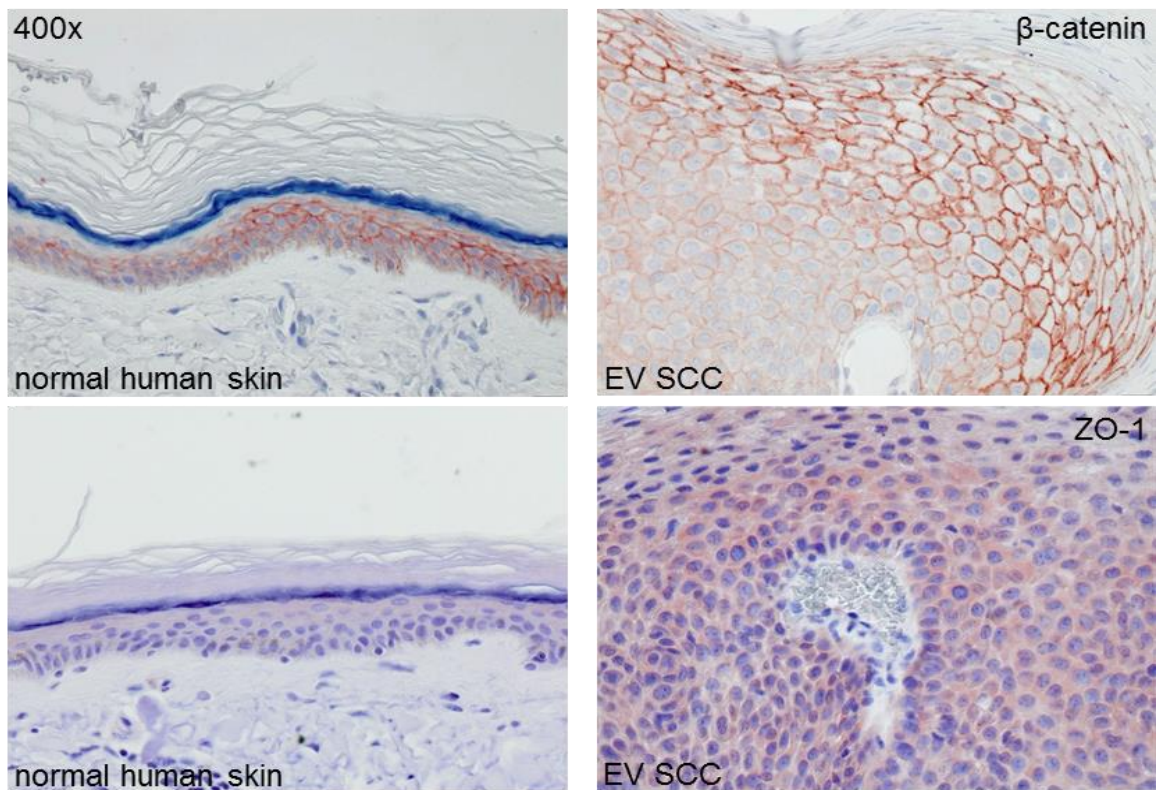
Figure 20. Increased expression of β-catenin and ZO-1 in HPV8 positive murine skin and human skin of EV-SCC. Representative immunohistochemical staining against β-catenin and ZO-1. (A) Elevated levels were determined in skin of K14-HPV8-CER transgenic mice compared to wt skin and (B) in human skin of EV-SCC (positive for HPV5, 8, 20, 23, 36, 50) compared to normal human skin. Tissue was counterstained with haematoxylin (magnification 400x).

4.3 Regulation of HPV8-E7 mediated invasion through keratinocyte-extracellular matrix (ECM) interaction

4.3.1 ECM proteins trigger HPV8-E7 mediated keratinocyte invasion

The importance of the matrix composition for HPV8-E7-mediated keratinocyte invasion was demonstrated by OSCs composed of 50% collagen I and 50% Matrigel, as described in the aims (see section 1.12). To establish an *in vitro* quantifiable invasion assay, Boyden chambers coated with Matrigel were used to test the invasive capacity of PHK expressing HPV8 oncogenes. The degree of invasion measured for PHK-8E7 (**p=0.0014) and PHK-8CER (**p=0.0091) was twofold higher compared to PHK expressing either HPV8-E2 or -E6 (figure 21 A).

To bypass potential variations between pools of PHK from different donors a stable cell line model of N/TERT keratinocytes expressing 8E7 and empty vector control was established. The 8E7 expression level in N/TERTs was determined by qRT-PCR, detecting 1.5 transcripts of 8E7 per GAPDH transcripts (***p<0.001, figure 21 B).

To further address the mechanism through which 8E7 triggers cell invasion, also N/TERTs were tested in Boyden chamber assays. Isogenic N/TERT-8E7 cells grown in RM+ medium did not show an enhanced invasive behaviour, when compared to the matched control cell line N/TERT-pLXSN. Interestingly, N/TERT-8E7 cells grown in KGM-Gold medium showed a 2-fold increase of invading cells (*p=0.0295, figure 21 C). This invasive capacity was comparable to the level of PHK-8E7 cells, which indicates that invasion in 8E7-expressing cells is exhibited only in KGM-Gold medium. All following experiments with N/TERT-8E7 were therefore performed in KGM-Gold medium. These data indicated that HPV8-E7-mediated invasion is triggered in cells with basal cell characteristics.

In order to identify the ECM proteins responsible for triggering invasion, Boyden chambers were either coated with collagen IV, laminin or fibronectin and used to assay N/TERT-8E7 cells. N/TERT-8E7 showed an about 2-fold enhanced invasion on all three matrices when compared to their matched controls (collagen IV: *p=0.0269, laminin: *p=0.0303, fibronectin: ***p<0.001, figure 21 D).
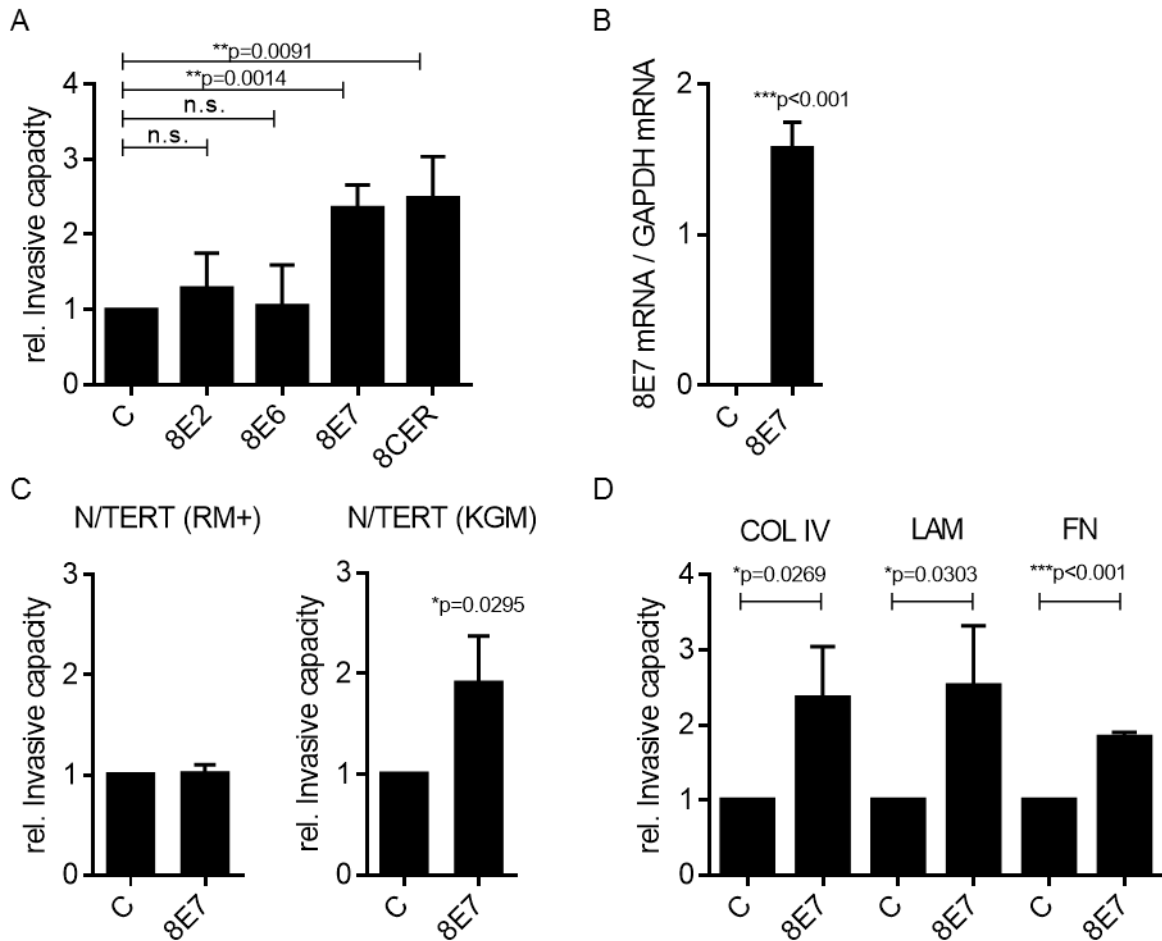
Figure 21. Invasive capacity of HPV8-E7 positive keratinocytes on ECM proteins. (A) Invasion capacity of PHK expressing either HPV8-E2, HPV8-E6, HPV8-E7 (**p=0.0014) or HPV8-CER (**p=0.0091) grown in KGM-Gold media, were analysed via Matrigel-coated Boyden chamber invasion assays and compared to empty vector. (B) qRT-PCR determining the absolute values of HPV8-E7 transcripts per GAPDH mRNA levels in N/TERT-8E7 (***p<0.001) cells compared to its empty vector control. (C) Determined invasive properties of isogenic N/TERT-8E7 cells grown either in RM+ or KGM-Gold (*p=0.0295) media by Matrigel-based Boyden chamber invasion assays. (D) Increased invasive capacity of N/TERT-8E7 cells tested on Boyden chamber invasion assays either coated with collagen IV (*p=0.0269), laminin (*p=0.0303) or fibronectin (***p<0.001).

4.3.2 A Cadherin switch increases motility of HPV8-E7 expressing cells on a fibronectin matrix

A cadherin switch associated with a decrease in E-cadherin and a subsequent increase in N-cadherin expression depicts a fundamental effect on cell phenotype and is considered to be a key molecular event during the first steps of cell invasion (van Roy 2014). E-cadherin staining intensity in OSCs established with PHK expressing 8E7 was significantly reduced compared to the control culture (figure 22).
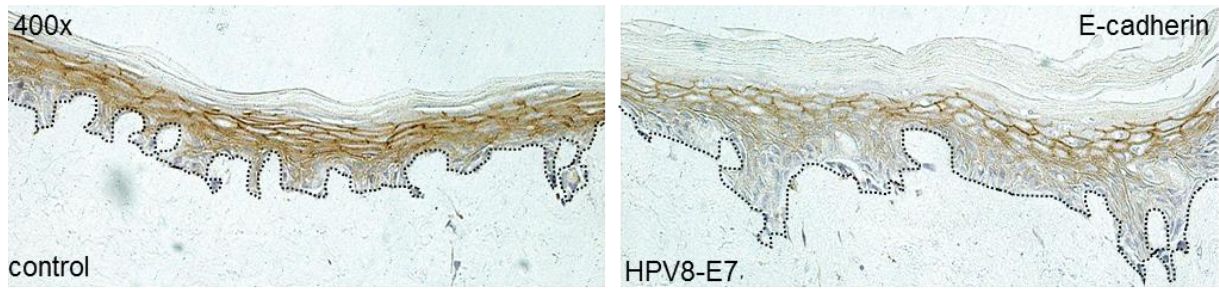
Figure 22. Decreased E-cadherin expression in regenerated epithelium of OSCs expressing HPV8-E7. Representative immunohistochemical staining of E-cadherin in OSCs repopulated with HPV8-E7 expressing keratinocytes or empty vector control. Decreased expression of E-cadherin at cell-cell junctions in suprabasal layers of HPV8-E7 OSCs. Tissue was counterstained with haematoxylin. Dashed line shows basement membrane zone (magnification 400x).

To identify the ECM protein triggering a cadherin switch in 8E7expressing keratinocytes the mRNA levels of E-cadherin and N-cadherin were measured via qRT-PCR in cells grown on cell culture plates coated either with collagen IV, laminin or fibronectin. Cells cultured on collagen IV showed a significant increase in E-cadherin (2-fold, *p=0.0138) and N-cadherin (1.5-fold, ***p<0.001) mRNA expression levels compared to the control culture (figure 23 A and B). When cells were grown on laminin, a significant twofold increase of N-cadherin (*p=0.0487) expression was detected. Interestingly, E-cadherin (***p<0.001) expression level was reduced by 50% in N/TERT-8E7 cells, when grown on fibronectin, which coincided with a 2-fold increase of N-cadherin (***p<0.001) expression (figure 23 A and B). The switch from E-cadherin to N-cadherin in N/TERT-8E7 cells grown on fibronectin was not associated with significant changes of the E-cadherin-regulating transcription factors Slug, Snail, and Twist. Also the mesenchymal and EMT marker vimentin was not changed upon 8E7 expression (figure 23 C). Thus, only fibronectin could be identified as an ECM protein inducing the cadherin switch in 8E7-positive keratinocytes.
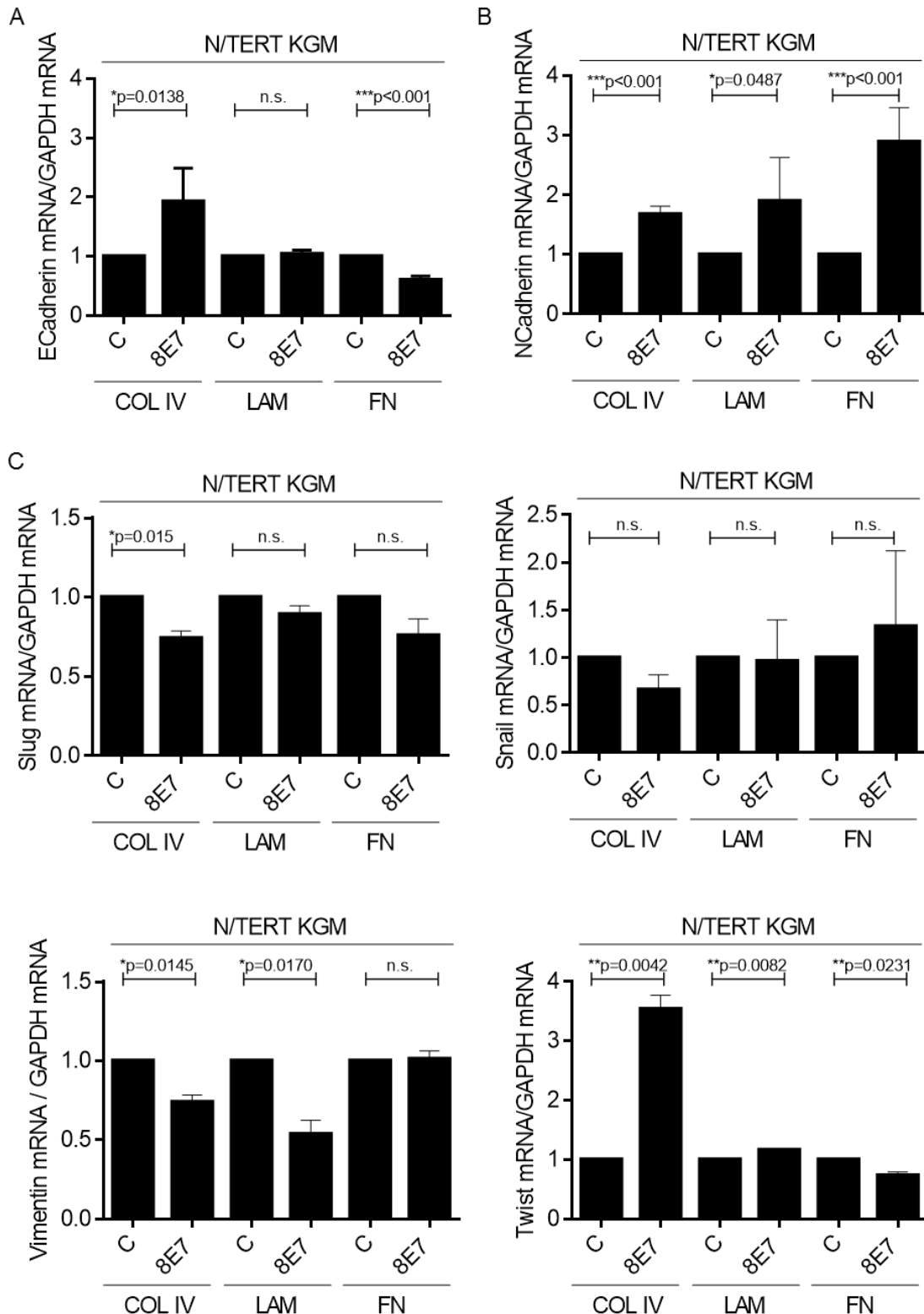
Figure 23. HPV8-E7 mediated EMT is induced upon cultivation on fibronectin. (A) mRNA expression levels of E-cadherin and N-cadherin in N/TERT-8E7 cells were determined via qRT-PCR. E-cadherin levels were upregulated in 8E7 expressing cells grown on collagen IV (*p=0.0138) and repressed on fibronectin (***p<0.001). N-cadherin mRNA expression levels were increased in N/TERT-8E7 cells when grown either on collagen IV (***p<0.001), laminin (*p=0.0487) or fibronectin (***p<0.001). In addition, mRNA expression levels of EMT associated transcription factors, including Slug, Snail, vimentin and Twist are illustrated for N/TERT-8E7 and control cells grown of collagen IV, laminin and fibronectin. mRNA expression levels of target genes were normalised to GAPDH mRNA levels and relative gene expression levels of the controls were set as 1. COL IV: collagen type IV; LAM: laminin; FN: fibronectin

4.3.3 Expression and secretion of fibronectin is altered by HPV8-E7

In HPV8-positive skin SCCs, the upregulation of fibronectin in peritumoral areas was significantly increased compared to betaHPV negative skin SCC. Furthermore, this upregulation of fibronectin could be confirmed in Western blot analysis of tissue extracts (cooperation Dr B. Akgül, Institute of Virology, Cologne with Prof C. Mauch and Dr P. Zigrino, Department of Dermatology, Cologne).

The increased deposition of fibronectin in the tumour matrix of HPV8 positive skin SCCs might be due to increased fibronectin expression and secretion from 8E7-positive keratinocytes. Therefore, mRNA expression levels of fibronectin in N/TERT keratinocytes expressing 8E7, grown on different matrices, were determined by qRT-PCR (figure 24 A). Elevated levels of fibronectin mRNA could be detected in N/TERT-8E7 positive cells grown either on collagen IV (3-fold increase, **p=0.006), laminin (3-fold increase, ***p<0.001) or fibronectin (3-fold increase, ***p<0.001). In addition, secretion of fibronectin by N/TERT-8E7 cells was determined in cell culture supernatants by immunoblotting. Fibronectin generates two isoforms due to alternative splicing, which contain an extra domain A (EDA) or B (EDB). The fibronectin^{EDA} plays an important role in wound healing, cell spreading and invasion (Sun *et al.* 2014). Significantly higher levels of total fibronectin and fibronectin^{EDA} were secreted by N/TERT-8E7 grown on laminin, collagen IV and fibronectin compared to their control (figure 24 B). In addition, to test whether 8E7-positive keratinocytes are able to stimulate fibronectin expression in fibroblasts, fibroblasts were treated with conditioned media from N/TERT-8E7 cells for 48h after which cell extracts were tested by Western blotting. As shown in figure 24 C, treatment of fibroblasts with conditioned media led to an increased expression of total fibronectin and fibronectin^{EDA}.
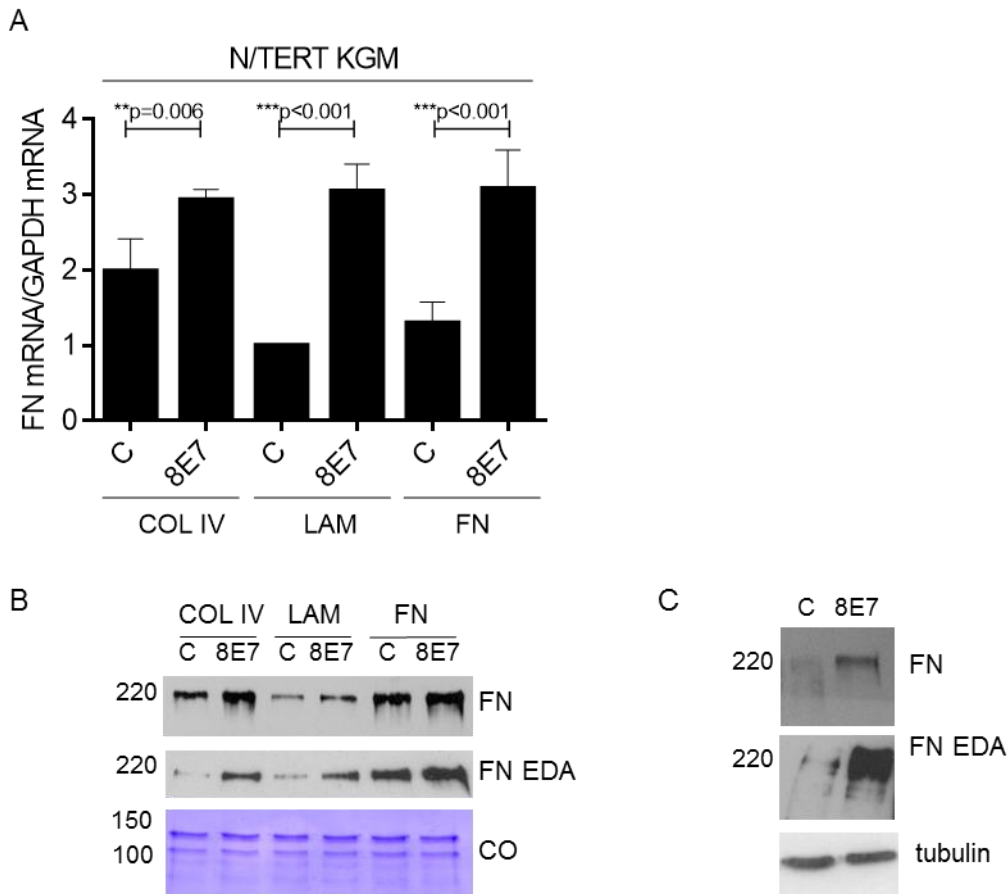
Figure 24. Increased fibronectin production and secretion by HPV8-E7. (A) qRT-PCR was performed to determine mRNA expression levels of fibronectin (FN) in N/TERT-8E7 cells grown on different matrices. Increased levels of fibronectin mRNA could be detected for N/TERT-8E7 cells either grown on collagen IV **p=0.006), laminin (***p<0.001) or fibronectin (***p<0.001). mRNA expression levels were normalised to transcript levels of GAPDH. Fibronectin mRNA expression level in control cells grown on laminin were set as 1. (B) Representative image of Western blot analysis showing secreted levels of total fibronectin and fibronectin[EDA] from N/TERT-8E7 cells. Equal loading was verified by Coomassie staining. (C) Total fibronectin and fibronectin[EDA] protein expression in primary fibroblasts stimulated with conditioned media from N/TERT-8E7 and control cells was determined via Western blot analysis. Equal loading was confirmed by immunoblotting for tubulin. COL IV: collagen type IV; LAM: laminin; FN: fibronectin

4.3.4 Regulation of the fibronectin promoter by HPV8-E7

To clarify the mechanism by which 8E7 induces fibronectin expression, we next tested whether fibronectin promoter activity is induced by 8E7. Luciferase promoter assays were performed with promoter constructs containing either the 1.2 kb promoter fragment of the human fibronectin promoter (pFN(1.2 kb)LUC) or the deletional mutants pFN(0.5 kb)LUC or pFN(0.2 kb)LUC (kindly provided by Dr J. Roman) (Michaelson *et al.* 2002). Keratinocytes were transiently transfected with the fibronectin promoter constructs together with increasing amounts of the pLXSN-8E7 or empty vector pLXSN. All tested fibronectin promoter constructs could dose-dependently be

activated by 8E7 (figure 25). A significant 2-fold activation was measured in all constructs (pFN(1.2 kb)LUC: *p=0.0427; pFN(0.5 kb)LUC: *p=0.032; pFN(0.2 kb)LUC: *p=0.0136). In order to predict transcription factors involved in 8E7-mediated activation of the fibronectin promoter, the 0.2 kb promoter proximal sequence was analysed using the TRANSFAC® database (http://www.biobase-international.com). This analysis led to the identification of a putative Sp1 binding site (5'-(G/T)GGGCGG(G/A)(G/A)(C/T)-3') at position $_{-134}$GGGGCGGGGC$_{-127}$ (Cawley *et al.* 2004). To test whether these Sp1 motifs have a role in mediating the 8E7 response, the pFN(0.2 kb)LUC construct was mutated at these sites (figure 26 A) and tested in luciferase assays. These luciferase promoter assays were performed in PHK co-transfected with the fibronectin constructs and 1 µg of pLXSN-8E7. The mutation of the Sp1 sites did not affect the overall activity of the fibronectin promoter (data not shown). Subsequent co-transfection experiments revealed that the 8E7-mediated activation of the 0.2 kb promoter fragment was abolished in the presence of mutated Sp1 sites within the pFN(0.2 kb)LUC-Sp1mut construct (figure 26 B).
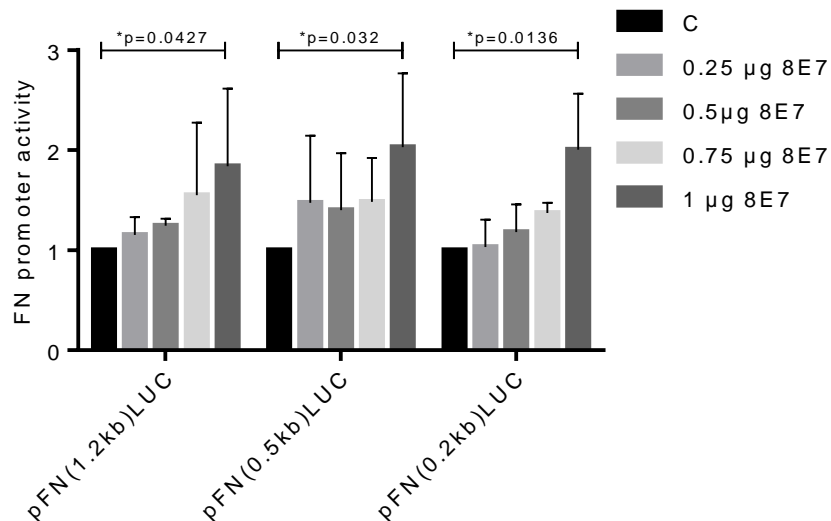
Figure 25. The fibronectin promoter activity is increased by HPV8-E7. Fibronectin promoter constructs were transfected into keratinocytes with increasing amounts of expression vector for 8E7. All fibronectin promoter constructs could be dose-dependently activated in the presence of increasing amounts of 8E7. Expression level of the corresponding co-transfected empty vector (control) was set as 1. FN: fibronectin

A

pFN(0.2 kb)LUC

5'-(G/T)**GGGCGG**(G/A)(G/A)(C/T)-3'   Sp1 consensus binding motif
GCGGGTGGGGTG**GGGCGGGGC**GGGGA   0.2 kb FN promoter sequence
GCGGGTGGGGTGGTTCGGTTCGGGGA   0.2 kb FN promoter sequence mut

B
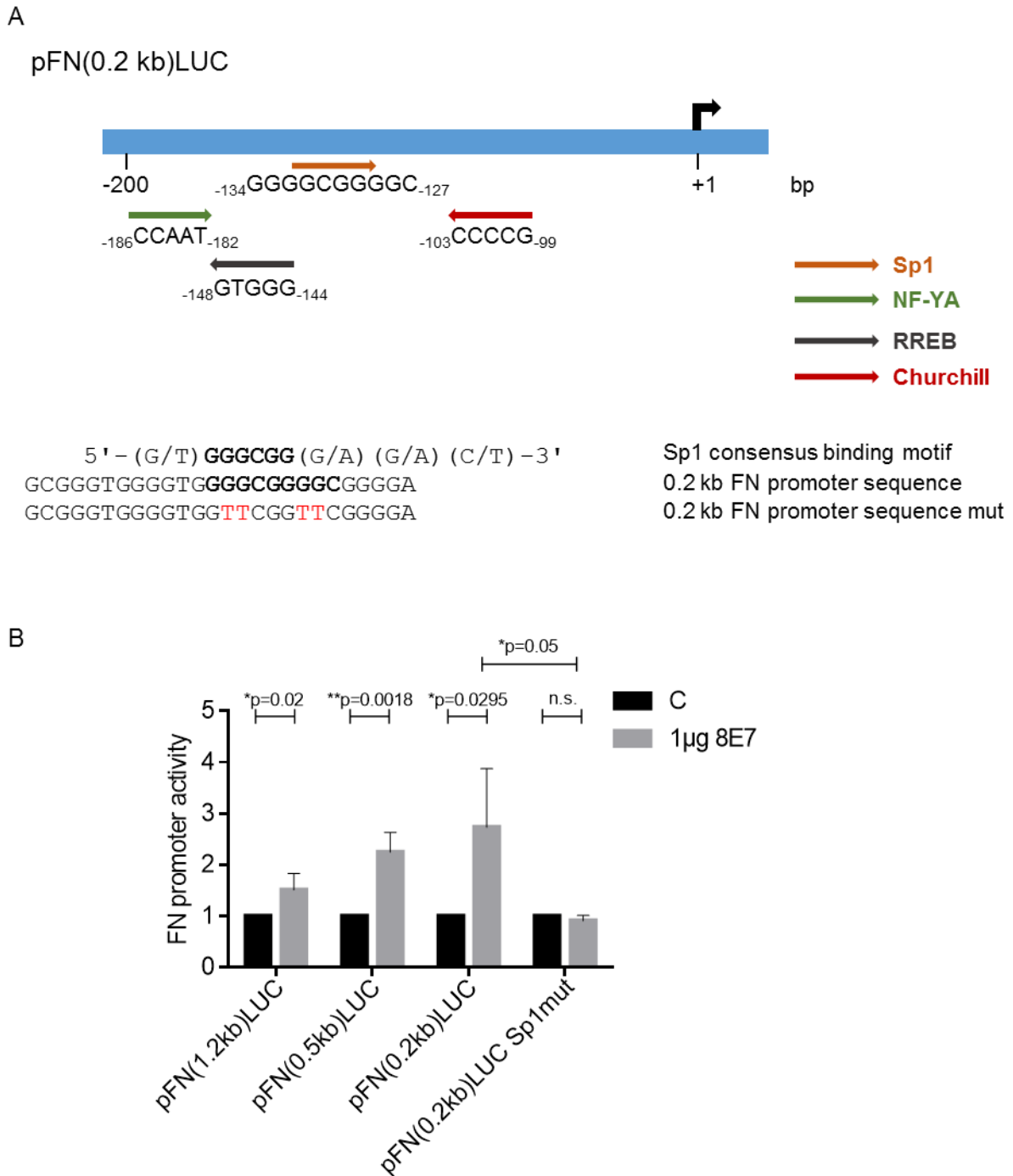
Figure 26. Fibronectin promoter activation by HPV8-E7 is dependent on functional Sp1 binding sites. (A) Schematic representation of putative transcription factor binding sites within the 200 bp fragment of the human fibronectin promoter. NF-YA, RREB, Churchill and Sp1 binding sites (BS) were predicted using TRANSFAC database analysis. The sequence alignment shows the consensus Sp1 BS, the sequence around the Sp1 BS within the 0.2 kb promoter and the mutation strategy of the Sp1 BS. (B) All promoter constructs were transfected into PHK together with 1 µg pLXSN-8E7. Increased promoter activity was reached ranging between 1.5-fold to 2.5-fold compared to controls (pFN(1.2 kb)LUC: 1.5-fold, *p=0.02; pFN(0.5 kb)LUC: 1.5-fold; **p=0.0018; pFN(0.2 kb)LUC: 2.5-fold, *p=0.0295). Due to the mutation of the Sp1 BS, the pFN(0.2 kb)LUC-Sp1mut reporter construct could not be stimulated by 8E7 anymore (*p=0.05). Firefly luciferase activity was normalised to co-transfected renilla luciferase. Relative promoter activity of the controls was set as 1. NF-Ya: nuclear transcription factor Y alpha, RREB: Ras responsive element binding protein 1, Churchill: Churchill domain containing 1, Sp1: specificity protein 1.

4.3.5 Fibronectin linked integrin regulation is associated with HPV8-E7 mediated invasion

4.3.5.1 Identification of integrin α3 chain on HPV8-E7 cells grown on fibronectin

Normal skin homeostasis is influenced by cell-ECM interactions, where changes are associated with disease (Watt and Fujiwara 2011). Keratinocytes are connected to the ECM via cell-matrix adhesion molecules, known as integrins, a family of glycoprotein receptors (Watt and Fujiwara 2011). Deregulation of several integrin chains has been associated with invasion and tumour development (De Franceschi *et al.* 2015). To analyse a correlation between altered integrin expression levels on the cell surface of 8E7 expressing keratinocytes with invasion, N/TERT-8E7 cells were cultured on collagen IV, laminin or fibronectin and analysed via qRT-PCR for integrin α2, α3, α5, αv and α6 and β1, β4, β5 and β6 chains. N/TERT-8E7 cells grown on laminin showed 1.5-fold increased expression levels of α2 (***$p<0.001$) and α6 (*$p=0.05$) chains, whereas 8E7 cells grown on collagen IV showed significantly increased levels of α2 (2-fold, ***$p<0.001$), α3 (3-fold, **$p=0.006$) and α5 (2.5-fold, *$p=0.04$, figure 27). Interestingly, only minor changes of integrin α chain expression was detected for cells grown on fibronectin. Figure 28 shows that β1 and β5 chain expression was significantly increased in N/TERT-8E7 cells grown on laminin. Integrin β5 chain mRNA expression was increased in N/TERT-8E7 cells grown on collagen IV. Only minor changes could be detected in N/TERT-8E7 cells grown on fibronectin.
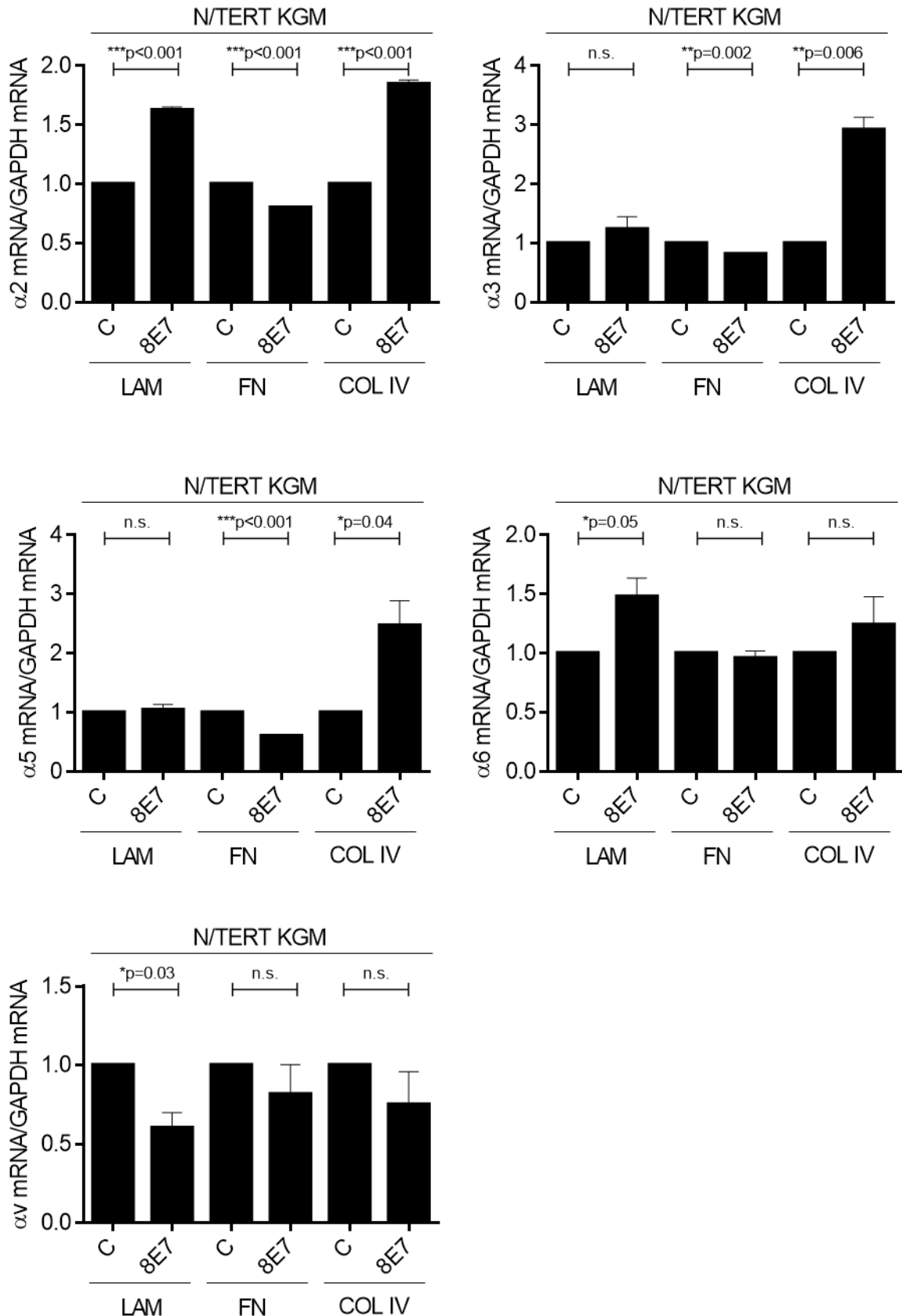
Figure 27. Changes in integrin α chain mRNA expression in N/TERT-8E7 grown on different ECM matrices. mRNA expression levels of different integrin α chains (α2, α3, α5, αv and α6) were determined by qRT-PCR for N/TERT-8E7 cells grown on collagen IV, laminin and fibronectin. The relative expression levels of the matched controls were set as 1 and GAPDH mRNA expression was used for normalisation. COL IV: collagen type IV; LAM: laminin; FN: fibronectin
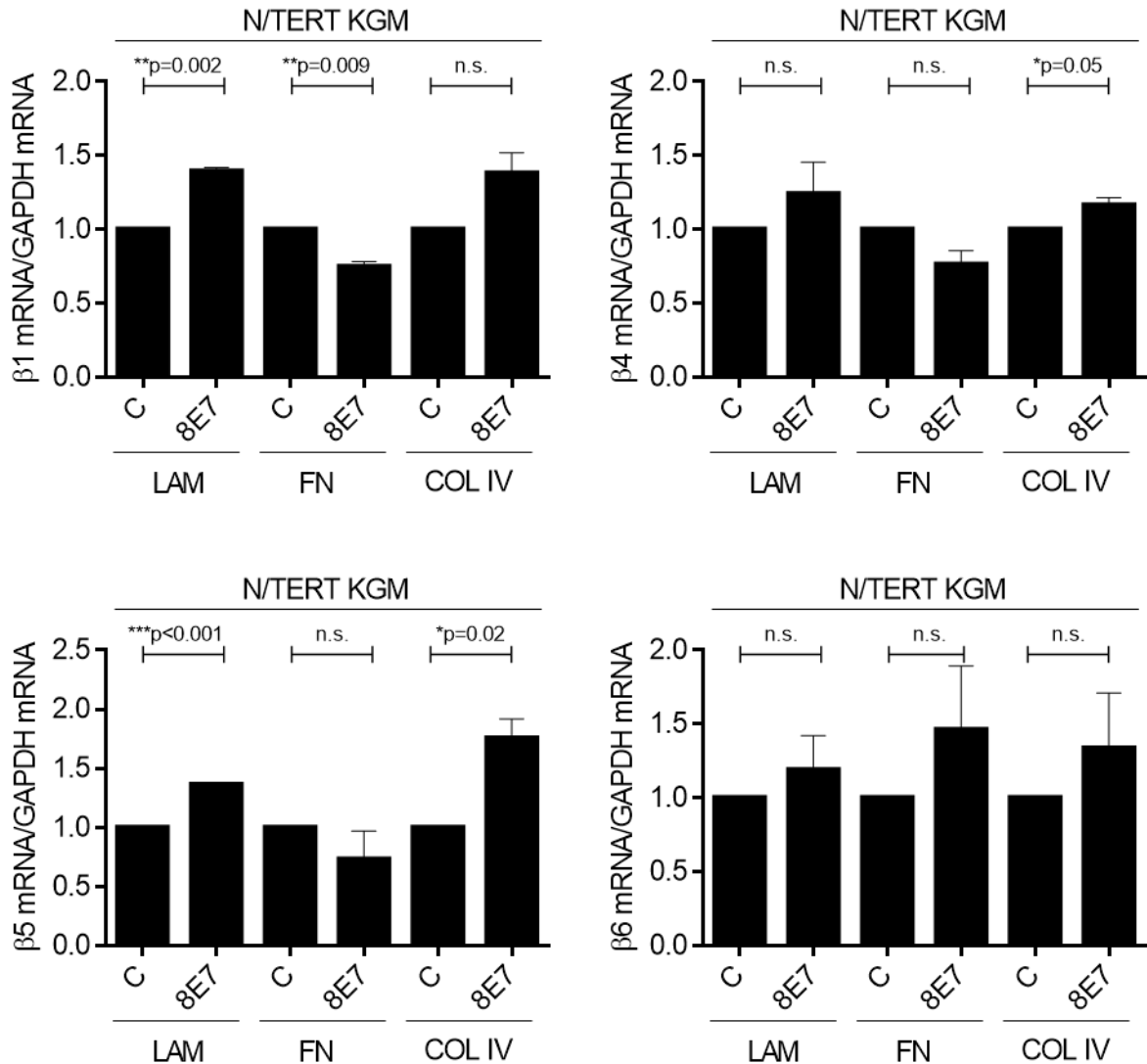
Figure 28. Changes in integrin β chain mRNA expression in N/TERT-8E7 grown on different ECM matrices. mRNA expression levels of different integrin β chains (β1, β4, β5 and β6) were determined by qRT-PCR for N/TERT-8E7 cells grown on collagen IV, laminin and fibronectin. The relative expression levels of the matched controls were set as 1 and GAPDH mRNA expression was used for normalisation. COL IV: collagen type IV; LAM: laminin; FN: fibronectin

To further address whether integrin α chains are elevated on the cell surface of 8E7 expressing keratinocytes, cells were analysed via FACS analysis to determine levels of integrin α2, α3, α5 and α6 chains. 8E7 and control cells were cultured either on laminin, collagen IV or fibronectin and harvested for FACS analysis. For 8E7 cells either cultured on collagen IV or laminin, no significant increase in integrin α chain cell surface localisation could be measured. Whereas, when the same cells were cultured on fibronectin, integrin α3 chain localisation was elevated on the cell surface by 30% (***p<0.001, figure 29). Although mRNA expression levels of integrin α3 chain in 8E7 cells grown on fibronectin showed no changes, elevated levels of integrin α3 on the cell surface were measured.
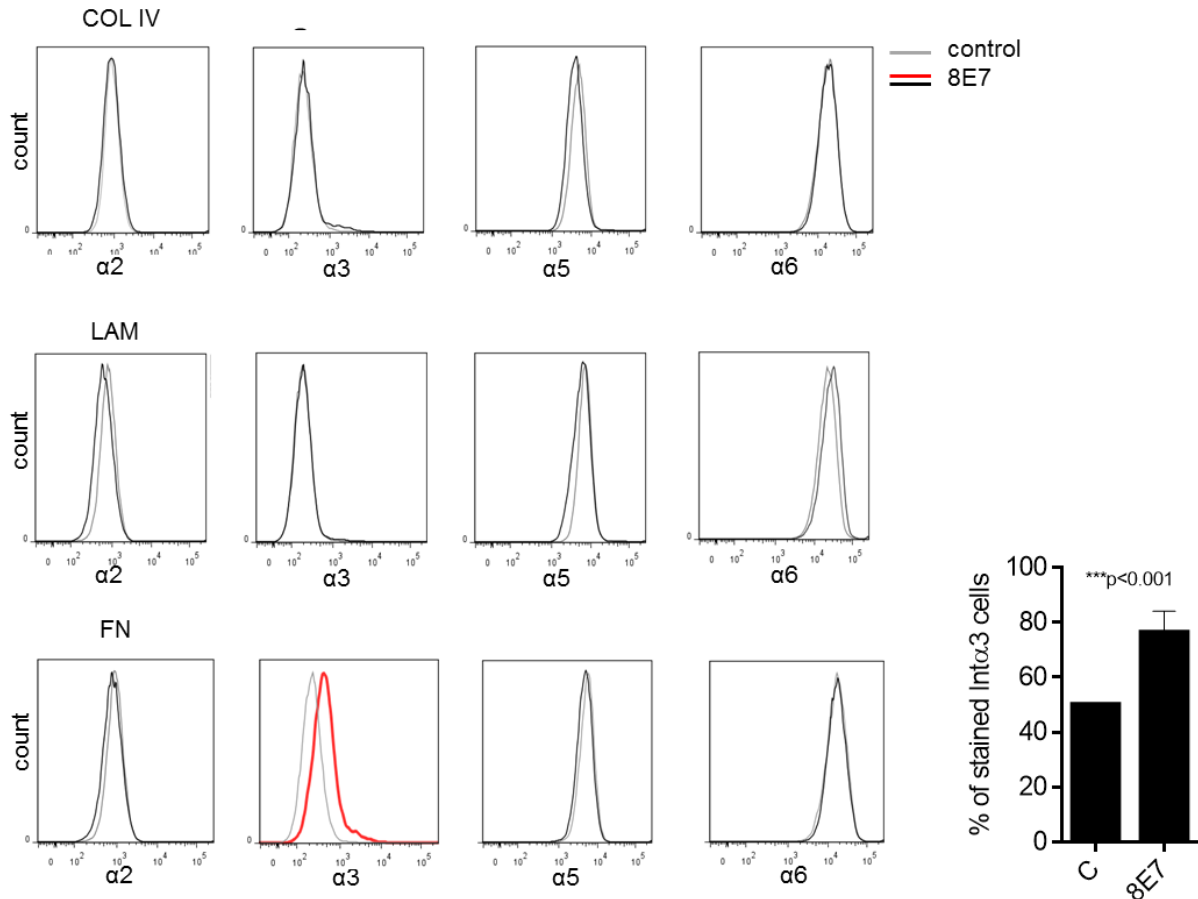
Figure 29. Increased expression of integrin α3 chain in HPV8-E7 expressing keratinocytes. Cell surface levels of integrin α2, α3, α5 and α6 chains were tested via FACS analysis on N/TERT-8E7 cells grown on different matrices. An increase of integrin α3 chain was determined for cells grown on fibronectin. The diagram on the left shows the percentage of cells showing increased integrin on the cell surface for N/TERT-8E7 cells grown on fibronectin. COL IV: collagen type IV; LAM: laminin; FN: fibronectin; C: control

To further verify enhanced integrin α3 expression levels whole cell extracts from N/TERT-8E7 cells either grown on Matrigel or fibronectin were used for immunoblotting. Figure 30 A shows that increased levels of integrin α3 were detected in 8E7-positive cells compared to their matching controls. In addition, fluorescence staining of OSCs established with N/TERT-8E7 cells showed enhanced levels of integrin α3 chain at the dermal-epidermal junction, whereas a weaker suprabasal expression was determined in the control culture (figure 30 B). The expression level of integrin α3 chain was also analysed in untreated and UV treated skin of wt and K14-HPV8-E7[ho] mice by fluorescence staining. Here, elevated levels of integrin α3 chain could be confirmed in chronically irradiated K14-HPV8-E7[ho] skin throughout basal and suprabasal layers compared to a weak suprabasal expression in irradiated wt skin (figure 31). Untreated wt and K14-HPV8-E7[ho] skin showed only very weak expression of integrin α3 chain. These findings led to the conclusion that 8E7 is able to regulate protein expression and cell surface levels of the integrin α3 chain.

A

B
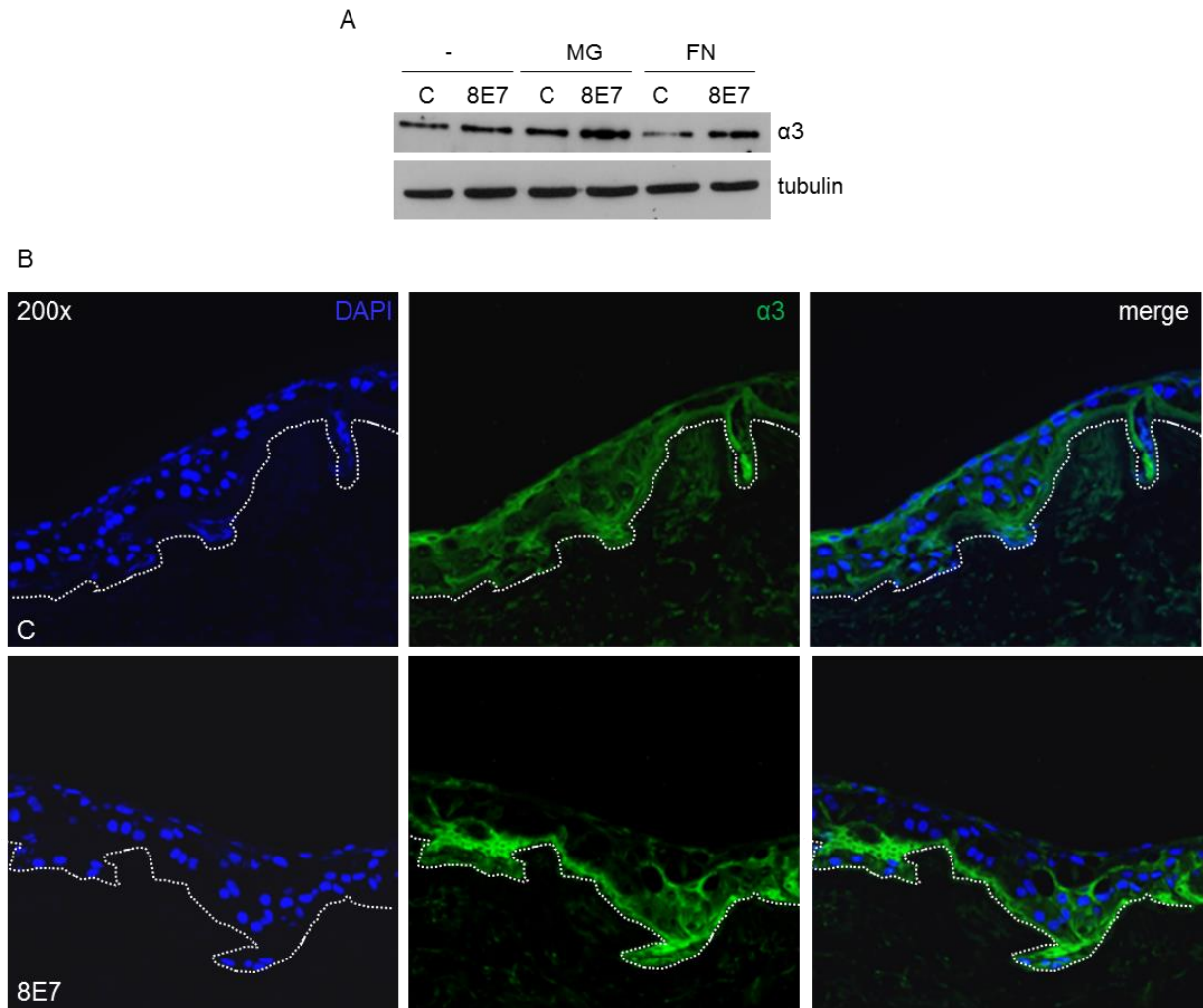
Figure 30. Elevated integrin α3 chain levels determined via Western blot and in fluorescence staining of OSCs. (A) Representative Western blot analysis of whole cell lysate from N/TERT-8E7 cells grown on Matrigel, fibronectin or without any coating. Elevated levels of integrin α3 chain were determined for 8E7 cells grown on Matrigel and fibronectin Equal loading was confirmed by immunoblotting for tubulin. (B) Immunofluorescence staining of integrin α3 chain (green) on OSCs established with N/TERT-8E7 and control cells. Tissue sections were counterstained with DAPI (blue) (original magnification 200x). MG: Matrigel; FN: fibronectin; C: control
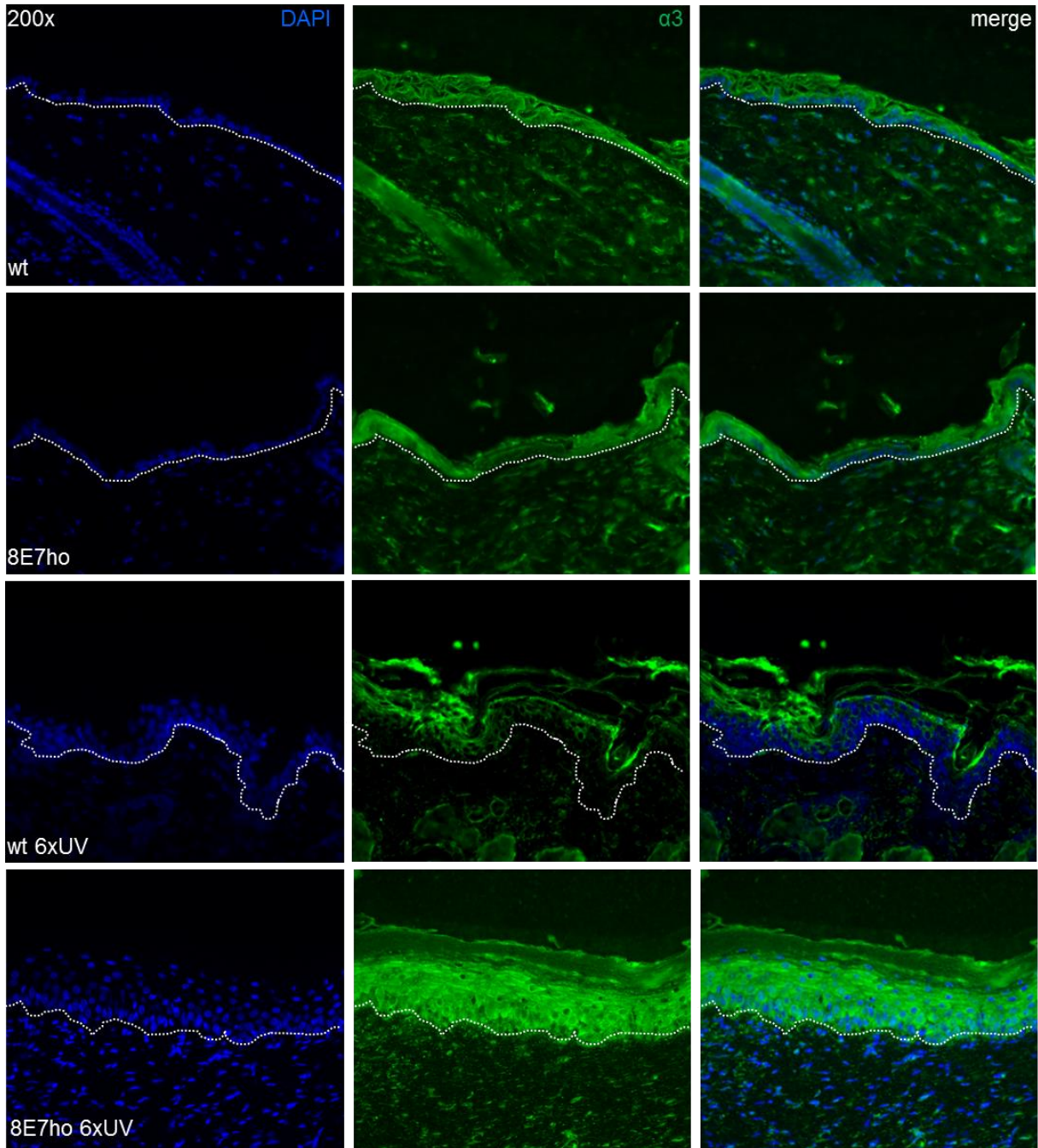
Figure 31. Increased expression of integrin α3 chain levels in chronically irradiated skin of K14-HPV8-E7^{ho} mice. Representative immunofluorescence staining of integrin α3 chain (green) on skin of untreated and UV treated skin of wt and K14-HPV8-E7^{ho} transgenic mice. Elevated levels of integrin α3 were detected in chronically irradiated skin of K14-HPV8-E7^{ho} mice. Tissue sections were counterstained with DAPI (blue) (original magnification 200x).

4.3.5.2   Proof of the role of integrin α3 chain in HPV8-E7 mediated invasion

a) Knockdown of integrin α3 chain

To confirm whether the elevated levels of the integrin α3 chain are involved in 8E7-mediated invasion, siRNA knockdown of the α3 chain was performed in N/TERT-8E7 keratinocytes and tested in Boyden chamber invasion assays. Figure 32 A shows the successful knockdown of integrin α3 chain in N/TERT-8E7 and control cells compared

to the cells transfected with control siRNA. No phenotypic changes could be observed due to siRNA knockdown of integrin α3 chain in N/TERT-pLXSN cells. Figure 32 B illustrates a significant reduction of the invasive capacity of N/TERT-8E7 cells due to the knockdown of integrin α3 chain compared to control cells. The level is reduced by about 50% (*p=0.03). Therefore, elevated levels of integrin α3 chain on the cell surface positively influence the invasive capacity of 8E7-expressing keratinocytes.
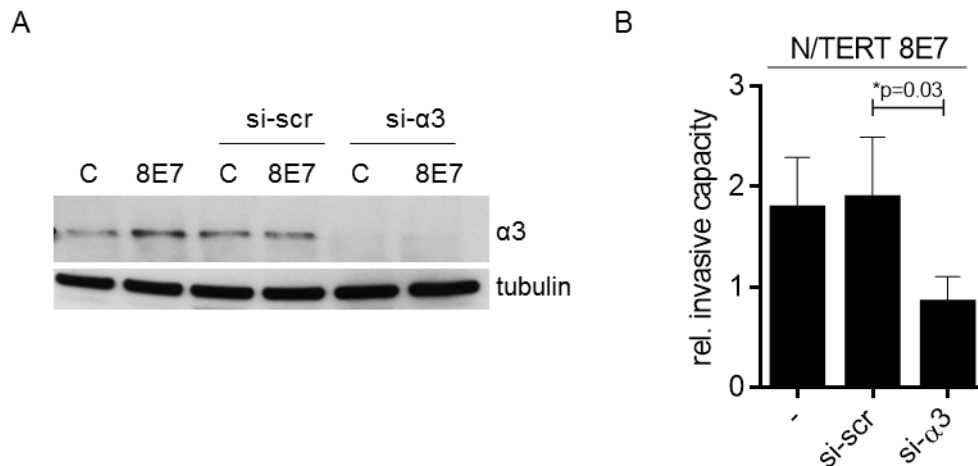
Figure 32. Integrin α3 chain knockdown is associated with reduced invasive capacity of N/TERT-8E7 cells. (A) Western blot analysis of whole protein lysates of N/TERT-8E7 and control cells, either untransfected, transfected with control siRNA (si-scr) or transfected with siRNA against integrin α3 (si-α3) was performed to confirm integrin α3 knockdown. Equal loading was confirmed via immunoblotting for tubulin. (B) Invasion was strongly reduced for N/TERT-8E7 cells with integrin α3 knockdown. Invasion capacity was determined via Boyden chamber invasion assays based on Matrigel. C: control

b) HPV8-E7 mutant, defective in integrin α3 upregulation, is not able to trigger keratinocyte invasion

No specific region of the HPV8-E7 oncoprotein has been known to be important for the control of keratinocyte invasion. The E7 proteins of all HPV types share amino acid homology to some extent, therefore an alignment of E7 sequences, including HPV1, 4, 5, 8, 16, 20 and 38, was performed (figure 33 A). One of the conserved aa in HPV5 and HPV8 E7 is the L at position 23. A site-directed mutagenesis was performed to mutate this conserved L in 8E7 to proof its influence on 8E7-mediated invasion. Therefore, we generated the 8E7 mutant L23A (8E7-L23A, figure 33 A). At first, the capacity of 8E7-L23A to degrade pRB was determined by immunoblotting to proof the functionality of this mutant protein. The degree of degradation of 8E7-L23A was comparable to 8E7wt (figure 33 B). Immunoblotting against integrin α3 chain showed that the expression was reduced in 8E7-L23A positive cells compared to 8E7wt grown on fibronectin (figure 33 C).
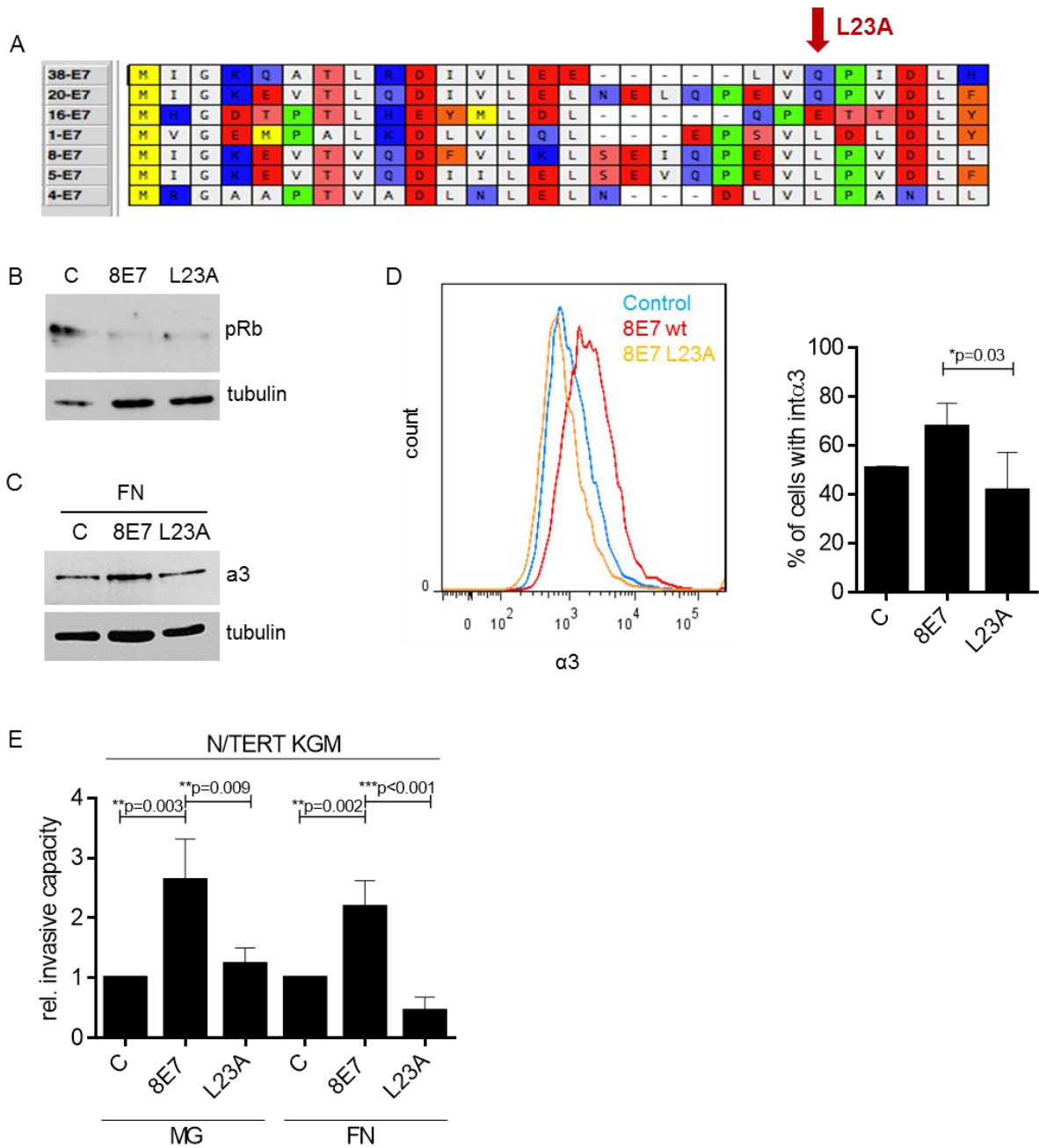
Figure 33. Integrin α3β1 induces invasive capacity of HPV8-E7 positive keratinocytes. (A) The alignment of several HPV-E7 protein sequences identified a conserved amino acid sequence in HPV5 and HPV8. To test whether this position is important for the invasive capacity, L23 was mutated via site-directed mutagenesis leading to 8E7-L23A. The arrow indicates the position L23. (B) Western blot analysis of whole protein lysates of N/TERT-8E7-wt and N/TERT-8E7-L23A demonstrated the degradation of pRB by 8E7wt and 8E7-L23A compared to control cells. (C) Immunoblotting against integrin α3 chain showed reduced levels in 8E7-L23A compared to 8E7wt for cells grown on fibronectin. Equal loading was confirmed by immunoblotting against tubulin. (D) Cell surface expression of integrin α3 chain was measured via FACS analysis in cells grown on fibronectin. N/TERT-8E7wt cells showed 68% integrin α3 chain positive cells compared to only 41% positivity in N/TERT-8E7-L23A (*p=0.03). (E) The invasive capacity of 8E7-L23A positive cells was tested in Boyden chamber assays either based on Matrigel or fibronectin. On both matrices N/TERT-8E7wt showed an about 2.5-fold (Matrigel: **p=0.003, fibronectin: **p=0.002) increased invasive capacity, however, N/TERT-8E7-L23A cells have a reduced invasive capacity (Matrigel: 1.2-fold, **p=0.009, fibronectin: 0.5-fold, ***p<0.001).

In addition, the cell surface expression level of integrin α3 chain was reduced on 8E7-L23A expressing cells grown on fibronectin compared to 8E7wt. For 8E7wt 70% of cells were positive for integrin α3, which was reduced to 40% (*p=0.03) in 8E7-L23A positive cells (figure 33 D). Furthermore, invasion was tested in Boyden chamber assays coated either with Matrigel or fibronectin. The invasive capacity of the 8E7-L23A was reduced by 60% on Matrigel (**p=0.009) and 80% on fibronectin (***p<0.001), compared to 8E7wt (figure 33 E). These results strengthen the findings that integrin α3β1 is the integrin mediating invasion of 8E7-positive keratinocytes.

4.3.6 Integrin α3 cell surface localisation on HPV8-E7 positive cells correlates with expression of epithelial stem cell markers

Our group could recently show that 8E7 expressing keratinocytes show cancer stem cell-like properties, which were attributed to increased cell surface expression of the epithelial stemness marker CD44 and epithelial cell adhesion molecule (EpCAM) (Hufbauer *et al.* 2013). Interestingly, α3β1 is also confined to the stem cells in the epidermis and co-immunoprecipitates with CD44 and EpCAM (Jones *et al.* 1995, Schmidt *et al.* 2004). To determine, whether the increased cell surface levels of integrin α3 chain can be associated with stem cell-like traits, cells were analysed by FACS analysis for CD44, EpCAM and a3. The top 10% of total control cells analysed for CD44 and EpCAM were gated and termed CD44^{high} and EpCAM^{high}. The 8E7-positive cells revealed a higher CD44^{high} / EpCAM^{high} population of about 25% (*p=0.0158, figure 34 A). When analysing the CD44^{high} / EpCAM^{high} population for α3 chain, an increase from 10% in the control cells to 21% in the 8E7-positive cells was observed (***p<0.001, figure 34 B).
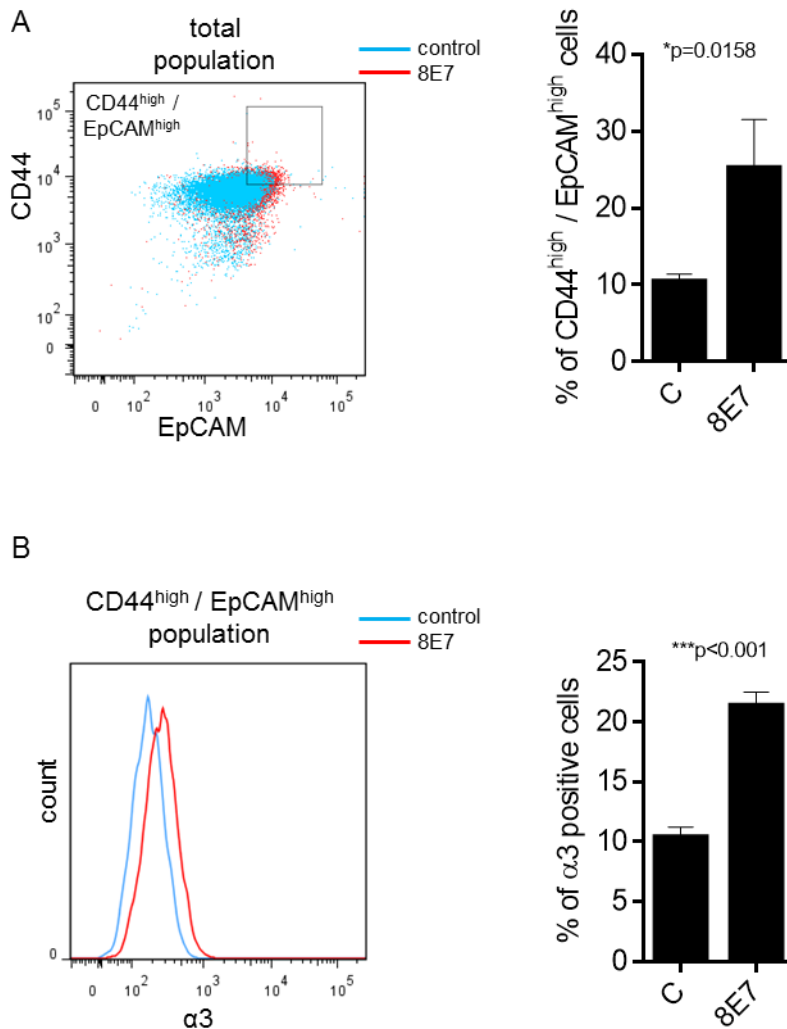
Figure 34. Stem cell-like properties of 8E7 positive cells correlate with increased α3 cell surface localisation. (A) For FACS analysis, the total cell population of N/TERT-8E7 and control cells was stained for CD44 and EpCAM. The top 10% of control cells were gated and termed CD44high / EpCAMhigh. The bar chart indicates the percentage of CD44high / EpCAMhigh N/TERT-8E7 and control cells. (B) The CD44high / EpCAMhigh population was further stained against integrin α3 chain. The bar diagram shows the percentage of integrin α3-positive cells of the CD44high / EpCAMhigh population of N/TERT-8E7 and control cells. C: control

4.3.7 HPV8-E7 increases expression of the ECM protein Fibulin-2

Integrin α3β1 is one of the major epidermal integrins and is highly expressed in epidermal keratinocytes (Watt and Fujiwara 2011). The α3β1 integrin is associated with the regulation of cell-autonomous and paracrine functions involved in wound healing and skin tumorigenesis (Missan *et al.* 2014). To characterise the influence of integrin α3β1 on the regulation of gene expression in transformed keratinocytes, Missan and colleagues recently performed a microarray analysis to identify genes regulated by integrin α3β1 in immortalised keratinocytes. This analysis identified induced expression of the cellular matrix protein Fibulin-2 by integrin α3β1, which contributed to the invasion properties of transformed keratinocytes (Missan *et al.*

2014). In addition, a role for integrin α3β1 in BM stability through the induction of Fibulin-2 was identified (Longmate *et al.* 2014). Fibulin-2 is a cellular matrix protein, known to bind to ECM proteins such as laminin and fibronectin, thereby participating in the organisation of extracellular supramolecular structures (Kobayashi *et al.* 2007, Kinsey *et al.* 2008). We therefore asked the question whether 8E7-mediated upregulation of integrin α3 chain also affects Fibulin-2 levels. Therefore, Fibulin-2 protein levels were determined in PHK-8E7 via immunoblotting. Fibulin-2 is upregulated in PHK-8E7 cells grown on Matrigel and fibronectin compared to their matched controls (figure 35 A). Knockdown of integrin α3 chain in PHK-8E7 cells lead to a reduction in Fibulin-2 levels, when grown on fibronectin (figure 35 B). To further verify enhanced levels of Fibulin-2 fluorescence staining of OSCs established with keratinocytes expressing 8E7 and untreated/treated skin of wt and K14-HPV8-E7[ho] mice was performed. In 8E7-positive OSCs Fibulin-2 expression was increased throughout the basal and suprabasal layers of the epidermis compared to a weaker signal in the more basal layers of the control culture (figure 35 C). Chronically irradiated skin of K14-HPV8-E7[ho] transgenic mice showed a similar staining of the basal and suprabasal layers of the epidermis compared the 8E7 positve OSCs. Weaker expression was detected in treated wt skin, whereas the skin of untreated wt and K14-HPV8-E7[ho] mice was faintly stained (figure 36). We therefore concluded, that 8E7 expression also leads to an α3β1-dependent upregulation of Fibulin-2.
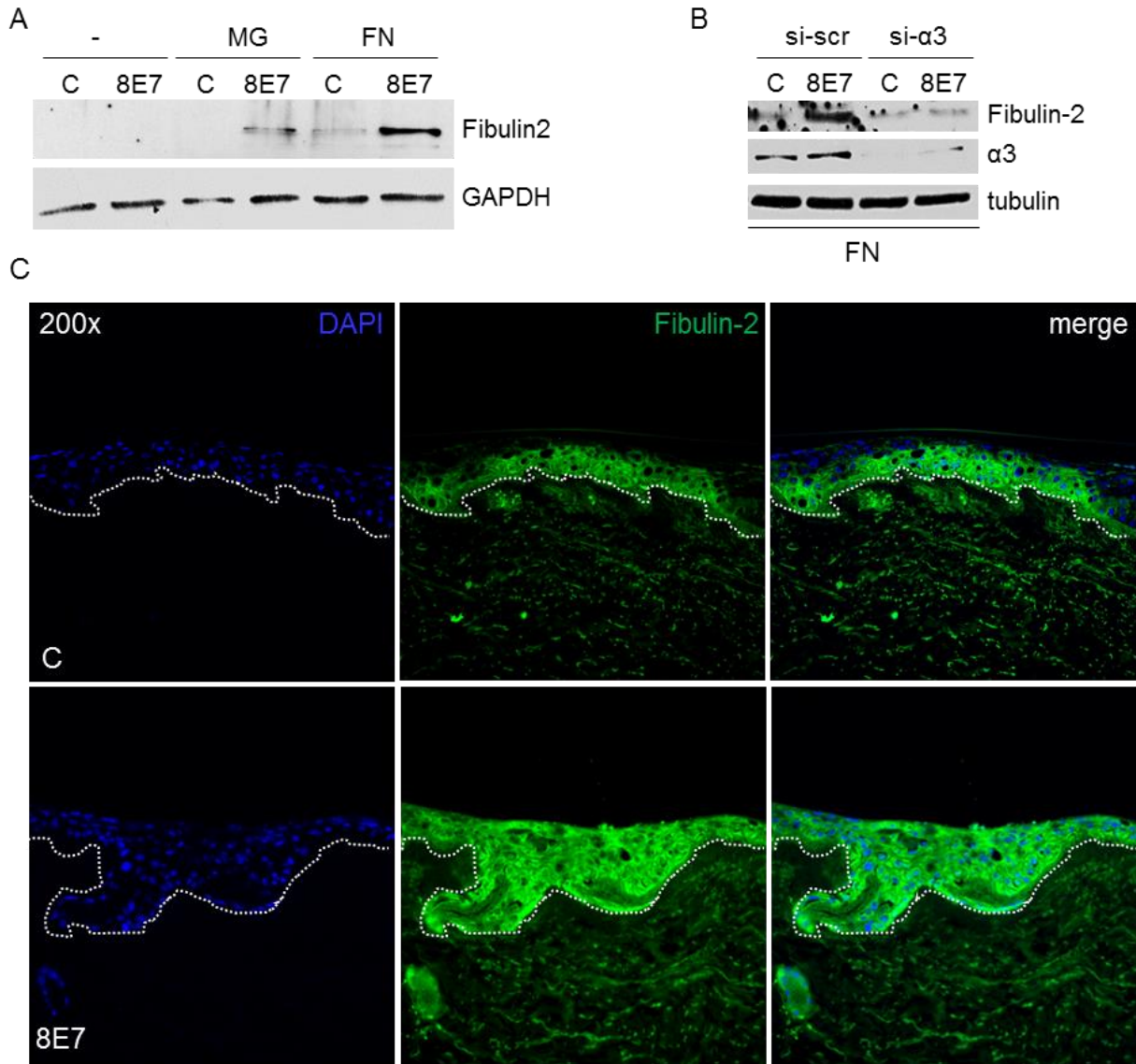
Figure 35. Elevated levels of Fibulin-2 in the presence of HPV8-E7. (A) Western blot analysis for Fibulin-2 of whole protein lysates of PHK-8E7 or control cells grown either on uncoated, Matrigel or fibronectin plates. Equal loading was confirmed by immunoblotting for GAPDH. (B) Western blot analysis for Fibulin-2 of whole protein lysates of PHK-8E7 and control cells when either transfected with control siRNA (si-scr) or si-α3 and grown on fibronectin. Equal loading was confirmed by immunoblotting for tubulin (C) Immunofluorescence staining of OSCs established with N/TERT-pLXSN or pLXSN-8E7 positive cells. Tissue sections were counterstained with DAPI (blue) (dashed line represents BM zone, magnification 200x).
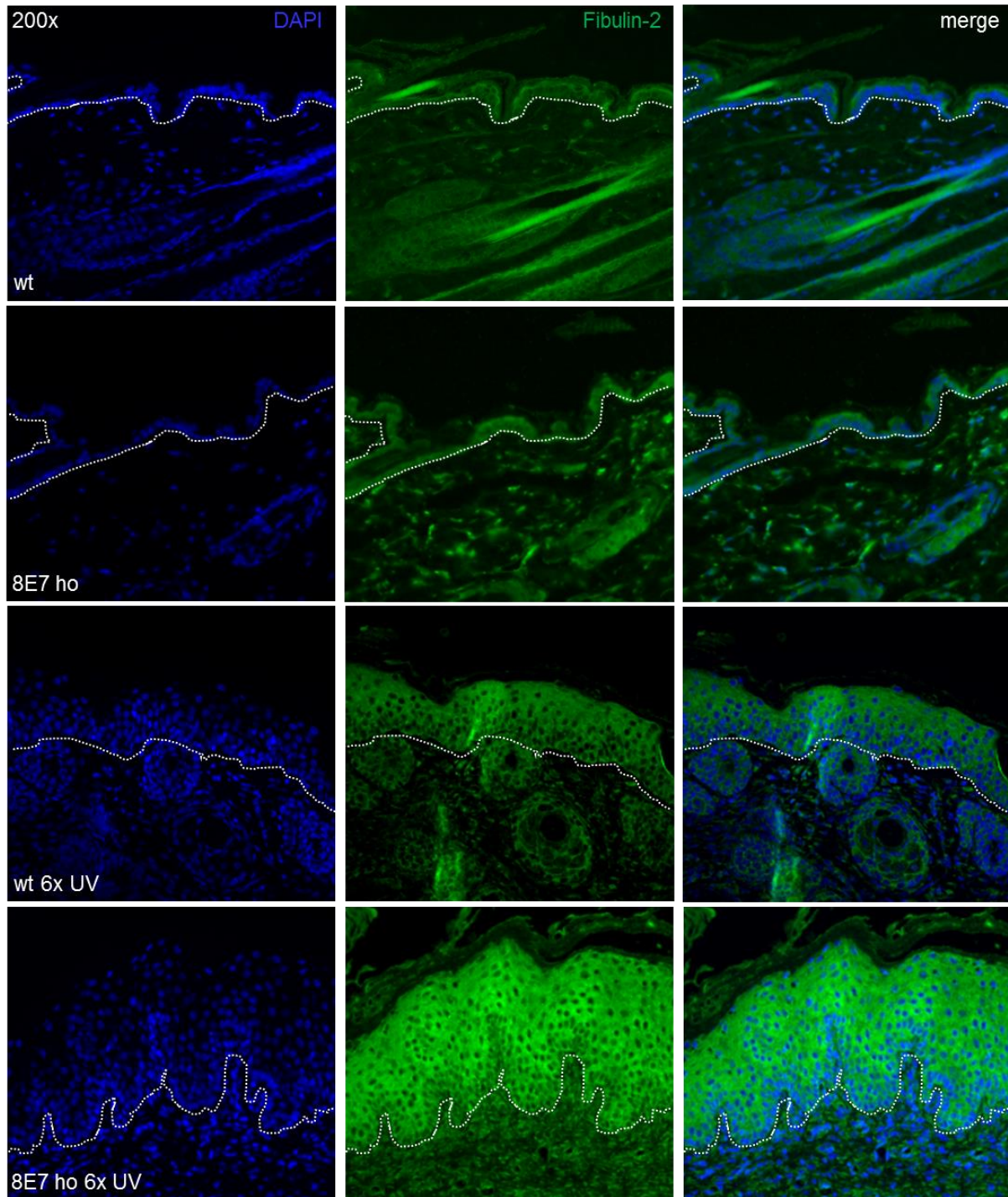
Figure 36. Elevated levels of Fibulin-2 in chronically irradiated skin of K14-HPV8-E7ho mice. Representative immunofluorescence staining for Fibulin-2 on FVB/n wt and K14-HPV8-E7ho transgenic mice skin sections. Increased levels of Fibulin-2 were detected in chronically irradiated skin of K14-HPV8-E7ho mice, weaker levels were also detected in treated skin of wt mice. Tissue was counterstained with DAPI (blue) (dashed line represents the BM zone, original magnification 200x).

4.4 Reduced affinity of HPV8-E7-L23A to cellular targets

4.4.1 HPV8-E7-L23A binds with low affinity to PTRF and ATP5B when compared to HPV8-E7wt

To identify cellular interaction partners for 8E7wt, C33a cells were transiently transfected with pCMV-8E7wt-FLAG and co-immunoprecipitated cellular proteins were analysed by mass-spectrometry. In addition, possible 8E7 interaction partners were identified in the yeast-two-hybrid (Y2H) system (Grigat 2004, Eker 2005). Predicted targets from both assays are presented in table 2. By comparing the results, the ATP synthase, H+ transporting, F1-complex, beta-polypeptide (ATP5B) and the polymerase I and transcript release factor (PTRF) were identified as matched targets. In order to confirm ATP5B and PTRF as 8E7 binding proteins and to test whether 8E7-L23A shows a different binding affinity to these proteins, FLAG-Co-IP experiments were performed. As shown in figure 37, ATP5B and PTRF could be confirmed as 8E7 binding proteins. Interestingly, 8E7-L23A showed significantly reduced affinity to these cellular proteins (figure 37 B).

To test whether 8E7 alters ATP5B and PTRF expression in PHK, we next probed total cell extracts from PHK-8E7wt and PHK-8E7-L23A, grown on fibronectin, for ATP5B and PTRF. Immunoblotting against ATP5B showed no changes in protein expression (figure 38). Since PTRF and PTRF-associated protein caveolin-1 are both associated with cancer cell invasion (Trimmer *et al.* 2013, Liu *et al.* 2014), both markers were tested by immunoblotting. Whereas, Caveolin-1 levels were not changed upon 8E7wt and 8E7-L23A expression, PTRF showed two protein bands in the 8E7wt lane and a very weak expression of the second band in the control and 8E7-L23A-positive extracts. In figure 39, immunocytochemical stainings of C33a cells transiently transfected with pCMV-FLAG, pCMV-8E7-FLAG and pCMV-8E7-L23A-FLAG identified PTRF predominantly in the nucleus. The staining for 8E7wt and 8E7-L23A using anti-FLAG antibodies overlapped with PTRF staining in the nucleus. Taken together, these results provide the first evidence that 8E7 binds to ATP5B and PTRF and that these factors might have a role in keratinocyte invasion.

Table 2. Predicted cellular interaction targets of HPV8-E7wt. The results of a yeast-two-hybrid (Y2H) assay were compared to the results of the Co-IP/mass spectrometry analysis of C33a cells transiently transfected with pCMV-8E7-FLAG or empty vector control. Targets are listed with gene names and subcellular localisation. Matches in both assays are indicated in bold red.

Y2H	Co-IP/MS	Gene name	Subcellular localisation
ATP5B	**ATP5B**	**ATP synthase, H+ transporting, F1-complex, beta-polypeptide**	**Mitochondria**
	ATP5A1	ATP Synthase, H+ Transporting F1 Complex, Alpha Subunit 1	Mitochondria
	ATP5C1	ATP Synthase, H+ Transporting, F1 Complex, Gamma Polypeptide 1	Mitochondria
	ATP5F1	ATP Synthase, H+ Transporting, Fo Complex, Subunit B1	Mitochondria
	ATP5L	ATP Synthase, H+ Transporting, Fo Complex, Subunit G	Mitochondria
MT-CO2		cytochrome c oxidase II	Mitochondria
MT-CO3		cytochrome c oxidase III	Mitochondria
ARFIP1		ADP-Ribosylation Factor Interacting Protein 1	Mitochondria
PARP		Poly (ADP-Ribose) Polymerase 1	Mitochondria
PTRF	**PTRF**	**polymerase I and transcript release factor**	**Nucleus, cell membrane**
NCOA4		nuclear receptor coactivator 4	Nucleus
BLM		Bloom Syndrome, RecQ Helicase-Like	Nucleus
AP1B1		Adaptor-Related Protein Complex 1, Beta 1 Subunit	Cytoplasm
RPL26		Ribosomal Protein L26	Cytoplasm
	RPL10	Ribosomal Protein L10	Cytoplasm
	RPL12	Ribosomal Protein L12	Cytoplasm
	RPL13a	Ribosomal Protein L13a	Cytoplasm
	RPL23	Ribosomal Protein L23	Cytoplasm
	RPL31	Ribosomal Protein L31	Cytoplasm
	RPLP0	Ribosomal Protein, Large, P0	Cytoplasm
ALMS1		Alstrom Syndrome Protein 1	Cytoplasm
GHITM/Derp2		growth hormone inducible transmembrane protein	Cytoplasm

A

B
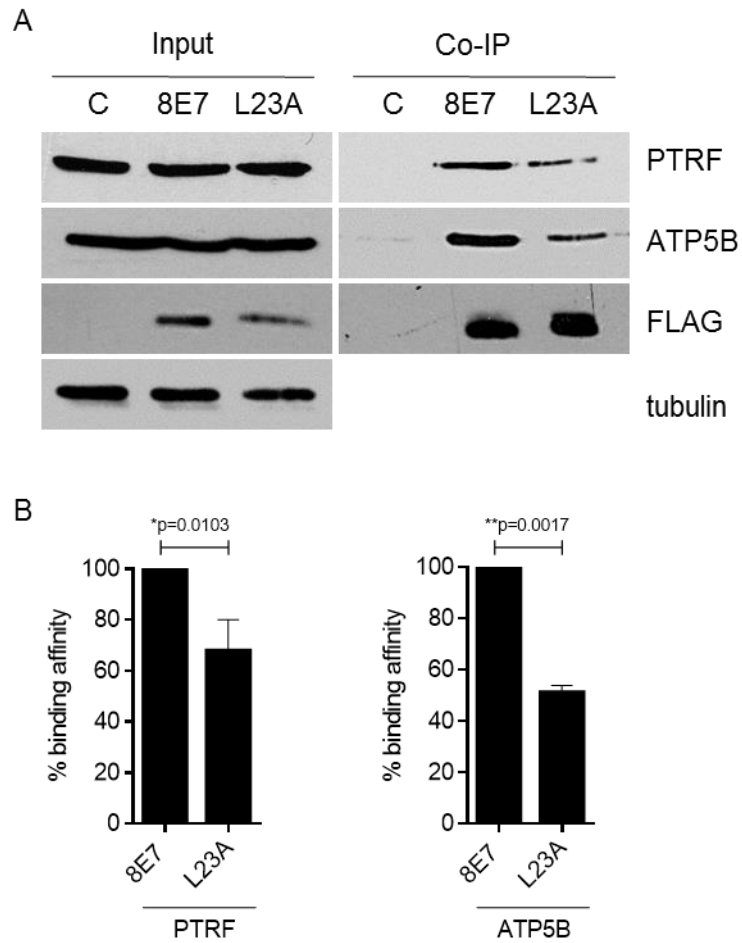
Figure 37. Identification of ATP5B and PTRF as HPV8-E7 binding partners. (A) Left blots: Representative input immunoblots of whole protein lysates of C33a cells either transfected with pCMV-FLAG empty vector or pCMV-8E7-FLAG and pCMV-8E7-L23A-FLAG. Equal loading was confirmed via immunoblotting for tubulin. Right blots: Cell extracts were incubated with M2-FLAG agarose beads and co-immunoprecipitated PTRF and ATP5B bound to FLAG-8E7 was detected by immunoblotting with specific antibodies. The expression of FLAG-8E7 was confirmed by a Western blot analysis against the FLAG. (B) Binding affinity of PTRF and ATP5B to 8E7wt and 8E7-L23A was determined by protein band quantification. Binding affinity of 8E7wt was set as 100%.
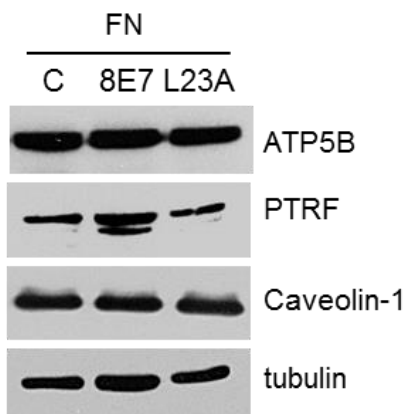
Figure 38. Expression levels of ATP5B, PTRF and Caveolin-1 in PHK-8E7wt and 8E7-L23A. Representative immunoblots of total cell extracts from PHK-8E7wt and PHK-8E7-L23A probed against ATP5B, PTRF and Caveolin-1. Equal loading was confirmed via immunoblotting against tubulin.
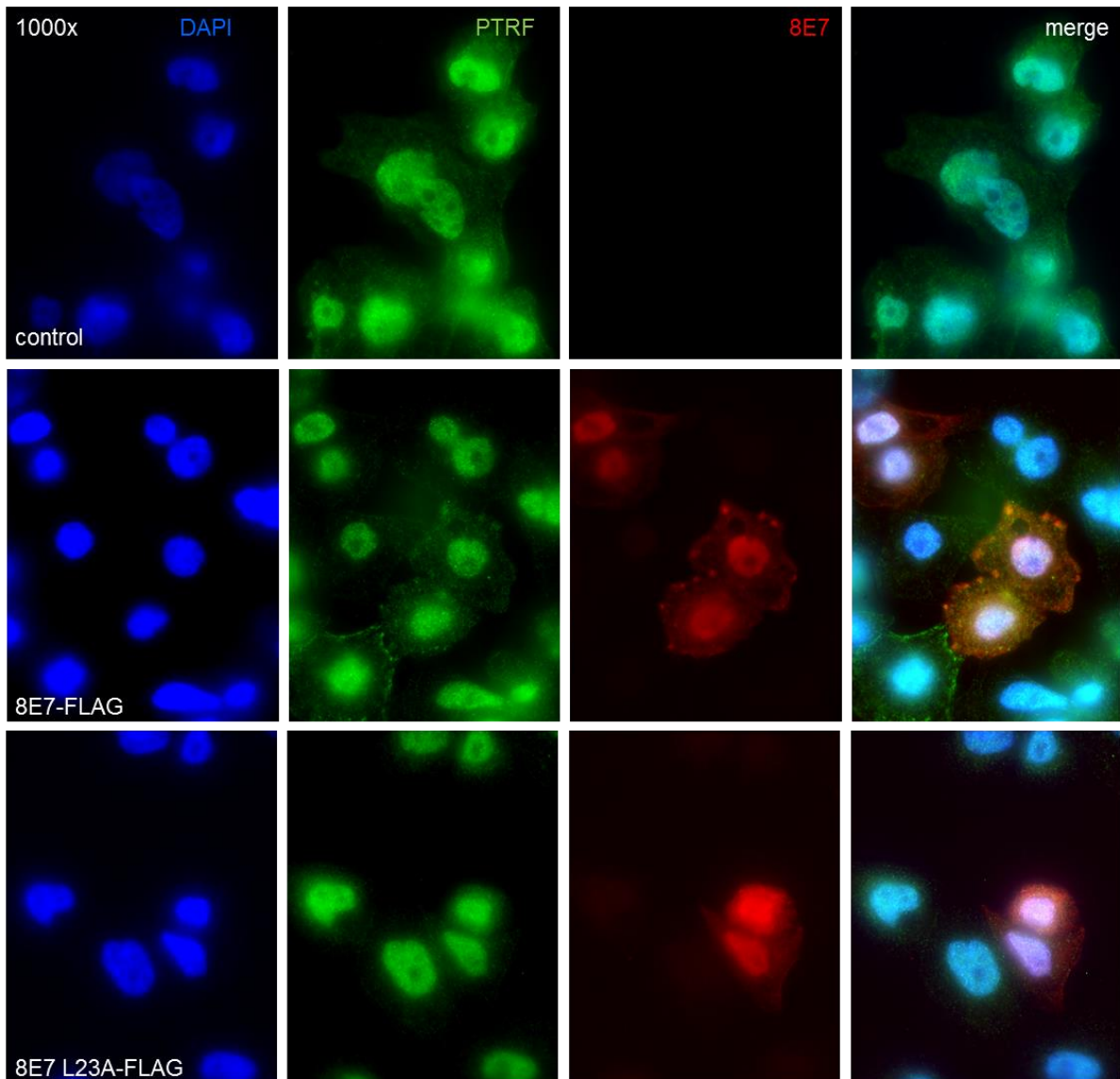
Figure 39. PTRF and 8E7wt/L23A co-localise in the nucleus of C33a cells. Representative images of immunocytochemical stainings of C33a cells transiently transfected with pCMV-FLAG, pCMV-8E7-FLAG or pCMV-8E7-L23A-FLAG were stained against PTRF (green) and 8E7wt or 8E7-L23A (red). Immunocytochemical staining with an α-FLAG antibody was performed to visualise 8E7. The 8E7wt and 8E7-L23A protein is predominantly located in the nucleus, whereas a light staining is also present in the cytoplasm. Nuclear HPV8-E7 overlaps with expression of PTRF. Cells were counterstained with DAPI (blue) (original magnification 1000x).

4.4.2 Modulation of mitochondrial respiratory capacity by HPV8-E7

ATP5B is a subunit of the mitochondrial ATP synthase, which catalyses ATP synthesis during oxidative phosphorylation (Hjerpe *et al.* 2013). To confirm localisation of 8E7 at the mitochondria, C33a cells were transfected either with pCMV-8E7-FLAG, pCMV-8E7-L23A-FLAG or empty vector control and active mitochondria were stained with MitoTracker prior immunocytochemistry. After fixation, the cells were stained against 8E7 by using an anti-FLAG antibody and a corresponding fluorescently labelled secondary antibody. Figure 40 shows that 8E7wt and 8E7-L23A are predominantly

localised in the nucleus, however, they also co-localise to mitochondria in the cytoplasm. In addition, co-immunofluorescence staining verified co-localization of ATP5B with 8E7wt and 8E7-L23A (figure 41).
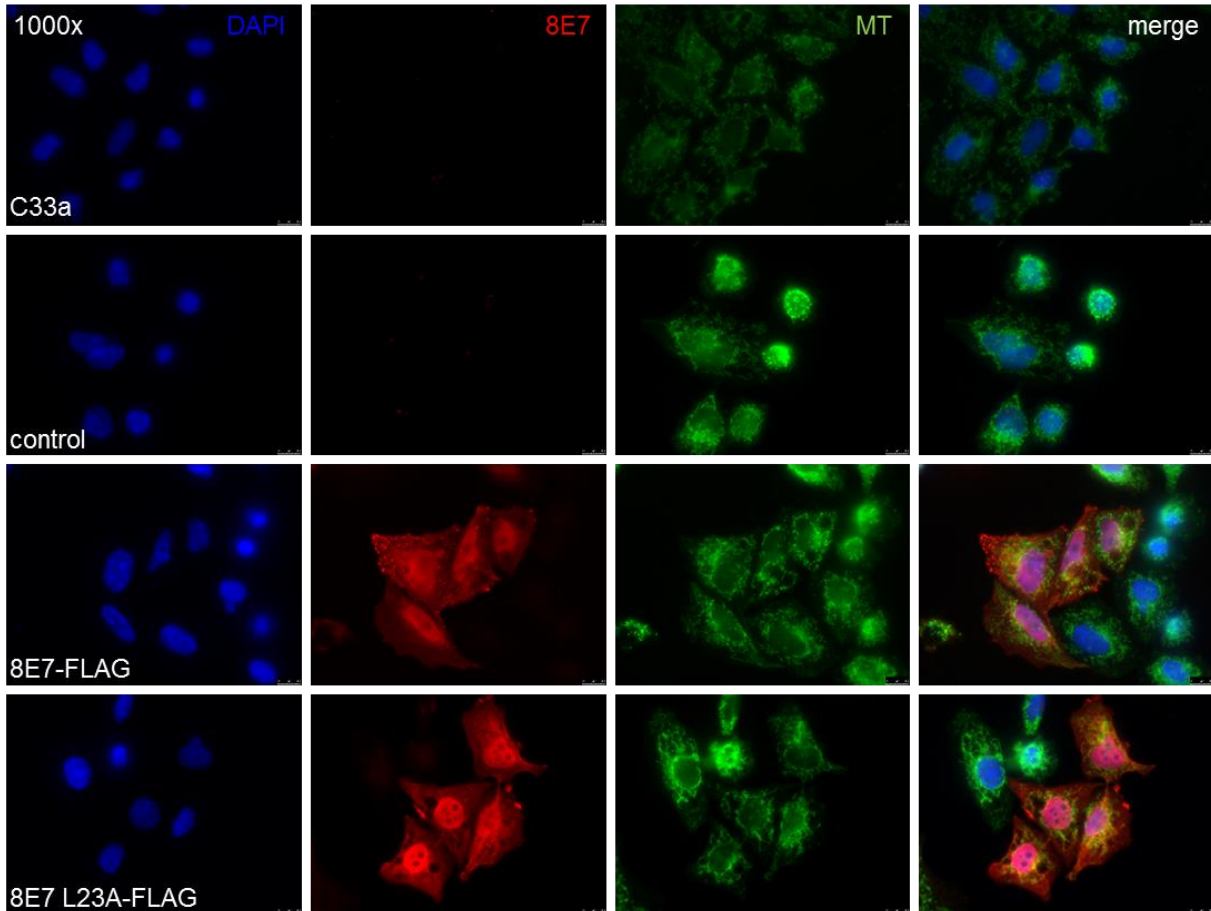
Figure 40. HPV8-E7 is expressed in the nucleus and cytoplasm and overlaps with mitochondrial staining. Representative images of C33a cells stained for mitochondria (green) by using a MitoTracker (MT) dye and against HPV8-E7 using an α-FLAG antibody (red). The top row shows the staining of empty C33a cells fixed after 48h. C33a cells were transiently transfected with pCMV-FLAG, pCMV-8E7-FLAG or pCMV-8E7-L23A-FLAG, stained for mitochondria after 48h and fixed with 4% paraformaldehyde. Immunocytochemical staining with an anti-FLAG antibody was performed to visualise HPV8-E7. The 8E7wt and 8E7-L23A protein is predominantly located in the nucleus, whereas a light staining is also present in the cytoplasm. The cytoplasmic 8E7 staining overlaps in some areas with the mitochondrial staining. Cells were counterstained with DAPI (blue) (magnification 1000x).
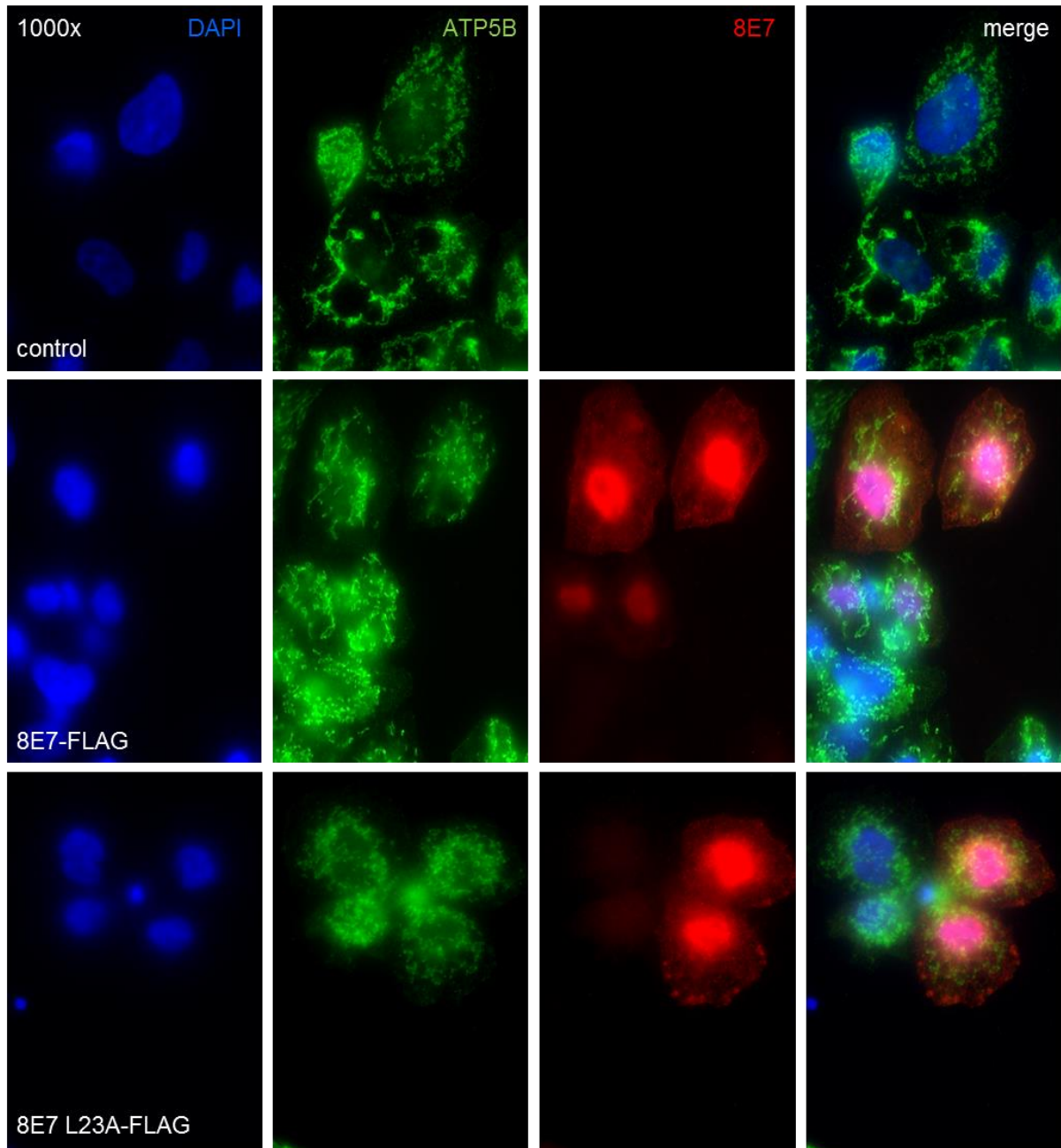
Figure 41. ATP5B and HPV8-E7 are co-localised in the cytoplasm. Representative images of immunocytochemical stainings of C33a cells transiently transfected with pCMV-FLAG, pCMV-8E7-FLAG or pCMV-8E7-L23A-FLAG against ATP5B (green) and 8E7 (red). The top row shows the staining of empty vector C33a cells fixed after 48h, only positive for ATP5B. Immunocytochemical staining with an α-FLAG antibody was performed to visualise 8E7. The 8E7wt and 8E7-L23A protein is predominantly located in the nucleus, whereas a light staining is also present in the cytoplasm. The cytoplasmic 8E7 stainings overlap in some areas with the staining against ATP5B. Cells were counterstained with DAPI (blue) (original magnification 1000x).

Since, in addition to ATP5B, additional mitochondrial proteins have also been predicted as potential 8E7 binding proteins (see table 2), we next asked the question whether the mitochondrial respiratory chain performance is affected by E7. Therefore, N/TERT-8E7wt cells were analysed using the Seahorse XF^{e}96 Extracellular Flux Analyser. Preliminary data of one experiment, performed in triplicate, could only be performed with cells cultured in RM+ media. In the Seahorse XF Mito Stress Test the basal respiration, the spare respiratory capacity, proton leak and ATP production were determined (figure 42 A). These parameters represent different functions of mitochondrial respiration, which can be determined by the oxygen consumption rate (OCR) during the specific experimental phases. Basal respiration was found to be slightly higher in N/TERT-8E7 compared to control cells (figure 42 B and C) and associated also with a slight increase in total ATP production. The addition of FCCP led to unhindered electron flow and maximal oxygen consumption of the cells allowing maximal respiration. The difference between maximal and basal respiration, named spare respiratory capacity, was found to be almost zero. Interestingly, a strong increase in spare respiratory capacity could be determined for N/TERT-8E7 cells (figure 42 B and C), suggesting that E7 might be able to drive the cell into a state where it can respond to increased energy demand.
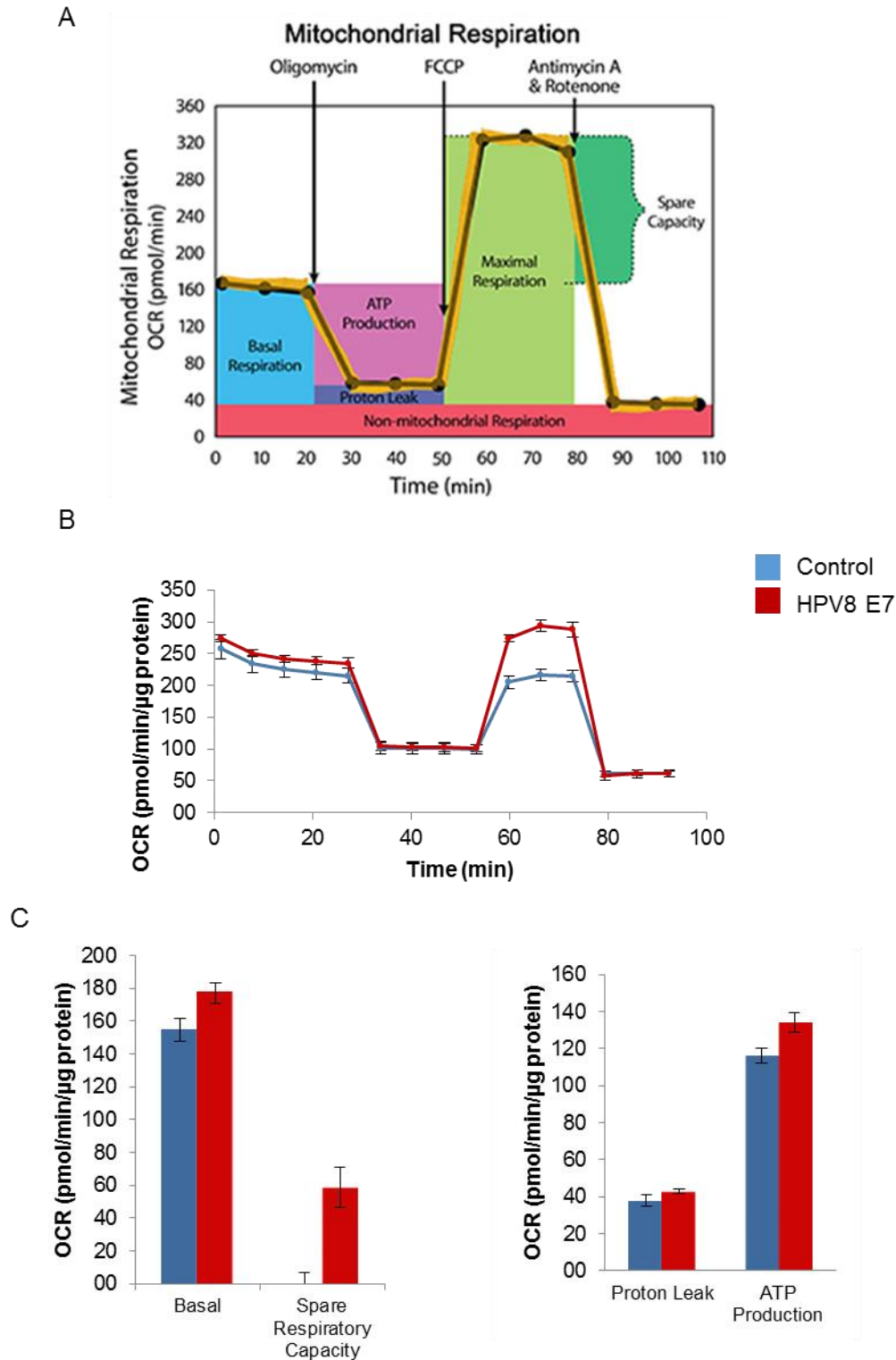
Figure 42. HPV8-E7 cells show modified mitochondrial functions. (A) Schematic diagram of the course of the Seahorse XF Cell Mito Stress Test. This assay uses the oxygen consumption rate (OCR) to analyse parameters of mitochondrial function. Different modulators (oligomycin, FCCP and rotenone/antimycin A) are serially added to the cells in the XF 96-well microtiter plate to modulate respiration by targeting the electron transport chain in the mitchondria determining basal respiration, ATP production, maximal respiration and non-mitochondrial respiration. The level of non-mitochondrial respiration is substracted from all parameter. (B) First results (n=1 in triplicate) of N/TERT-8E7 (grown in RM+ media) and control cells analysed by Cell Mito Stress assay. (C) Bar charts show OCR levels representing specific parameters of the mitchrondrial respiratory performance. All measurements were normalised to protein levels.

4.4.3 HPV8-E7wt and HPV8-E7-L23A differ in their binding affinity to phospholipids

4.4.3.1 HPV8-E7wt binds to the phospholipid phosphatidylserine

Recent studies indicated that phosphatidylinositides and their metabolizing enzymes are associated with various pathophysiological disorders, including cancer. They control various aspects of cell biology in part by interacting with and regulating downstream protein partners (Fiume *et al.* 2015).

To analyse possible phospholipid binding properties of 8E7, a protein-lipid overlay assay system on PIP-Strips (Echelon Biosciences, Salt Lake City, USA) was used. This assay has 15 different phospholipids spotted on a nitrocellulose membrane, which was overlaid with total cell extracts of C33a cells either transfected with pCMV-8E7wt-FLAG, pCMV-8E7-L23A-FLAG or empty vector control. FLAG antibodies were used to develop the overlay assay. 8E7wt showed a strong binding specificity to phosphatidylserine (PS), which was significantly reduced in strength for 8E7-L23A (figure 43).
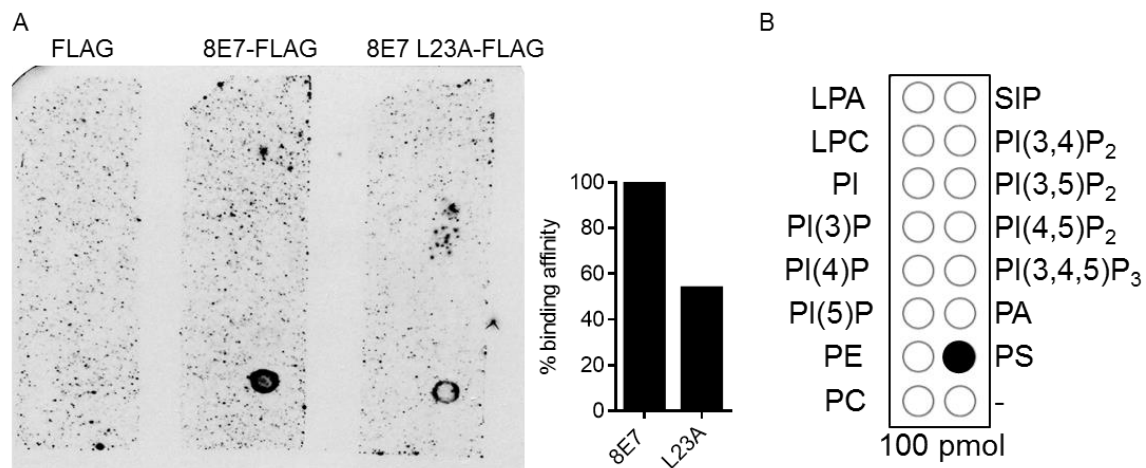
Figure 43. Identification of phosphatidylserine as HPV8-E7 binding phospholipid. (A) Representative image of PIP-Strips incubated with total cell extracts of C33a cells transiently transfected with pCMV2-FLAG, pCMV2-8E7-FLAG or pCMV2-8E7-L23A-FLAG. Membranes were washed and lipid-bound 8E7-FLAG and 8E7-L23A-FLAG was detected with a monoclonal anti-FLAG antibody. Binding affinity for 8E7-L23A compared to 8E7 was reduced by 50%. (B) Schematic diagram of the nitrocellulose membrane with immobilised phospholipids in 100 picomole spots (PIP-Strip) is shown, with the positive result for 8E7-FLAG to bind to phosphatidylserine. LPA: lysophosphatidic acid; LPC: lysophosphocholine; PI: phosphatidylinositol; PI(3)P: phosphatidylinositol (3) phosphate, PI(4)P: phosphatidylinositol (4) phosphate, PI(5)P: phosphatidylinositol (5) phosphate PE: phosphatidylethanolamine; PC: phosphatidylcholine; SIP: sphingosine-1-phosphate; PI(3,4)P$_2$: phosphatidylinositol (3,4) biphosphate, PI(4,5)P$_2$: phosphatidylinositol (4,5) biphosphate, PI(3,4,5)P$_3$: phosphatidylinositol (3,4,5) triphosphate, PA: phosphatidic acid; PS: phosphatidylserine.

4.4.3.2   HPV8-E7 induces PI(4,5)P$_2$ production probably by PIP5KIγ

Our group recently demonstrated that HPV8-E6 expression leads to the increase of nuclear phosphatidylinositol-4,5-bisphosphate (PI(4,5)P$_2$) with a potential clinical significance for HPV induced cancer development (Marx and Akgül, unpublished). PI(4,5)P$_2$ is a membrane phospholipid, which is indirectly involved in the process of cell invasion (Wu *et al.* 2011, Goni *et al.* 2014). PI(4,5)P$_2$ is synthesised in mammalian cells either due to the phosphorylation of phosphatidylinositol-4-bisphosphate (PI5P) by phosphatidylinositol-5-phosphate-4-kinase type II (PIP4KII) or, primarily, by type I phosphatidylinositol 4-phosphate 5-kinase (PIP5KI), which phosphorylates phosphatidylinositol-4-phosphate (PI(4)P). Three isoforms of PIP5KI, namely PIP5KI-α, -β and –γ, exist in humans (Wu *et al.* 2011).
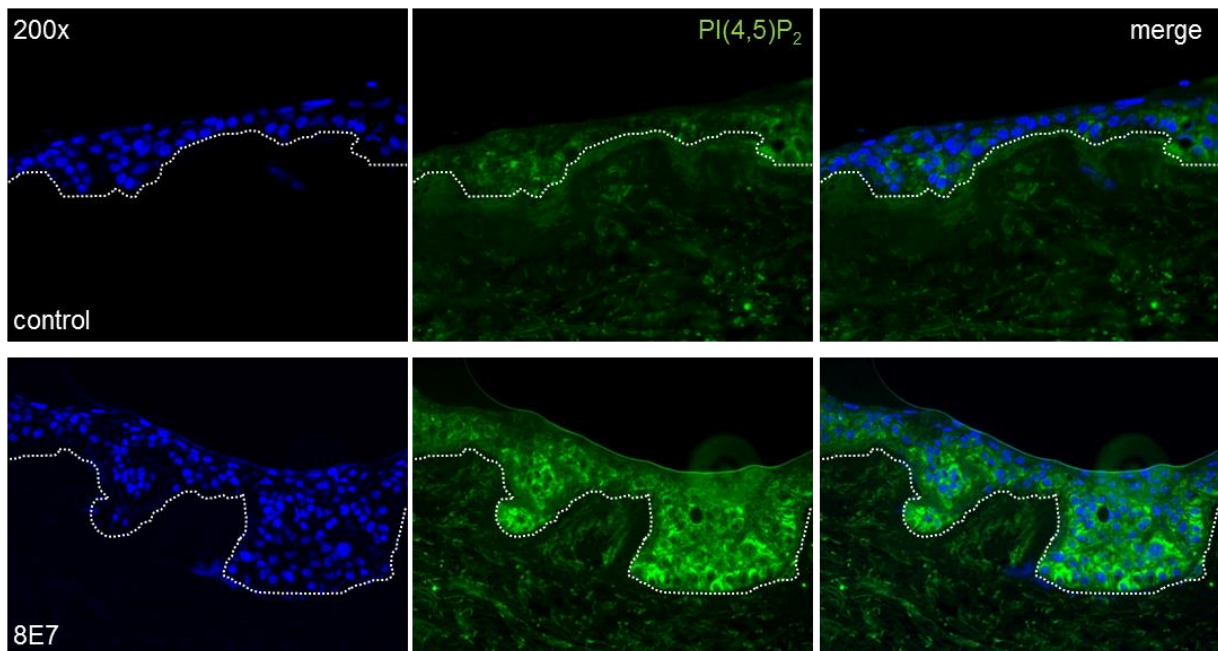
Figure 44. Increased PI(4,5)P$_2$ levels in HPV8-E7 positive OSCs. Representative immunofluorescence staining of OSCs established with keratinocytes expressing either 8E7 or empty vector control against PI(4,5)P$_2$ (green). Increased cytoplasmic levels of PI(4,5)P$_2$ were detected for 8E7 positive OSCs compared to control. Tissue was counterstained with DAPI (blue) (magnification 200x).

Although 8E7 did not bind to PI(4,5)P$_2$ in the PIP-Strip assay, we still analysed whether elevated levels of PI(4,5)P$_2$ can be found in 8E7 positive keratinocytes. Therefore, immunofluorescence staining against PI(4,5)P$_2$ on OSCs and murine skin was performed. The regenerated epithelium of OSCs established with N/TERT-8E7 expressing keratinocytes showed indeed elevated levels of cytoplasmic PI(4,5)P$_2$, compared to empty vector control (figure 44). For untreated K14-HPV8-E7^{ho} skin, only a fussy fluorescent signal was determined. However, chronically irradiated skin of K14-HPV8-E7^{ho} mice showed strongly elevated levels of cytoplasmic PI(4,5)P$_2$ throughout

the suprabasal layers of the skin, whereas chronically irradiated wt skin showed only neglectable changes (figure 45). Unfortunately, no data could be generated for the effect of 8E7-L23A on PI(4,5)P$_2$ due to the lack of OSCs and transgenic skin.
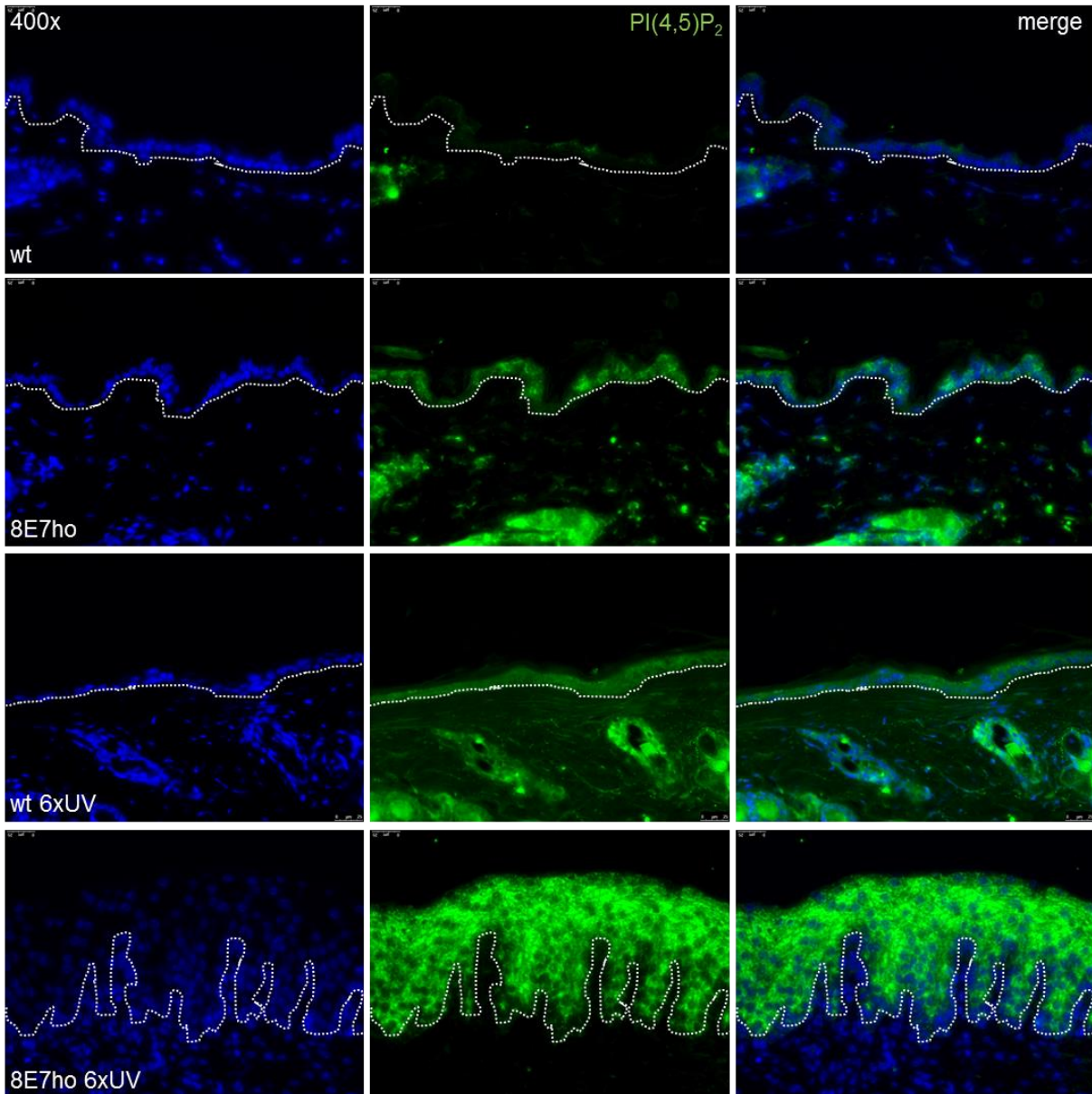
Figure 45. Elevated levels of PI(4,5)P$_2$ in UV treated skin of K14-HPV8-E7^{ho} mice. Representative immunofluorescence staining of untreated and UV treated skin of wt and K14-HPV8-E7^{ho} mice against PI(4,5)P$_2$ (green). Increased levels of PI(4,5)P$_2$ were detected in basal and suprabasal layers of treated K14-HPV8-E7^{ho} skin, located in the cytoplasm. Tissue was counterstained with DAPI (blue) (magnification 200x).

To determine whether increased PI(4,5)P$_2$ levels can be associated with changes in PIP5KI expression levels, qRT-PCRs were performed for N/TERT-8E7 grown on Matrigel and fibronectin. In figure 46, expression levels for PIP5KIγ were measured in N/TERT-8E7 cells and significant increases were detected for cells grown on Matrigel (1.5 fold) and fibronectin (2-fold) compared to control cells. The 2-fold increase of

PIP5KIγ in N/TERT-8E7 on fibronectin was reduced to 0.5-fold, in N/TERT-8E7-L23A cells grown on fibronectin. Taken together, these data indicate that enhanced levels of PI(4,5)P$_2$ and PIP5KIγ may be involved in 8E7-mediated invasion.
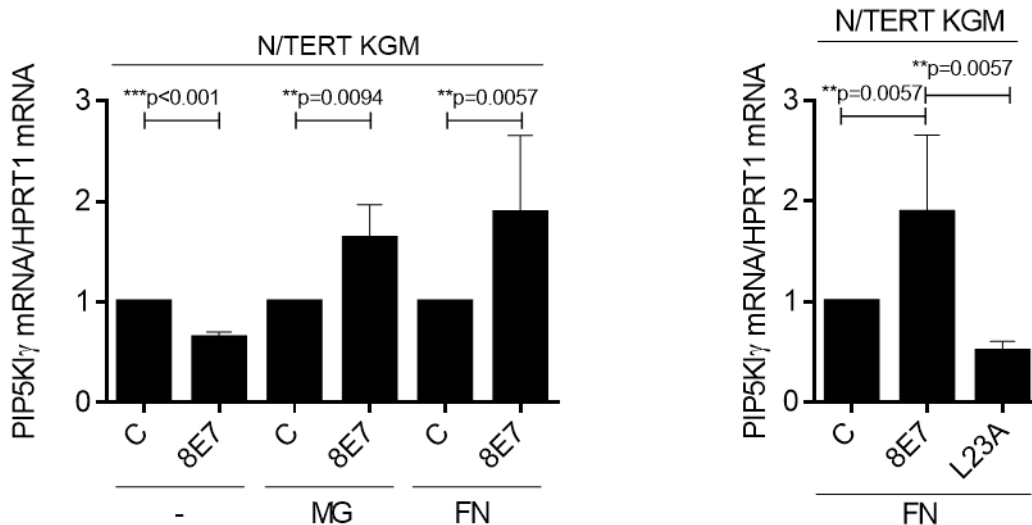
Figure 46. Increased expression of PIP5KIγ in HPV8-E7 positive keratinocytes. Expression levels of PIP5KIγ were determined via qRT-PCR in N/TERT-8E7, N/TERT-8E7-L23A and empty vector cells grown on plastic, Matrigel or fibronectin for 4 days. On the left, a significant increase in PIP5KIγ expression levels was determined in N/TERT-8E7 cells either grown on Matrigel (increase to 1.5-fold, **p=0.0094) or fibronectin (increase to 2-fold, **p=0.0057) compared to their matched controls. The right image shows that the PIP5KIγ mRNA levels were reduced in N/TERT-8E7-L23A cells to 0.5-fold when grown on fibronectin (**p=0.0057). Relative expression levels of the corresponding controls were set as 1. MG: Matrigel, FN: fibronectin, C: control

4.5   Effect of HPV8-E7wt and HPV8-E7-L23A on HPV8 replication

To finally analyse the effect of 8E7-L23 on the viral life cycle, we analysed its effect on DNA replication. In a previous study, Iftner and colleagues demonstrated that replication efficiency was higher in the presence of 8E7 leading to the suggestion that 8E7 positively acts on viral replication (Iftner *et al.* 1988).

To test whether 8E7-L23A has a different effect on HPV8 replication compared to 8E7wt, we mutated the HPV8 genome containing plasmid pVE34 (Steger *et al.* 1990) and transfected pVE34wt and pVE34-L23A in RTS3b cells to allow transient replication. After 72h, episomal DNA was extracted, halved whereby one half was digested with *Dpn*I to cut the transfected bacterially generated input DNA. The number of replicated pVE34 was quantified by using HPV8-E2 specific PCR primers. Interestingly, the number of pVE34-L23A plasmids increased 5-fold, when compared to pVE34wt (figure 47). This led to the conclusion that the position L23 in 8E7 is not only crucial for invasion, but also surprisingly impeding genome replication.
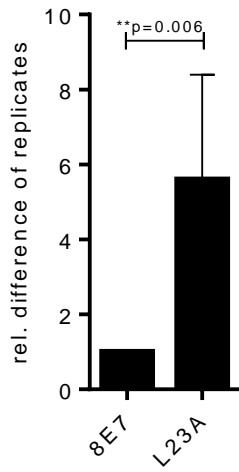
Figure 47. Increased replicative capacity of HPV8-E7-L23A determined in transient replication assays. RTS3b cells were transfected either with pVE34 (including the whole HPV8 genome) or with pVE34-L23A, harvested after 72h and qRT-PCR was performed on episomal DNA to test the number of replicates. A 5-fold increase in the number of replicates was determined for cells transfected with pVE34-L23A compared to the pVE34wt.

5. Discussion

To unravel the oncogenic mechanism of HPV8-E7 *in vitro* and *in vivo*, different experimental approaches were used analysing the effects of ECM proteins and coupled downstream processes on keratinocyte invasion. The K14-HPV8-E7 transgenic mice, generated within this study, spontaneously developed skin tumours characterised by keratinocyte hyperplasia in 43% of animals within the observation period of 28 months, although E7 mRNA levels were relatively low. A single UV treatment was successfully used in previous studies of K14-HPV8-E2, K14-HPV8-E6 and K14-HPV8-CER transgenic animals (Schaper *et al.* 2005, Pfefferle *et al.* 2008, Marcuzzi *et al.* 2009) to induce papilloma growth by activating the human K14-promoter and increasing oncoprotein levels (Hufbauer *et al.* 2010b). Six UV irradiations led to an increase of HPV8-E7 mRNA levels and to the development of flat to polypus skin tumours, characterised by strong hyperplasia and areas with carcinoma *in situ*. Interestingly, no papilloma formation was observed in E7 mice, which was a strong characteristic of the E2, E6 and CER animals. We speculate that the E7-associated effects within the CER animals could not be specified after UV irradiation due to fast E6-associated papilloma formation. The observation that E7-mediated severity of tumour grade was dose-dependent is in line with the previously described association between E2-mRNA levels and tumour formation rate in K14-HPV8-E2 mice, leading to the suggestion that a certain threshold of oncogene expression is critical for tumour formation (Pfefferle *et al.* 2008). The establishment of the K14-HPV8-E7 transgenic mouse line was associated with difficulties allowing the generation of only one low-level expressing founder animal. In addition, only minor differences of E7 expression levels were determined between hemizygous and homozygous animals. For HPV16, it could be demonstrated that E7 is able to increase apoptosis (Stöppler *et al.* 1998, McLaughlin-Drubin and Münger 2009). Therefore, it might be suggested that high levels of E7 are associated with lethality and thereby represent some kind of natural selection for low E7 levels. However, the development of carcinoma *in situ* in mice with low E7 expression levels clearly indicates a strong carcinogenic potential of this viral oncoprotein. Nevertheless, it remains to be verified that metastatic SCCs can develop in E7-positive mice and whether mutagenic effects of UV may have contributed to carcinoma *in situ* formation. In line with observations of the K14-HPV8-E7 mice, K14-HPV38-E6/E7 (another betaHPV type) mice developed only minor skin alterations after

single UV treatment, but actinic keratosis and SCCs after chronic UV irradiation (Viarisio *et al.* 2011). Recent case control studies led to the suggestion that betaHPV infection associated with SCC development in the general population implicates its role in cancer initiation rather than its maintenance, which was strengthened by increased prevalence and viral loads of betaHPV in precancerous lesions (Weissenborn *et al.* 2005, Iannacone *et al.* 2014, Howley and Pfister 2015). Therefore, to strengthen the fact that HPV8 is involved in SCC development due to its presence in the early stages of tumour initiation, the generation of inducible transgenic mouse models for HPV8 should be considered. In addition, an inducible HPV8-E7 system will probably solve the difficulties to establish transgenic mouse lines with higher E7 expression levels. The quantitative and time-controlled expression of HPV8 early proteins will provide further evidence for the role of HPV8 in skin cancer initiation and development.

The invasive phenotype of cells is the result of a gradual process including several intermediate steps, including changes in cell-cell interactions. During the dissolution of cell-cell interactions in EMT, β-catenin is no longer able to interact with E-cadherin and is either degraded or protected from degradation in response to Wnt signalling (Lamouille *et al.* 2014). OSCs established with HPV5-E7 and HPV8-E7 showed a strong overexpression of cytoplasmic and mainly membrane-tethered β-catenin levels in the granular layer. However, elevated levels of β-catenin could not be associated with the activation of the canonical Wnt pathway. This disagrees with the findings of β-catenin relocalisation from the plasma membrane to the nucleus in the presence of HPV16-E6/E7 (Uren *et al.* 2005, Stenner *et al.* 2011). However, in line with our observation, increased β-catenin levels were localised at plasma membranes in respiratory papilloma caused by HPV6 or 11 (Lucs *et al.* 2014). In addition, β-catenin is also important for the organisation of the actin cytoskeleton by the interaction with α-catenin, thereby recruiting actin to the plasma membrane (Baum and Georgiou 2011). Enhanced actin staining of HPV5-E7 and HPV8-E7 positive tissues may indicate that the E7 proteins disturb β-catenin functions in the differentiation-dependent anchoring of actin-filaments to cell junctions. This is in association with the identification of deregulated proteins involved in the organisation of the actin cytoskeleton, which were determined in HPV8-E7 expressing cells by 2D-DIGE experiments (Akgül *et al.* 2009).

The interaction between occludin and ZO-1 is important to maintain the structure of tight junctions, in which occludin is linked to the actin cytoskeleton. The tight junction protein ZO-1 is also found outside of distinct membrane structures, suggesting tight junction-structure-dependent and structure-independent functions (Brandner *et al.* 2015). ZO-1 is described to be downregulated in most cancer tissues, allowing increased motility (Kalluri and Weinberg 2009). However, first evidence of upregulated expression levels of ZO-1 in cancer were identified in human melanoma, in which increased ZO-1 expression contributed to the oncogenic behaviour (Smalley *et al.* 2005), which supports our finding of increased levels of ZO-1 in association with HPV5-E7 and HPV8-E7 expression. A broader expression pattern of ZO-1 in epidermal layers has previously been shown in skin SCCs, which suggests that ZO-1 contributes to tumour progression, largely in a tight junction independent manner (Morita *et al.* 2004, Brandner *et al.* 2015). Thus HPV5-E7 and HPV8-E7 induced ZO-1 levels may be involved in cellular processes enabling keratinocyte invasion, whereby the classical downregulation of ZO-1 during EMT does not play a role. Elevated expression of β-catenin and ZO-1 in the skin of transgenic HPV8 mice and EV lesions supports a possible clinical relevance of these data. Taken together, changes in β-catenin and ZO-1 expression in betaHPV-positive epithelia may disturb adherens and tight junction composition, thereby unbalancing cell homeostasis and contributing to HPV5 and HPV8 mediated carcinogenic processes. This is in line with the description of partial EMT, that invading cells do not necessarily need to possess all EMT characteristic changes (Lamouille *et al.* 2014).

Cell invasion is not only achieved by the dissolution of cell-cell adhesion, but also due to the reorganisation of cell-ECM interactions, whereby the loss of epithelial cell characteristics is associated with the gain of mesenchymal-like properties, representing another hallmark of cancer (Guan 2015, Aneta *et al.* 2016). Migrating cells utilise different modes of cell migration, including collective and single cell invasion, which are associated with differently expressed epithelial and mesenchymal cell characteristics (Aneta *et al.* 2016). The expression of HPV8-E7 led to a reduction of E-cadherin in the suprabasal cell layers of OSCs. This observation is in line with a weak expression of E-cadherin in skin SCCs and their precursor lesions (Kurtz *et al.* 2006, Margulis *et al.* 2006) and further corroborates to recent data showing that 16E7 decreased E-cadherin levels and induced the expression of N-cadherin in PHK grown

as monolayer cultures (Hellner *et al.* 2009). In contact with ECM proteins, 8E7 probably induces different modes of invasion. Without inducing a cadherin switch, 8E7 might promote collective cell invasion in contact with collagen IV and laminin, whereby 8E7-positive cells, when grown on fibronectin induce a cadherin switch and EMT. The presence of fibronectin has an important effect on the ability of the epidermal keratinocytes to migrate (Juhasz *et al.* 1993), whereby adhesion of cancer cells to fibronectin is known to enhance their tumorigenicity (Han and Roman 2006). The EMT-mediated invasion of 8E7 cells may be associated with single-cell invasion, a mode accepted to increase metastatic efficiency of a cancer (Krakhmal *et al.* 2015).

The ECM protein fibronectin is organised into a fibrillary network through direct interactions with different cell surface receptors, including integrins, and is secreted from different cells as a soluble, inactive, disulphide-bonded dimer, responsible for matrix stability (Mao and Schwarzbauer 2005, Sabatier *et al.* 2009). Different fibronectin isoforms are generated by alternative splicing containing an extra domain A (EDA) or B (EDB). Fibronectin[EDA] has been implicated in the regulation of wound healing and is more potent in promoting cell spreading and migration irrespective of the presence or absence of EDB (Grinnell 1984, Manabe *et al.* 1997, Sun *et al.* 2014). 8E7 stimulates fibronectin and fibronectin[EDA] expression and secretion in keratinocytes, as well as fibronectin expression in fibroblasts, both of which may have contributed to the deposition of fibronectin in the peritumoral stroma of betaHPV-positive skin SCCs. Interestingly, 8E7 was able to increase fibronectin promoter activity, which was reduced to normal levels due to a mutated Sp1 site of the fibronectin promoter. It needs to be clarified, whether E7 controls fibronectin promoter activity in cis, in a complex with Sp1, or in trans, through controlling Sp1 levels by the amount of pRB (Kim *et al.* 1992, Rey *et al.* 2000, Akgül *et al.* 2007). However, currently it cannot be excluded that other transcription factors are involved in E7-mediated fibronectin promoter regulation. In line with these observations it could be shown that 16E7 and 18E6/E7 can also stimulate fibronectin expression (McCormack *et al.* 1997, Hellner *et al.* 2009). In 18E6/E7-immortalised keratinocytes fibronectin expression was paralleled by increased expression and activity of the FAK, which is an early mediator of integrin-mediated signalling regulating cell motility and proliferation (McCormack *et al.* 1997, Chen *et al.* 2010).

Changed cell adhesion to the ECM, in conjunction with integrin interaction, is an important regulator of keratinocyte invasion, whereby upregulated integrin subunits can be used as an indicator for invasive cells (Pawelek and Chakraborty 2008). Therefore, a further link to invasion is the ability of 8E7 to induce the cell surface levels of the integrin α3 chain. The mechanistic link is supported by the effect of siRNA-mediated α3 knockdown, depleting the invasive character of 8E7-positive keratinocytes. Furthermore, the invasion-defective mutant 8E7-L23A showed reduced levels of integrin α3 on the cell surface. Therefore, a role of integrin α3 chain in 8E7-mediated invasion could be confirmed. Numerous studies using primary or immortalised keratinocytes have identified a role of integrin α3β1 in a range of cell functions including tumour progression, ECM organisation and invasion (Margadant *et al.* 2010, Aggarwal *et al.* 2014, Missan *et al.* 2014). The involvement of α3β1 in skin tumorigenesis has recently been demonstrated *in vivo* in epidermal-specific deletion leading to reduced tumour development. However, tumours which developed in those mice progressed more rapidly to invasive carcinoma, indicating a requirement for increased α3β1 cell surface location in tumour initiation and early growth, and reduced integrin α3β1 levels during the progression of skin SCC at later stages. In addition, *in vitro* analysis of cell lines representative of several stages of skin carcinogenesis described that integrin α3 chain is inversely correlated with the progression stage (Sachs *et al.* 2012). Although integrin α3β1 is known to bind predominantly to laminin-5, it also binds weaker to collagen IV and fibronectin (DiPersio *et al.* 1997). A previous study described integrin α3β1 as a trans-dominant inhibitor of the main fibronectin receptor integrin α5β1 in non-migratory keratinocytes, whereby a migratory mode can be reached by altered interactions of laminin-5 with integrin α3β1, due to conformational changes in both proteins, relieving trans-dominant inhibitory functions on integrin α5β1 (Hodivala-Dilke *et al.* 1998). Whether high levels of α3β1 lead to conformational changes of laminin-5 and thereby drive E7 cells into a migratory mode needs to be determined. Therefore, increased levels of integrin α3β1 in presence of 8E7 enable a stronger migratory phenotype, inhibiting other integrins on the cell surface, which occurs simultaneously with increased activation of the fibronectin promoter by 8E7.

EMT has been identified to generate cells that either exhibit stem-cell like properties or are poised to enter into the stem cell state. This acquisition of stem cell-like properties holds important implications for the successful completion of the invasion-

metastasis cascade by disseminated cancer cells (Mani *et al.* 2008, Tam and Weinberg 2013). A universal surface marker for epithelial stem cells has not been identified yet. However, in cutaneous SCC cell lines, the epithelial cancer stem cell population can be identified by high cell surface expression of CD44 and EpCAM (Biddle *et al.* 2011). A recent study of our group could show that 8E7 confers cancer stem cell-like traits on keratinocytes, which could be attributed to the pool of CD44^{high}/EpCAM^{high} cells (Hufbauer *et al.* 2013). Here, the CD44^{high}/EpCAM^{high} cell population of 8E7-positive cells showed a higher proportion of integrin α3 chain positivity. This finding suggests that 8E7 may generate invasive malignant stem-like cells through integrin α3β1 cell surface presentation.

A wide range of potential mechanisms, whereby integrins may regulate tumour cell behaviour is known. Interestingly, Missan and colleagues demonstrated that SV40 largeT antigen transformed keratinocytes show high cell surface levels of α3β1, which promotes expression of Fibulin-2 and thereby promoted keratinocyte invasion. Fibulins are a family of extracellular glycoproteins, with the largest protein, Fibulin-2, localised at basement membranes, elastic fibres and other connective tissue structures. Furthermore, Fibulins possess overlapping binding sites for several BM proteins, including fibronectin, participating in the formation of supramolecular structures (Timpl *et al.* 2003). Fibulin-2 has been described as a promoter of malignancy and as tumour suppressor (Schiemann *et al.* 2002, Ramaswamy *et al.* 2003, Gallagher *et al.* 2005). In adenocarcinoma, Fibulin-2 was found to be associated with metastasis and with malignant progression of lung adenocarcinoma (Ramaswamy *et al.* 2003, Baird *et al.* 2013). 8E7 was able to induce increased levels of Fibulin-2, which was verified in 8E7 positive OSCs and in the skin of K14-HPV8-E7 mice. Knockdown experiments of integrin α3 chain verified that 8E7-mediated upregulation of Fibulin-2 was α3-dependent. Therefore, one might suggest that the mechanism of integrin α3-mediated induction of Fibulin-2 and the resulting invasion may share functional similarities in SV40 largeT antigen and HPV8-E7 positive keratinocytes. Surprisingly, increased levels of Fibulin-2 were located in basal and suprabasal layers of the epidermis, rather than in the ECM, which might lead to the suggestion that 8E7 is able to block Fibulin-2 secretion from keratinocytes. Measuring invasion of 8E7 positive cells on a fibronectin matrix and knocked down Fibulin-2 expression will clarify the role of Fibulin-2 in E7-mediated invasion.

The position L23, located few amino acids in front of the conserved pRB binding motif LXCXE (figure 48), has so far not been described to be involved in any protein-protein interactions. Compared to the list of 16E7 interaction partners, only a few interacting proteins are known for 8E7. To gain more insight into possible 8E7 molecular processes, Y2H and Co-IP/MS experiments led to the identification of ATP5B, mitochondrial ATP synthase beta subunit, and PTRF/cavin-1 as E7 interaction factors. Mitochondria play a central role in the physiology of eukaryotic cells, whereby malfunctioning is implicated in the pathogenesis of different human diseases, including cancer (Willers *et al.* 2010).
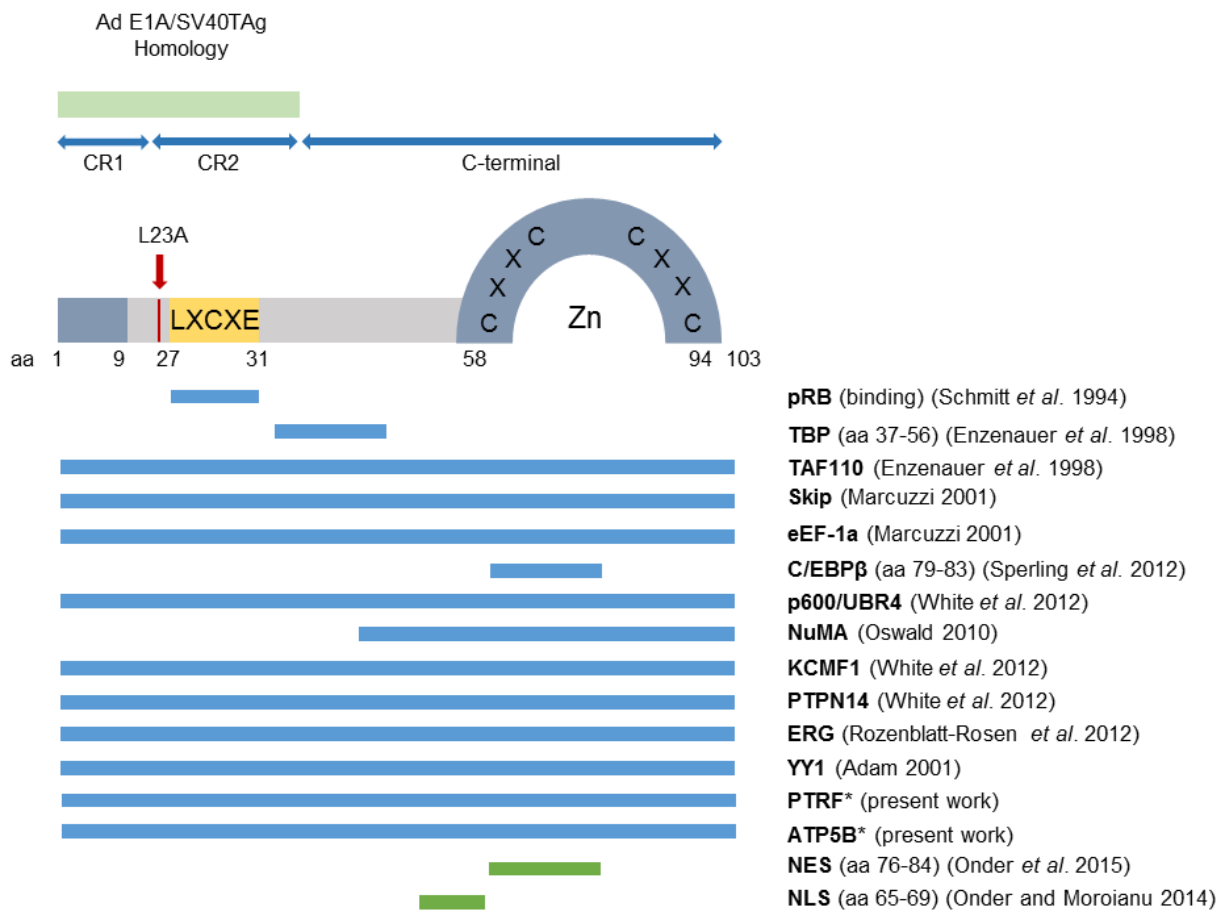
Figure 48. Schematic diagram of the HPV8-E7 protein and interacting cellular proteins (adapted from Münger *et al.* (2001)). Schematic representation of the HPV8-E7-protein with the CR1, CR2 and C-terminal domains. The CR1 and CR2 domains are homologous to the conserved region 1 and 2 of Adenovirus E1A protein. The pRB binding site (LXCXE) is located within the CR2 domain. Biochemical and/or functional interaction domains with cellular proteins are indicated by blue bars. Green bars indicate the nuclear localisation signal (NLS) and the nuclear export signal (NES). The red arrow indicates an amino acid exchange leading to the mutational variant HPV8-E7-L23A (Full-length blue bar: no specific binding motif was determined; asterisks: newly identified 8E7 interaction partner).

To support transformation, differentiation and invasion of malignant cells, cancer cells produce ATP mainly via aerobic glycolysis (Phelan *et al.* 2014). The ATP synthase is involved in ATP synthesis during oxidative phosphorylation being a catalyst by creating an electrochemical proton gradient across the inner membrane of mitochondria (Senior 2007). Decreased expression of ATP5B is associated with different types of tumours (Willers *et al.* 2010). Interestingly 8E7-L23A not able to trigger keratinocyte invasion showed also weaker affinity to ATP5B, when compared to 8E7wt. Since, we could confirm co-localisation of E7 with ATP5B at the mitochondria, we next tested the mitochondrial respiratory chain performance of 8E7 cells. Preliminary data suggest that 8E7 cells have an increased respiratory capacity, which might be used to respond to increased energy demands, required during invasive cell growth and probably during the viral life cycle.

PTRF, also known as cavin-1, belongs to the protein family of cavins, which forms together with caveolins, a complex network establishing the formation of caveolae. Interestingly, PTRF has, like 8E7, a high binding affinity for PS, which promotes the incorporation of PTRF into caveolae (Low and Nicholson 2014). Increased expression of these proteins has been reported to be associated with the development of different diseases and cancer by mediating focal adhesion turnover and FAK stabilization (Urra *et al.* 2012, Faggi *et al.* 2015). In addition, PI(4,5)P$_2$, PIP5KIγ and fibronectin, all upregulated by 8E7, can also target FAK activity during migration (Ling *et al.* 2007, van den Bout and Divecha 2009, Goni *et al.* 2014) This might envision a scenario at the cells leading edge, an area of focal adhesion formation, in which 8E7 may manipulate caveolae formation and focal adhesion turnover leading to an enhanced invasive capacity of 8E7 positive cells. This scenario can be strengthened by the observation that the invasive-defective 8E7-L23A binds weaker to PTRF and does not target PIP5KIγ expression. In line with this hypothesis, a previous study demonstrated that depletion of PIP5KIγ reduces strength of cell adhesion to fibronectin and thereby inhibits invasion of colon cancer cells, which coincided with reduced levels of PI(4,5)P$_2$ (Wu *et al.* 2011).

Additionally to its cell transforming activities, 8E7 is also known to positively influence E1/E2-dependent viral replication (Iftner *et al.* 1989). Interestingly, the HPV8 replication plasmid containing the 8E7-L23A showed a higher replication efficiency compared to E7wt containing vectors. As higher replication rates would probably destroy the natural adaptation of HPV8 in the skin by the activation of immune

responses, the mutation at position L23 did not become prominent as a result of natural selection. Since betaHPV-E7 is expressed in basal as well as differentiating keratinocytes within an EV lesion, the characterisation of cellular factors, differentially binding to E7wt and E7-L23A (probably factors characterised in figure 48), will shed light on the differentiation-dependent maintenance and amplification phases of HPV8 DNA replication (Haller *et al.* 1995).
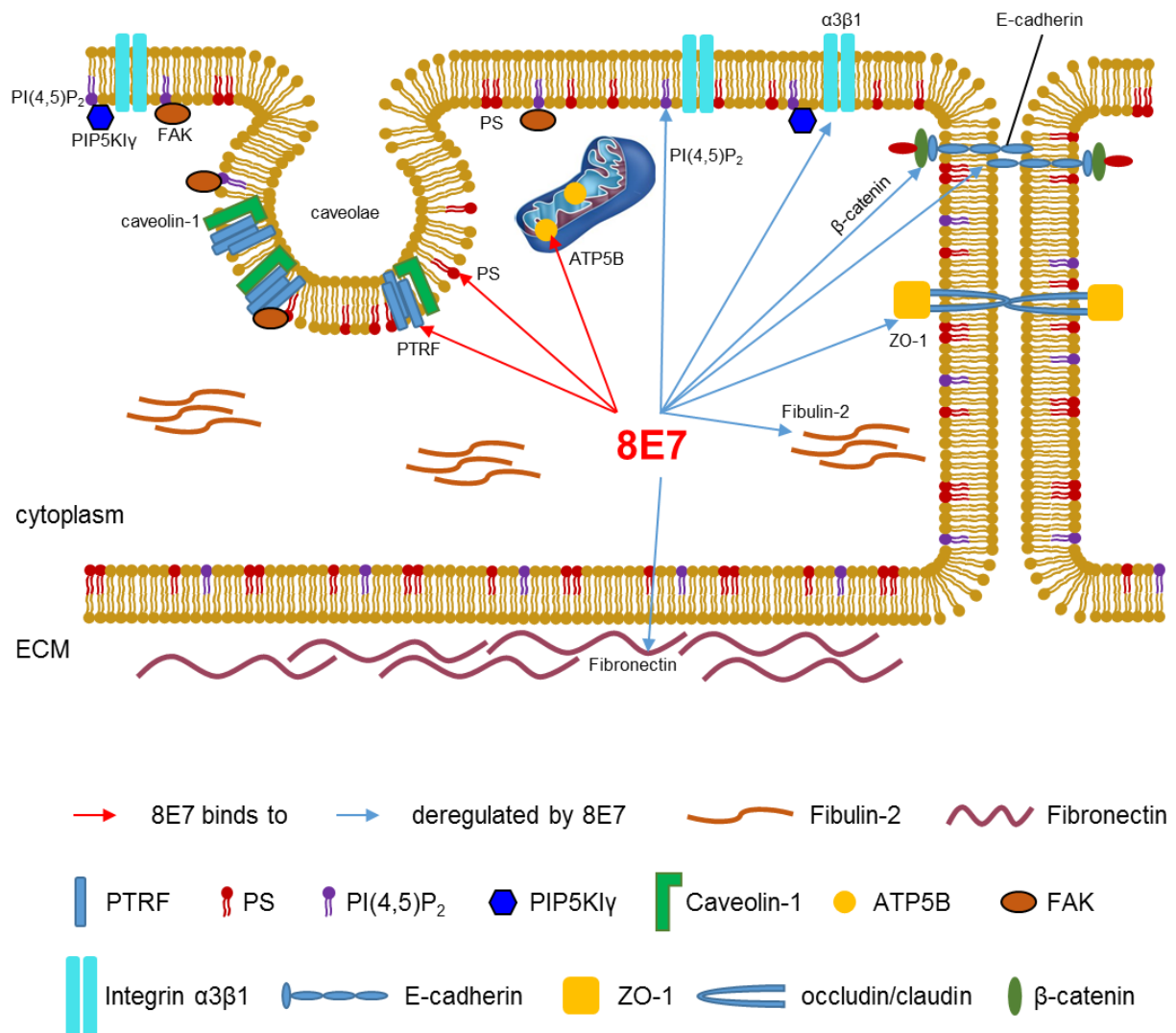
Figure 49. Schematic representation of cellular targets deregulated by 8E7. Red arrows indicate new identified interacting cellular targets of HPV8-E7. Blue arrows indicate all cellular targets deregulated by HPV8-E7.

The aim of this study was to identify and clarify possible molecular processes involved in 8E7-mediated keratinocyte invasion. Several key events of EMT, associated with the development of an invasive phenotype, were identified to play an important role in the invasive capacity of 8E7-positive keratinocytes. The transgenic mouse model, despite low 8E7 expression levels, was useful to strengthen the oncogenic potential of

8E7. This study led to new insights into changed ECM protein composition induced by 8E7, whereby the understanding of the role of 8E7-targeted cellular pathways would probably help to develop new therapeutic strategies against betaHPV associated skin cancer.

6. References

Accardi, R., W. Dong, A. Smet, R. Cui, A. Hautefeuille, A. S. Gabet, B. S. Sylla, L. Gissmann, P. Hainaut and M. Tommasino (2006). "Skin human papillomavirus type 38 alters p53 functions by accumulation of deltaNp73." EMBO Rep **7**(3): 334-340.

Adam, M. (2001). Rolle des zellulären Transkriptionsfaktors YY1 bei der Kontrolle der Replikation und Transkription des humanen Papillomvirus 8 Diploma thesis, University of Cologne.

Aggarwal, A., R. N. Al-Rohil, A. Batra, P. J. Feustel, D. M. Jones and C. M. DiPersio (2014). "Expression of integrin alpha3beta1 and cyclooxygenase-2 (COX2) are positively correlated in human breast cancer." BMC Cancer **14**: 459.

Ajiro, M. and Z. M. Zheng (2014). "Oncogenes and RNA splicing of human tumor viruses." Emerg Microbes Infect **3**(9): e63.

Akgül, B., B. Bauer, P. Zigrino, A. Storey, C. Mauch and H. Pfister (2011a). "Upregulation of lipocalin-2 in human papillomavirus-positive keratinocytes and cutaneous squamous cell carcinomas." J Gen Virol **92**(Pt 2): 395-401.

Akgül, B., R. Garcia-Escudero, C. Ekechi, G. Steger, H. Navsaria, H. Pfister and A. Storey (2011b). "The E2 protein of human papillomavirus type 8 increases the expression of matrix metalloproteinase-9 in human keratinocytes and organotypic skin cultures." Med Microbiol Immunol **200**(2): 127-135.

Akgül, B., R. Garcia-Escudero, L. Ghali, H. J. Pfister, P. G. Fuchs, H. Navsaria and A. Storey (2005). "The E7 protein of cutaneous human papillomavirus type 8 causes invasion of human keratinocytes into the dermis in organotypic cultures of skin." Cancer Res **65**(6): 2216-2223.

Akgül, B., L. Ghali, D. Davies, H. Pfister, I. M. Leigh and A. Storey (2007). "HPV8 early genes modulate differentiation and cell cycle of primary human adult keratinocytes." Exp Dermatol **16**(7): 590-599.

Akgül, B., P. Karle, M. Adam, P. G. Fuchs and H. J. Pfister (2003). "Dual role of tumor suppressor p53 in regulation of DNA replication and oncogene E6-promoter activity of epidermodysplasia verruciformis-associated human papillomavirus type 8." Virology **308**(2): 279-290.

Akgül, B., P. Zigrino, D. Frith, S. Hanrahan and A. Storey (2009). "Proteomic analysis reveals the actin cytoskeleton as cellular target for the human papillomavirus type 8." Virology **386**(1): 1-5.

Aneta, G., V. Tomas, R. Daniel and B. Jan (2016). "Cell polarity signaling in the plasticity of cancer cell invasiveness." Oncotarget.

Auersperg, N. (1969). "Histogenetic behavior of tumors. I. Morphologic variation in vitro and in vivo of two related human carcinoma cell lines." J Natl Cancer Inst **43**(1): 151-173.

Baird, B. N., M. J. Schliekelman, Y. H. Ahn, Y. Chen, J. D. Roybal, B. J. Gill, D. K. Mishra, B. Erez, M. O'Reilly, Y. Yang, M. Patel, X. Liu, N. Thilaganathan, I. V. Larina, M. E. Dickinson, J. L. West, D. L. Gibbons, D. D. Liu, M. P. Kim, J. M. Hicks, Wistuba, II, S. M. Hanash and J. M. Kurie (2013). "Fibulin-2 is a driver of malignant progression in lung adenocarcinoma." PLoS One **8**(6): e67054.

Barbosa, M. S., W. C. Vass, D. R. Lowy and J. T. Schiller (1991). "In vitro biological activities of the E6 and E7 genes vary among human papillomaviruses of different oncogenic potential." J Virol **65**(1): 292-298.

Barsky, S. H., G. P. Siegal, F. Jannotta and L. A. Liotta (1983). "Loss of basement membrane components by invasive tumors but not by their benign counterparts." Lab Invest **49**(2): 140-147.

Baum, B. and M. Georgiou (2011). "Dynamics of adherens junctions in epithelial establishment, maintenance, and remodeling." J Cell Biol **192**(6): 907-917.

Bedard, K. M., M. P. Underbrink, H. L. Howie and D. A. Galloway (2008). "The E6 oncoproteins from human betapapillomaviruses differentially activate telomerase through an E6AP-dependent mechanism and prolong the lifespan of primary keratinocytes." J Virol **82**(8): 3894-3902.

Bergvall, M., T. Melendy and J. Archambault (2013). "The E1 proteins." Virology **445**(1-2): 35-56.

Biddle, A., X. Liang, L. Gammon, B. Fazil, L. J. Harper, H. Emich, D. E. Costea and I. C. Mackenzie (2011). "Cancer stem cells in squamous cell carcinoma switch between two distinct phenotypes that are preferentially migratory or proliferative." Cancer Res **71**(15): 5317-5326.

Birnboim, H. C. and J. Doly (1979). "A rapid alkaline extraction procedure for screening recombinant plasmid DNA." Nucleic Acids Res **7**(6): 1513-1523.

Borgogna, C., S. Lanfredini, A. Peretti, M. De Andrea, E. Zavattaro, E. Colombo, M. Quaglia, R. Boldorini, U. Miglio, J. Doorbar, J. N. Bavinck, K. D. Quint, M. N. de Koning, S. Landolfo and M. Gariglio (2014). "Improved detection reveals active beta-papillomavirus infection in skin lesions from kidney transplant recipients." Mod Pathol **27**(8): 1101-1115.

Borgogna, C., E. Zavattaro, M. De Andrea, H. M. Griffin, V. Dell'Oste, B. Azzimonti, M. M. Landini, W. L. Peh, H. Pfister, J. Doorbar, S. Landolfo and M. Gariglio (2012). "Characterization of beta papillomavirus E4 expression in tumours from Epidermodysplasia Verruciformis patients and in experimental models." Virology **423**(2): 195-204.

Bouvard, V., R. Baan, K. Straif, Y. Grosse, B. Secretan, F. El Ghissassi, L. Benbrahim-Tallaa, N. Guha, C. Freeman, L. Galichet, V. Cogliano and W. H. O. I. A. f. R. o. C. M. W. Group (2009). "A review of human carcinogens--Part B: biological agents." Lancet Oncol **10**(4): 321-322.

Boxman, I. L., L. H. Mulder, F. Noya, V. de Waard, S. Gibbs, T. R. Broker, F. ten Kate, L. T. Chow and J. ter Schegget (2001). "Transduction of the E6 and E7 genes of epidermodysplasia-verruciformis-associated human papillomaviruses alters human keratinocyte growth and differentiation in organotypic cultures." J Invest Dermatol **117**(6): 1397-1404.

Boyer, S. N., D. E. Wazer and V. Band (1996). "E7 protein of human papilloma virus-16 induces degradation of retinoblastoma protein through the ubiquitin-proteasome pathway." Cancer Res **56**(20): 4620-4624.

Brandner, J. M., M. Zorn-Kruppa, T. Yoshida, I. Moll, L. A. Beck and A. De Benedetto (2015). "Epidermal tight junctions in health and disease." Tissue Barriers **3**(1-2): e974451.

Breitkreutz, D., I. Koxholt, K. Thiemann and R. Nischt (2013). "Skin basement membrane: the foundation of epidermal integrity--BM functions and diverse roles of bridging molecules nidogen and perlecan." Biomed Res Int **2013**: 179784.

Brimer, N., C. Lyons, A. E. Wallberg and S. B. Vande Pol (2012). "Cutaneous papillomavirus E6 oncoproteins associate with MAML1 to repress transactivation and NOTCH signaling." Oncogene **31**(43): 4639-4646.

Brooks, P. C., S. Stromblad, L. C. Sanders, T. L. von Schalscha, R. T. Aimes, W. G. Stetler-Stevenson, J. P. Quigley and D. A. Cheresh (1996). "Localization of matrix metalloproteinase MMP-2 to the surface of invasive cells by interaction with integrin alpha v beta 3." Cell **85**(5): 683-693.

Cawley, S., S. Bekiranov, H. H. Ng, P. Kapranov, E. A. Sekinger, D. Kampa, A. Piccolboni, V. Sementchenko, J. Cheng, A. J. Williams, R. Wheeler, B. Wong, J. Drenkow, M. Yamanaka, S. Patel, S. Brubaker, H. Tammana, G. Helt, K. Struhl and T. R. Gingeras (2004). "Unbiased mapping of transcription factor binding sites along human chromosomes 21 and 22 points to widespread regulation of noncoding RNAs." Cell **116**(4): 499-509.

Chen, S. H., C. Y. Lin, L. T. Lee, G. D. Chang, P. P. Lee, C. C. Hung, W. T. Kao, P. H. Tsai, A. V. Schally, J. J. Hwang and M. T. Lee (2010). "Up-regulation of fibronectin and tissue transglutaminase promotes cell invasion involving increased association with integrin and MMP expression in A431 cells." Anticancer Res **30**(10): 4177-4186.

Chow, L. T., S. S. Reilly, T. R. Broker and L. B. Taichman (1987). "Identification and mapping of human papillomavirus type 1 RNA transcripts recovered from plantar warts and infected epithelial cell cultures." J Virol **61**(6): 1913-1918.

Ciuffo, G. (1907). "Innesto positivo con filtrato di verruca volgare." Giornala Ital. Mal. Ven. Pelle **48**: 12-17.

Cleary, C., J. E. Leeman, D. S. Higginson, N. Katabi, E. Sherman, L. Morris, S. McBride, N. Lee and N. Riaz (2016). "Biological Features of Human Papillomavirus-related Head and Neck Cancers Contributing to Improved Response." Clin Oncol (R Coll Radiol).

Clower, R. V., J. C. Fisk and T. Melendy (2006). "Papillomavirus E1 protein binds to and stimulates human topoisomerase I." J Virol **80**(3): 1584-1587.

Crawford, L. V. (1965). "A study of human papilloma virus DNA." J Mol Biol **13**(2): 362-372.

Crequer, A., C. Picard, E. Patin, A. D'Amico, A. Abhyankar, M. Munzer, M. Debre, S. Y. Zhang, G. de Saint-Basile, A. Fischer, L. Abel, G. Orth, J. L. Casanova and E. Jouanguy (2012a). "Inherited MST1 deficiency underlies susceptibility to EV-HPV infections." PLoS One **7**(8): e44010.

Crequer, A., A. Troeger, E. Patin, C. S. Ma, C. Picard, V. Pedergnana, C. Fieschi, A. Lim, A. Abhyankar, L. Gineau, I. Mueller-Fleckenstein, M. Schmidt, A. Taieb, J. Krueger, L. Abel, S. G. Tangye, G. Orth, D. A. Williams, J. L. Casanova and E. Jouanguy (2012b). "Human RHOH deficiency causes T cell defects and susceptibility to EV-HPV infections." J Clin Invest **122**(9): 3239-3247.

Cueille, N., R. Nougarede, F. Mechali, M. Philippe and C. Bonne-Andrea (1998). "Functional interaction between the bovine papillomavirus virus type 1 replicative helicase E1 and cyclin E-Cdk2." J Virol **72**(9): 7255-7262.

Culp, T. D., L. R. Budgeon, M. P. Marinkovich, G. Meneguzzi and N. D. Christensen (2006). "Keratinocyte-secreted laminin 5 can function as a transient receptor for human papillomaviruses by binding virions and transferring them to adjacent cells." J Virol **80**(18): 8940-8950.

De Andrea, M., M. Ritta, M. M. Landini, C. Borgogna, M. Mondini, F. Kern, K. Ehrenreiter, M. Baccarini, G. P. Marcuzzi, S. Smola, H. Pfister, S. Landolfo and M. Gariglio (2010). "Keratinocyte-specific stat3 heterozygosity impairs development of skin tumors in human papillomavirus 8 transgenic mice." Cancer Res **70**(20): 7938-7948.

De Franceschi, N., H. Hamidi, J. Alanko, P. Sahgal and J. Ivaska (2015). "Integrin traffic - the update." J Cell Sci **128**(5): 839-852.

de Koning, M. N., S. J. Weissenborn, D. Abeni, J. N. Bouwes Bavinck, S. Euvrard, A. C. Green, C. A. Harwood, L. Naldi, R. Neale, I. Nindl, C. M. Proby, W. G. Quint, F. Sampogna, J. ter Schegget, L. Struijk, U. Wieland, H. J. Pfister, M. C. Feltkamp and E.-H.-U.-C. group (2009). "Prevalence and associated factors of betapapillomavirus infections in individuals without cutaneous squamous cell carcinoma." J Gen Virol **90**(Pt 7): 1611-1621.

de Villiers, E. M., C. Fauquet, T. R. Broker, H. U. Bernard and H. zur Hausen (2004). "Classification of papillomaviruses." Virology **324**(1): 17-27.

Dell'Oste, V., B. Azzimonti, M. De Andrea, M. Mondini, E. Zavattaro, G. Leigheb, S. J. Weissenborn, H. Pfister, K. M. Michael, T. Waterboer, M. Pawlita, A. Amantea, S. Landolfo and M. Gariglio (2009). "High beta-HPV DNA loads and strong seroreactivity are present in epidermodysplasia verruciformis." J Invest Dermatol **129**(4): 1026-1034.

Dickson, M. A., W. C. Hahn, Y. Ino, V. Ronfard, J. Y. Wu, R. A. Weinberg, D. N. Louis, F. P. Li and J. G. Rheinwald (2000). "Human keratinocytes that express hTERT and also bypass a p16(INK4a)-enforced mechanism that limits life span become immortal yet retain normal growth and differentiation characteristics." Mol Cell Biol **20**(4): 1436-1447.

DiPersio, C. M., K. M. Hodivala-Dilke, R. Jaenisch, J. A. Kreidberg and R. O. Hynes (1997). "alpha3beta1 Integrin is required for normal development of the epidermal basement membrane." J Cell Biol **137**(3): 729-742.

Dong, W., U. Kloz, R. Accardi, S. Caldeira, W. M. Tong, Z. Q. Wang, L. Jansen, M. Durst, B. S. Sylla, L. Gissmann and M. Tommasino (2005). "Skin hyperproliferation and susceptibility to chemical carcinogenesis in transgenic mice expressing E6 and E7 of human papillomavirus type 38." J Virol **79**(23): 14899-14908.

Doorbar, J. (2013). "The E4 protein; structure, function and patterns of expression." Virology **445**(1-2): 80-98.

Doorbar, J. (2016). "Model systems of human papillomavirus-associated disease." J Pathol **238**(2): 166-179.

Doorbar, J., S. Ely, J. Sterling, C. McLean and L. Crawford (1991). "Specific interaction between HPV-16 E1-E4 and cytokeratins results in collapse of the epithelial cell intermediate filament network." Nature **352**(6338): 824-827.

Doorbar, J., W. Quint, L. Banks, I. G. Bravo, M. Stoler, T. R. Broker and M. A. Stanley (2012). "The biology and life-cycle of human papillomaviruses." Vaccine **30 Suppl 5**: F55-70.

Dyson, N., P. Guida, K. Munger and E. Harlow (1992). "Homologous sequences in adenovirus E1A and human papillomavirus E7 proteins mediate interaction with the same set of cellular proteins." J Virol **66**(12): 6893-6902.

Dyson, N., P. M. Howley, K. Munger and E. Harlow (1989). "The human papilloma virus-16 E7 oncoprotein is able to bind to the retinoblastoma gene product." Science **243**(4893): 934-937.

Egawa, N., K. Egawa, H. Griffin and J. Doorbar (2015). "Human Papillomaviruses; Epithelial Tropisms, and the Development of Neoplasia." Viruses **7**(7): 3863-3890.

Eker, E. (2005). Charakterisierung zellulärer Interaktionspartner des E7 Proteins des humanen Papillomvirus 8 Diploma thesis, University of Cologne.

Enzenauer, C., G. Mengus, A. Lavigne, I. Davidson, H. Pfister and M. May (1998). "Interaction of human papillomavirus 8 regulatory proteins E2, E6 and E7 with components of the TFIID complex." Intervirology **41**(2-3): 80-90.

Esser, S., A. Kreuter, M. Oette, A. Gingelmaier, F. Mosthaf, M. L. Sautter-Bihl, J. Jongen, N. H. Brockmeyer, G. Eldering, J. Swoboda, N. Postel, O. Degen, H. Schalk, A. Jessen, H. Knechten, J. Thoden, H. J. Stellbrink, A. Schafberger and U. Wieland (2015). "German-Austrian guidelines on anal dysplasia and anal cancer in HIV-positive individuals: prevention, diagnosis, and treatment." J Dtsch Dermatol Ges **13**(12): 1302-1319.

Evander, M., I. H. Frazer, E. Payne, Y. M. Qi, K. Hengst and N. A. McMillan (1997). "Identification of the alpha6 integrin as a candidate receptor for papillomaviruses." J Virol **71**(3): 2449-2456.

Faggi, F., N. Chiarelli, M. Colombi, S. Mitola, R. Ronca, L. Madaro, M. Bouche, P. L. Poliani, M. Vezzoli, F. Longhena, E. Monti, B. Salani, D. Maggi, C. Keller and A. Fanzani (2015). "Cavin-1 and Caveolin-1 are both required to support cell proliferation, migration and anchorage-independent cell growth in rhabdomyosarcoma." Lab Invest **95**(6): 585-602.

Favre, M., F. Breitburd, O. Croissant and G. Orth (1977). "Chromatin-like structures obtained after alkaline disruption of bovine and human papillomaviruses." J Virol **21**(3): 1205-1209.

Favre, M., N. Ramoz and G. Orth (1997). "Human papillomaviruses: general features." Clin Dermatol **15**(2): 181-198.

Fiume, R., Y. Stijf-Bultsma, Z. H. Shah, W. J. Keune, D. R. Jones, J. G. Jude and N. Divecha (2015). "PIP4K and the role of nuclear phosphoinositides in tumour suppression." Biochim Biophys Acta **1851**(6): 898-910.

Gallagher, W. M., C. A. Currid and L. C. Whelan (2005). "Fibulins and cancer: friend or foe?" Trends Mol Med **11**(7): 336-340.

Gomez, D. S., JL (2007). Human Papillomavirus infection and cervical cancer: pathogenesis and epidermiology. Communicating Current Research and Educational Topics and Trends in Applied Microbiology. A. Mendez-Vilas**:** 680-688.

Goni, G. M., C. Epifano, J. Boskovic, M. Camacho-Artacho, J. Zhou, A. Bronowska, M. T. Martin, M. J. Eck, L. Kremer, F. Grater, F. L. Gervasio, M. Perez-Moreno and D. Lietha (2014). "Phosphatidylinositol 4,5-bisphosphate triggers activation of focal adhesion kinase by inducing clustering and conformational changes." Proc Natl Acad Sci U S A **111**(31): E3177-3186.

Grigat, S. (2004). Interaktionen der zelltransformierenden Proteine E6 und E7 des hautspezifischen Papillomavirus Typ 8 mit zellulären Faktoren Diploma thesis, University of Cologne.

Grinnell, F. (1984). "Fibronectin and wound healing." J Cell Biochem **26**(2): 107-116.

Guan, X. (2015). "Cancer metastases: challenges and opportunities." Acta Pharm Sin B **5**(5): 402-418.

Haller, K., F. Stubenrauch and H. Pfister (1995). "Differentiation-dependent transcription of the epidermodysplasia verruciformis-associated human papillomavirus type 5 in benign lesions." Virology **214**(1): 245-255.

Hammes, A. a. S., A. (2000). Generation of transgenic mice from plasmids, BACs and YACs. Mouse Genetics and Transgenics: a Practical Approach. I. J. Jackson, Abbot, C.M. New York**:** 217-245.

Han, S. W. and J. Roman (2006). "Fibronectin induces cell proliferation and inhibits apoptosis in human bronchial epithelial cells: pro-oncogenic effects mediated by PI3-kinase and NF-kappa B." Oncogene **25**(31): 4341-4349.

Hanahan, D. and R. A. Weinberg (2000). "The hallmarks of cancer." Cell **100**(1): 57-70.

Hartsock, A. and W. J. Nelson (2008). "Adherens and tight junctions: structure, function and connections to the actin cytoskeleton." Biochim Biophys Acta **1778**(3): 660-669.

Hellner, K., J. Mar, F. Fang, J. Quackenbush and K. Munger (2009). "HPV16 E7 oncogene expression in normal human epithelial cells causes molecular changes indicative of an epithelial to mesenchymal transition." Virology **391**(1): 57-63.

Hjerpe, E., S. Egyhazi Brage, J. Carlson, M. Frostvik Stolt, K. Schedvins, H. Johansson, M. Shoshan and E. Avall-Lundqvist (2013). "Metabolic markers GAPDH, PKM2, ATP5B and BEC-index in advanced serous ovarian cancer." BMC Clin Pathol **13**(1): 30.

Hodivala-Dilke, K. M., C. M. DiPersio, J. A. Kreidberg and R. O. Hynes (1998). "Novel roles for alpha3beta1 integrin as a regulator of cytoskeletal assembly and as a trans-dominant inhibitor of integrin receptor function in mouse keratinocytes." J Cell Biol **142**(5): 1357-1369.

Howie, H. L., R. A. Katzenellenbogen and D. A. Galloway (2009). "Papillomavirus E6 proteins." Virology **384**(2): 324-334.

Howie, H. L., J. I. Koop, J. Weese, K. Robinson, G. Wipf, L. Kim and D. A. Galloway (2011). "Beta-HPV 5 and 8 E6 promote p300 degradation by blocking AKT/p300 association." PLoS Pathog **7**(8): e1002211.

Howley, P. M. and H. J. Pfister (2015). "Beta genus papillomaviruses and skin cancer." Virology **479-480**: 290-296.

Hübbers, C. U. and B. Akgül (2015). "HPV and cancer of the oral cavity." Virulence **6**(3): 244-248.

Hufbauer, M., A. Biddle, C. Borgogna, M. Gariglio, J. Doorbar, A. Storey, H. Pfister, I. Mackenzie and B. Akgul (2013). "Expression of betapapillomavirus oncogenes increases the number of keratinocytes with stem cell-like properties." J Virol **87**(22): 12158-12165.

Hufbauer, M., J. Cooke, G. T. van der Horst, H. Pfister, A. Storey and B. Akgul (2015). "Human papillomavirus mediated inhibition of DNA damage sensing and repair drives skin carcinogenesis." Mol Cancer **14**(1): 183.

Hufbauer, M., D. Lazic, B. Akgul, J. L. Brandsma, H. Pfister and S. J. Weissenborn (2010a). "Enhanced human papillomavirus type 8 oncogene expression levels are crucial for skin tumorigenesis in transgenic mice." Virology **403**(2): 128-136.

Hufbauer, M., D. Lazic, B. Akgül, J. L. Brandsma, H. Pfister and S. J. Weissenborn (2010b). "Enhanced human papillomavirus type 8 oncogene expression levels are crucial for skin tumorigenesis in transgenic mice." Virology **403**(2): 128-136.

Iannacone, M. R., T. Gheit, H. Pfister, A. R. Giuliano, J. L. Messina, N. A. Fenske, B. S. Cherpelis, V. K. Sondak, R. G. Roetzheim, S. Silling, M. Pawlita, M. Tommasino and D. E. Rollison (2014). "Case-control study of genus-beta human papillomaviruses in plucked eyebrow hairs and cutaneous squamous cell carcinoma." Int J Cancer **134**(9): 2231-2244.

Iftner, T., S. Bierfelder, Z. Csapo and H. Pfister (1988). "Involvement of human papillomavirus type 8 genes E6 and E7 in transformation and replication." J Virol **62**(10): 3655-3661.

Iftner, T., P. G. Fuchs and H. Pfister (1989). "Two independently transforming functions of human papillomavirus 8." Curr Top Microbiol Immunol **144**: 167-173.

Jackson, S., C. Harwood, M. Thomas, L. Banks and A. Storey (2000). "Role of Bak in UV-induced apoptosis in skin cancer and abrogation by HPV E6 proteins." Genes Dev **14**(23): 3065-3073.

Jackson, S. and A. Storey (2000). "E6 proteins from diverse cutaneous HPV types inhibit apoptosis in response to UV damage." Oncogene **19**(4): 592-598.

Janes, S. M. and F. M. Watt (2006). "New roles for integrins in squamous-cell carcinoma." Nat Rev Cancer **6**(3): 175-183.

Jones, D. L. and K. Munger (1996). "Interactions of the human papillomavirus E7 protein with cell cycle regulators." Semin Cancer Biol **7**(6): 327-337.

Jones, P. H., S. Harper and F. M. Watt (1995). "Stem cell patterning and fate in human epidermis." Cell **80**(1): 83-93.

Juhasz, I., G. F. Murphy, H. C. Yan, M. Herlyn and S. M. Albelda (1993). "Regulation of extracellular matrix proteins and integrin cell substratum adhesion receptors on epithelium during cutaneous human wound healing in vivo." Am J Pathol **143**(5): 1458-1469.

Kalluri, R. (2003). "Basement membranes: structure, assembly and role in tumour angiogenesis." Nat Rev Cancer **3**(6): 422-433.

Kalluri, R. and R. A. Weinberg (2009). "The basics of epithelial-mesenchymal transition." J Clin Invest **119**(6): 1420-1428.

Kanitakis, J. (2002). "Anatomy, histology and immunohistochemistry of normal human skin." Eur J Dermatol **12**(4): 390-399; quiz 400-391.

Kim, S. J., U. S. Onwuta, Y. I. Lee, R. Li, M. R. Botchan and P. D. Robbins (1992). "The retinoblastoma gene product regulates Sp1-mediated transcription." Mol Cell Biol **12**(6): 2455-2463.

Kines, R. C., R. J. Cerio, J. N. Roberts, C. D. Thompson, E. de Los Pinos, D. R. Lowy and J. T. Schiller (2016). "Human papillomavirus capsids preferentially bind and infect tumor cells." Int J Cancer **138**(4): 901-911.

Kinsey, R., M. R. Williamson, S. Chaudhry, K. T. Mellody, A. McGovern, S. Takahashi, C. A. Shuttleworth and C. M. Kielty (2008). "Fibrillin-1 microfibril deposition is dependent on fibronectin assembly." J Cell Sci **121**(Pt 16): 2696-2704.

Klug, A. and J. T. Finch (1965). "Structure of Viruses of the Papilloma-Polyoma Type. I. Human Wart Virus." J Mol Biol **11**: 403-423.

Kobayashi, N., G. Kostka, J. H. Garbe, D. R. Keene, H. P. Bachinger, F. G. Hanisch, D. Markova, T. Tsuda, R. Timpl, M. L. Chu and T. Sasaki (2007). "A comparative analysis of the fibulin protein family. Biochemical characterization, binding interactions, and tissue localization." J Biol Chem **282**(16): 11805-11816.

Kohler, A., T. Forschner, T. Meyer, C. Ulrich, M. Gottschling, E. Stockfleth and I. Nindl (2007). "Multifocal distribution of cutaneous human papillomavirus types in hairs from different skin areas." Br J Dermatol **156**(5): 1078-1080.

Kolk, A., K. D. Wolff, R. Smeets, M. Kesting, R. Hein and A. W. Eckert (2014). "Melanotic and non-melanotic malignancies of the face and external ear - A review of current treatment concepts and future options." Cancer Treat Rev **40**(7): 819-837.

Komiya, Y. and R. Habas (2008). "Wnt signal transduction pathways." Organogenesis **4**(2): 68-75.

Krakhmal, N. V., M. V. Zavyalova, E. V. Denisov, S. V. Vtorushin and V. M. Perelmuter (2015). "Cancer Invasion: Patterns and Mechanisms." Acta Naturae **7**(2): 17-28.

Kreimer, A. R., G. M. Clifford, P. Boyle and S. Franceschi (2005). "Human papillomavirus types in head and neck squamous cell carcinomas worldwide: a systematic review." Cancer Epidemiol Biomarkers Prev **14**(2): 467-475.

Kurtz, K. A., H. T. Hoffman, M. B. Zimmerman and R. A. Robinson (2006). "Decreased E-cadherin but not beta-catenin expression is associated with vascular invasion and decreased survival in head and neck squamous carcinomas." Otolaryngol Head Neck Surg **134**(1): 142-146.

Lamouille, S., J. Xu and R. Derynck (2014). "Molecular mechanisms of epithelial-mesenchymal transition." Nat Rev Mol Cell Biol **15**(3): 178-196.

Lazarczyk, M., P. Cassonnet, C. Pons, Y. Jacob and M. Favre (2009). "The EVER proteins as a natural barrier against papillomaviruses: a new insight into the pathogenesis of human papillomavirus infections." Microbiol Mol Biol Rev **73**(2): 348-370.

Lazic, D., M. Hufbauer, P. Zigrino, S. Buchholz, S. Kazem, M. C. Feltkamp, C. Mauch, G. Steger, H. Pfister and B. Akgul (2012). "Human papillomavirus type 8 E6 oncoprotein inhibits transcription of the PDZ protein syntenin-2." J Virol **86**(15): 7943-7952.

Leverrier, S., D. Bergamaschi, L. Ghali, A. Ola, G. Warnes, B. Akgul, K. Blight, R. Garcia-Escudero, A. Penna, A. Eddaoudi and A. Storey (2007). "Role of HPV E6 proteins in preventing UVB-induced release of pro-apoptotic factors from the mitochondria." Apoptosis **12**(3): 549-560.

Liberti, M. V. and J. W. Locasale (2016). "The Warburg Effect: How Does it Benefit Cancer Cells?" Trends Biochem Sci **41**(3): 211-218.

Ling, K., S. F. Bairstow, C. Carbonara, D. A. Turbin, D. G. Huntsman and R. A. Anderson (2007). "Type I gamma phosphatidylinositol phosphate kinase modulates adherens junction and E-cadherin trafficking via a direct interaction with mu 1B adaptin." J Cell Biol **176**(3): 343-353.

Liu, L., H. X. Xu, W. Q. Wang, C. T. Wu, T. Chen, Y. Qin, C. Liu, J. Xu, J. Long, B. Zhang, Y. F. Xu, Q. X. Ni, M. Li and X. J. Yu (2014). "Cavin-1 is essential for the tumor-promoting effect of caveolin-1 and enhances its prognostic potency in pancreatic cancer." Oncogene **33**(21): 2728-2736.

Liu, X., H. Yuan, B. Fu, G. L. Disbrow, T. Apolinario, V. Tomaic, M. L. Kelley, C. C. Baker, J. Huibregtse and R. Schlegel (2005). "The E6AP ubiquitin ligase is required for transactivation of the hTERT promoter by the human papillomavirus E6 oncoprotein." J Biol Chem **280**(11): 10807-10816.

Longmate, W. M., R. Monichan, M. L. Chu, T. Tsuda, M. G. Mahoney and C. M. DiPersio (2014). "Reduced fibulin-2 contributes to loss of basement membrane integrity and skin blistering in mice lacking integrin alpha3beta1 in the epidermis." J Invest Dermatol **134**(6): 1609-1617.

Low, J. Y. and H. D. Nicholson (2014). "Emerging role of polymerase-1 and transcript release factor (PTRF/ Cavin-1) in health and disease." Cell Tissue Res **357**(3): 505-513.

Lucs, A. V., A. L. Abramson and B. M. Steinberg (2014). "Overexpressed beta-catenin localizes to plasma membrane in respiratory papillomas." J Invest Dermatol **134**(6): 1760-1763.

Majewski, S., S. Jablonska and G. Orth (1997). "Epidermodysplasia verruciformis. Immunological and nonimmunological surveillance mechanisms: role in tumor progression." Clin Dermatol **15**(3): 321-334.

Malik, T., M. Imran and R. Jayaraman (2016). "Optimal control with multiple human papillomavirus vaccines." J Theor Biol **393**: 179-193.

Manabe, R., N. Ohe, T. Maeda, T. Fukuda and K. Sekiguchi (1997). "Modulation of cell-adhesive activity of fibronectin by the alternatively spliced EDA segment." J Cell Biol **139**(1): 295-307.

Mani, S. A., W. Guo, M. J. Liao, E. N. Eaton, A. Ayyanan, A. Y. Zhou, M. Brooks, F. Reinhard, C. C. Zhang, M. Shipitsin, L. L. Campbell, K. Polyak, C. Brisken, J. Yang and R. A. Weinberg (2008). "The epithelial-mesenchymal transition generates cells with properties of stem cells." Cell **133**(4): 704-715.

Mantovani, F. and L. Banks (2001). "The human papillomavirus E6 protein and its contribution to malignant progression." Oncogene **20**(54): 7874-7887.

Mao, Y. and J. E. Schwarzbauer (2005). "Fibronectin fibrillogenesis, a cell-mediated matrix assembly process." Matrix Biol **24**(6): 389-399.

Marcuzzi, G. P. (2001). Untersuchungen zu Interaktionen der zelltransformierenden E7 Proteine hautspezifischer Papillomviren mit zellulären Faktoren Diploma thesis, University of Cologne.

Marcuzzi, G. P., M. Hufbauer, H. U. Kasper, S. J. Weissenborn, S. Smola and H. Pfister (2009). "Spontaneous tumour development in human papillomavirus type 8 E6 transgenic mice and rapid induction by UV-light exposure and wounding." J Gen Virol **90**(Pt 12): 2855-2864.

Margadant, C., R. A. Charafeddine and A. Sonnenberg (2010). "Unique and redundant functions of integrins in the epidermis." FASEB J **24**(11): 4133-4152.

Margulis, A., W. Zhang, A. Alt-Holland, S. Pawagi, P. Prabhu, J. Cao, S. Zucker, L. Pfeiffer, J. Garfield, N. E. Fusenig and J. A. Garlick (2006). "Loss of intercellular adhesion activates a transition from low- to high-grade human squamous cell carcinoma." Int J Cancer **118**(4): 821-831.

Maubant, S., B. Tesson, V. Maire, M. Ye, G. Rigaill, D. Gentien, F. Cruzalegui, G. C. Tucker, S. Roman-Roman and T. Dubois (2015). "Transcriptome analysis of Wnt3a-treated triple-negative breast cancer cells." PLoS One **10**(4): e0122333.

McBride, A. A. (2008). "Replication and partitioning of papillomavirus genomes." Adv Virus Res **72**: 155-205.

McBride, A. A. (2013). "The papillomavirus E2 proteins." Virology **445**(1-2): 57-79.

McCormack, S. J., S. E. Brazinski, J. L. Moore, Jr., B. A. Werness and D. J. Goldstein (1997). "Activation of the focal adhesion kinase signal transduction pathway in cervical carcinoma cell lines and human genital epithelial cells immortalized with human papillomavirus type 18." Oncogene **15**(3): 265-274.

McLaughlin-Drubin, M. E. and K. Münger (2009). "The human papillomavirus E7 oncoprotein." Virology **384**(2): 335-344.

Mesri, E. A., M. A. Feitelson and K. Munger (2014). "Human viral oncogenesis: a cancer hallmarks analysis." Cell Host Microbe **15**(3): 266-282.

Meyers, J. M., J. M. Spangle and K. Munger (2013). "The human papillomavirus type 8 E6 protein interferes with NOTCH activation during keratinocyte differentiation." J Virol **87**(8): 4762-4767.

Michaelson, J. E., J. D. Ritzenthaler and J. Roman (2002). "Regulation of serum-induced fibronectin expression by protein kinases, cytoskeletal integrity, and CREB." Am J Physiol Lung Cell Mol Physiol **282**(2): L291-301.

Michel, A., A. Kopp-Schneider, H. Zentgraf, A. D. Gruber and E. M. de Villiers (2006). "E6/E7 expression of human papillomavirus type 20 (HPV-20) and HPV-27 influences proliferation and differentiation of the skin in UV-irradiated SKH-hr1 transgenic mice." J Virol **80**(22): 11153-11164.

Miller, A. D. and F. Chen (1996). "Retrovirus packaging cells based on 10A1 murine leukemia virus for production of vectors that use multiple receptors for cell entry." J Virol **70**(8): 5564-5571.

Missan, D. S., S. V. Chittur and C. M. DiPersio (2014). "Regulation of fibulin-2 gene expression by integrin alpha3beta1 contributes to the invasive phenotype of transformed keratinocytes." J Invest Dermatol **134**(9): 2418-2427.

Moody, C. A. and L. A. Laimins (2010). "Human papillomavirus oncoproteins: pathways to transformation." Nat Rev Cancer **10**(8): 550-560.

Morita, K., S. Tsukita and Y. Miyachi (2004). "Tight junction-associated proteins (occludin, ZO-1, claudin-1, claudin-4) in squamous cell carcinoma and Bowen's disease." Br J Dermatol **151**(2): 328-334.

Muller, A., A. Ritzkowsky and G. Steger (2002). "Cooperative activation of human papillomavirus type 8 gene expression by the E2 protein and the cellular coactivator p300." J Virol **76**(21): 11042-11053.

Mullis, K. B. and F. A. Faloona (1987). "Specific synthesis of DNA in vitro via a polymerase-catalyzed chain reaction." Methods Enzymol **155**: 335-350.

Münger, K., J. R. Basile, S. Duensing, A. Eichten, S. L. Gonzalez, M. Grace and V. L. Zacny (2001). "Biological activities and molecular targets of the human papillomavirus E7 oncoprotein." Oncogene **20**(54): 7888-7898.

Münger, K. and P. M. Howley (2002). "Human papillomavirus immortalization and transformation functions." Virus Res **89**(2): 213-228.

Neale, R. E., S. Weissenborn, D. Abeni, J. N. Bavinck, S. Euvrard, M. C. Feltkamp, A. C. Green, C. Harwood, M. de Koning, L. Naldi, I. Nindl, M. Pawlita, C. Proby, W. G. Quint, T. Waterboer, U. Wieland and H. Pfister (2013). "Human papillomavirus load in eyebrow hair follicles and risk of cutaneous squamous cell carcinoma." Cancer Epidemiol Biomarkers Prev **22**(4): 719-727.

Nindl, I., M. Gottschling and E. Stockfleth (2007). "Human papillomaviruses and non-melanoma skin cancer: basic virology and clinical manifestations." Dis Markers **23**(4): 247-259.

Nindl, I. and F. Rösl (2008). "Molecular concepts of virus infections causing skin cancer in organ transplant recipients." Am J Transplant **8**(11): 2199-2204.

O'Shaughnessy, R. F., B. Akgül, A. Storey, H. Pfister, C. A. Harwood and C. Byrne (2007). "Cutaneous human papillomaviruses down-regulate AKT1, whereas AKT2 up-regulation and activation associates with tumors." Cancer Res **67**(17): 8207-8215.

Oldak, M., H. Smola, M. Aumailley, F. Rivero, H. Pfister and S. Smola-Hess (2004). "The human papillomavirus type 8 E2 protein suppresses beta4-integrin expression in primary human keratinocytes." J Virol **78**(19): 10738-10746.

Oliveira, J. G., L. A. Colf and A. A. McBride (2006). "Variations in the association of papillomavirus E2 proteins with mitotic chromosomes." Proc Natl Acad Sci U S A **103**(4): 1047-1052.

Onder, Z., V. Chang and J. Moroianu (2015). "Nuclear export of cutaneous HPV8 E7 oncoprotein is mediated by a leucine-rich nuclear export signal via a CRM1 pathway." Virology **474**: 28-33.

Onder, Z. and J. Moroianu (2014). "Nuclear import of cutaneous beta genus HPV8 E7 oncoprotein is mediated by hydrophobic interactions between its zinc-binding domain and FG nucleoporins." Virology **449**: 150-162.

Orth, G., S. Jablonska, M. Favre, O. Croissant, M. Jarzabek-Chorzelska and G. Rzesa (1978). "Characterization of two types of human papillomaviruses in lesions of epidermodysplasia verruciformis." Proc Natl Acad Sci U S A **75**(3): 1537-1541.

Oswald, E. (2010). Bindung und Modulation der zellulären Funktionen von NuMA und NM1 durch das E7-Protein der humanen beta-Papillomaviren HPV5 und HPV8 PhD thesis, Ruprecht-Karls-Universität Heidelberg.

Patel, T., L. K. Morrison, P. Rady and S. Tyring (2010). "Epidermodysplasia verruciformis and susceptibility to HPV." Dis Markers **29**(3-4): 199-206.

Pawelek, J. M. and A. K. Chakraborty (2008). "Fusion of tumour cells with bone marrow-derived cells: a unifying explanation for metastasis." Nat Rev Cancer **8**(5): 377-386.

Pfefferle, R., G. P. Marcuzzi, B. Akgul, H. U. Kasper, F. Schulze, I. Haase, C. Wickenhauser and H. Pfister (2008). "The human papillomavirus type 8 E2 protein induces skin tumors in transgenic mice." J Invest Dermatol **128**(9): 2310-2315.

Pfister, H. and P. G. Fuchs (1994). "Anatomy, taxonomy and evolution of papillomaviruses." Intervirology **37**(3-4): 143-149.

Pfister, H. and H. zur Hausen (1978). "Characterization of proteins of human papilloma viruses (HPV) and antibody response to HPV 1." Med Microbiol Immunol **166**(1-4): 13-19.

Phelan, J. J., F. MacCarthy, R. Feighery, N. J. O'Farrell, N. Lynam-Lennon, B. Doyle, D. O'Toole, N. Ravi, J. V. Reynolds and J. O'Sullivan (2014). "Differential expression of mitochondrial energy metabolism profiles across the metaplasia-dysplasia-adenocarcinoma disease sequence in Barrett's oesophagus." Cancer Lett **354**(1): 122-131.

Philips, N., S. Auler, R. Hugo and S. Gonzalez (2011). "Beneficial regulation of matrix metalloproteinases for skin health." Enzyme Res **2011**: 427285.

Pickup, M. W., J. K. Mouw and V. M. Weaver (2014). "The extracellular matrix modulates the hallmarks of cancer." EMBO Rep **15**(12): 1243-1253.

Poddar, A., S. C. Reed, M. G. McPhillips, J. E. Spindler and A. A. McBride (2009). "The human papillomavirus type 8 E2 tethering protein targets the ribosomal DNA loci of host mitotic chromosomes." J Virol **83**(2): 640-650.

Profumo, V. and P. Gandellini (2013). "MicroRNAs: cobblestones on the road to cancer metastasis." Crit Rev Oncog **18**(4): 341-355.

Proksch, E., J. M. Brandner and J. M. Jensen (2008). "The skin: an indispensable barrier." Exp Dermatol **17**(12): 1063-1072.

Purdie, K. J., C. J. Sexton, C. M. Proby, M. T. Glover, A. T. Williams, J. N. Stables and I. M. Leigh (1993). "Malignant transformation of cutaneous lesions in renal allograft patients: a role for human papillomavirus." Cancer Res **53**(21): 5328-5333.

Quint, K. D., R. E. Genders, M. N. de Koning, C. Borgogna, M. Gariglio, J. N. Bouwes Bavinck, J. Doorbar and M. C. Feltkamp (2015). "Human Beta-papillomavirus infection and keratinocyte carcinomas." J Pathol **235**(2): 342-354.

Raff, A. B., A. W. Woodham, L. M. Raff, J. G. Skeate, L. Yan, D. M. Da Silva, M. Schelhaas and W. M. Kast (2013). "The evolving field of human papillomavirus receptor research: a review of binding and entry." J Virol **87**(11): 6062-6072.

Ramaswamy, S., K. N. Ross, E. S. Lander and T. R. Golub (2003). "A molecular signature of metastasis in primary solid tumors." Nat Genet **33**(1): 49-54.

Ramoz, N., L. A. Rueda, B. Bouadjar, L. S. Montoya, G. Orth and M. Favre (2002). "Mutations in two adjacent novel genes are associated with epidermodysplasia verruciformis." Nat Genet **32**(4): 579-581.

Ramoz, N., A. Taieb, L. A. Rueda, L. S. Montoya, B. Bouadjar, M. Favre and G. Orth (2000). "Evidence for a nonallelic heterogeneity of epidermodysplasia verruciformis with two susceptibility loci mapped to chromosome regions 2p21-p24 and 17q25." J Invest Dermatol **114**(6): 1148-1153.

Rey, O., S. Lee and N. H. Park (2000). "Human papillomavirus type 16 E7 oncoprotein represses transcription of human fibronectin." J Virol **74**(10): 4912-4918.

Riethmuller, D., A. C. Jacquard, J. Lacau St Guily, F. Aubin, X. Carcopino, P. Pradat, A. Dahlab and J. L. Pretet (2015). "Potential impact of a nonavalent HPV vaccine on the occurrence of HPV-related diseases in France." BMC Public Health **15**: 453.

Rous, P. and J. G. Kidd (1938). "The Carcinogenic Effect of a Papilloma Virus on the Tarred Skin of Rabbits : I. Description of the Phenomenon." J Exp Med **67**(3): 399-428.

Rozenblatt-Rosen, O., R. C. Deo, M. Padi, G. Adelmant, M. A. Calderwood, T. Rolland, M. Grace, A. Dricot, M. Askenazi, M. Tavares, S. J. Pevzner, F. Abderazzaq, D. Byrdsong, A. R. Carvunis, A. A. Chen, J. Cheng, M. Correll, M. Duarte, C. Fan, M. C. Feltkamp, S. B. Ficarro, R. Franchi, B. K. Garg, N. Gulbahce, T. Hao, A. M. Holthaus, R. James, A. Korkhin, L. Litovchick, J. C. Mar, T. R. Pak, S. Rabello, R. Rubio, Y. Shen, S. Singh, J. M. Spangle, M. Tasan, S. Wanamaker, J. T. Webber, J. Roecklein-Canfield, E. Johannsen, A. L. Barabasi, R. Beroukhim, E. Kieff, M. E. Cusick, D. E. Hill, K. Munger, J. A. Marto, J. Quackenbush, F. P. Roth, J. A. DeCaprio and M. Vidal (2012). "Interpreting cancer genomes using systematic host network perturbations by tumour virus proteins." Nature **487**(7408): 491-495.

Sabatier, L., D. Chen, C. Fagotto-Kaufmann, D. Hubmacher, M. D. McKee, D. S. Annis, D. F. Mosher and D. P. Reinhardt (2009). "Fibrillin assembly requires fibronectin." Mol Biol Cell **20**(3): 846-858.

Sachs, N., P. Secades, L. van Hulst, M. Kreft, J. Y. Song and A. Sonnenberg (2012). "Loss of integrin alpha3 prevents skin tumor formation by promoting epidermal turnover and depletion of slow-cycling cells." Proc Natl Acad Sci U S A **109**(52): 21468-21473.

Sambrook, J., Fritsch, E.F., Maniatis, T. (1989). Molecular cloning: a laboratory manual, Cold Spring Habor Laboratory Press, Cold Spring Harbor, N.Y.

Sang, B. C. and M. S. Barbosa (1992). "Single amino acid substitutions in "low-risk" human papillomavirus (HPV) type 6 E7 protein enhance features characteristic of the "high-risk" HPV E7 oncoproteins." Proc Natl Acad Sci U S A **89**(17): 8063-8067.

Sankovski, E., A. Mannik, J. Geimanen, E. Ustav and M. Ustav (2014). "Mapping of betapapillomavirus human papillomavirus 5 transcription and characterization of viral-genome replication function." J Virol **88**(2): 961-973.

Schaper, I. D., G. P. Marcuzzi, S. J. Weissenborn, H. U. Kasper, V. Dries, N. Smyth, P. Fuchs and H. Pfister (2005). "Development of skin tumors in mice transgenic for early genes of human papillomavirus type 8." Cancer Res **65**(4): 1394-1400.

Schelhaas, M., B. Shah, M. Holzer, P. Blattmann, L. Kuhling, P. M. Day, J. T. Schiller and A. Helenius (2012). "Entry of human papillomavirus type 16 by actin-dependent, clathrin- and lipid raft-independent endocytosis." PLoS Pathog **8**(4): e1002657.

Schiemann, W. P., G. C. Blobe, D. E. Kalume, A. Pandey and H. F. Lodish (2002). "Context-specific effects of fibulin-5 (DANCE/EVEC) on cell proliferation, motility, and invasion. Fibulin-5 is induced by transforming growth factor-beta and affects protein kinase cascades." J Biol Chem **277**(30): 27367-27377.

Schiller, J. T. and M. Muller (2015). "Next generation prophylactic human papillomavirus vaccines." Lancet Oncol **16**(5): e217-225.

Schlaepfer, D. D., K. C. Jones and T. Hunter (1998). "Multiple Grb2-mediated integrin-stimulated signaling pathways to ERK2/mitogen-activated protein kinase: summation of both c-Src- and focal adhesion kinase-initiated tyrosine phosphorylation events." Mol Cell Biol **18**(5): 2571-2585.

Schmidt, D. S., P. Klingbeil, M. Schnolzer and M. Zoller (2004). "CD44 variant isoforms associate with tetraspanins and EpCAM." Exp Cell Res 297(2): 329-347.

Schmitt, A., J. B. Harry, B. Rapp, F. O. Wettstein and T. Iftner (1994). "Comparison of the properties of the E6 and E7 genes of low- and high-risk cutaneous papillomaviruses reveals strongly transforming and high Rb-binding activity for the E7 protein of the low-risk human papillomavirus type 1." J Virol 68(11): 7051-7059.

Sedman, J. and A. Stenlund (1995). "Co-operative interaction between the initiator E1 and the transcriptional activator E2 is required for replicator specific DNA replication of bovine papillomavirus in vivo and in vitro." EMBO J 14(24): 6218-6228.

Seifert, U. and S. J. Klug (2014). "[Early detection of cervical cancer in Germany: evidence and implementation]." Bundesgesundheitsblatt Gesundheitsforschung Gesundheitsschutz 57(3): 294-301.

Senior, A. E. (2007). "ATP synthase: motoring to the finish line." Cell 130(2): 220-221.

Simpson, C. L., D. M. Patel and K. J. Green (2011). "Deconstructing the skin: cytoarchitectural determinants of epidermal morphogenesis." Nat Rev Mol Cell Biol 12(9): 565-580.

Smalley, K. S., P. Brafford, N. K. Haass, J. M. Brandner, E. Brown and M. Herlyn (2005). "Up-regulated expression of zonula occludens protein-1 in human melanoma associates with N-cadherin and contributes to invasion and adhesion." Am J Pathol 166(5): 1541-1554.

Smola-Hess, S., J. Pahne, C. Mauch, P. Zigrino, H. Smola and H. J. Pfister (2005). "Expression of membrane type 1 matrix metalloproteinase in papillomavirus-positive cells: role of the human papillomavirus (HPV) 16 and HPV8 E7 gene products." J Gen Virol 86(Pt 5): 1291-1296.

Soave, D. F., Nunes Celes, M.R., Oliveira-Costa, J.P., da Silveira, G.G., Riedo Zanetti, B., Oliveira, L.R. and Ribeiro-Silva, A. (2013). The Role of Human Papillomavirus in Pre-Cancerous Lesions and Oral Cancers. Human Papillomavirus and Related Diseases from Bench to Bedside A Diagnostic and Preventive Perspective. D. D. V. Broeck.

Sperling, T., M. Oldak, B. Walch-Ruckheim, C. Wickenhauser, J. Doorbar, H. Pfister, M. Malejczyk, S. Majewski, A. C. Keates and S. Smola (2012). "Human papillomavirus type 8 interferes with a novel C/EBPbeta-mediated mechanism of keratinocyte CCL20 chemokine expression and Langerhans cell migration." PLoS Pathog 8(7): e1002833.

Staal, F. J., M. van Noort, G. J. Strous and H. C. Clevers (2002). "Wnt signals are transmitted through N-terminally dephosphorylated beta-catenin." EMBO Rep 3(1): 63-68.

Steger, G., M. Olszewsky, E. Stockfleth and H. Pfister (1990). "Prevalence of antibodies to human papillomavirus type 8 in human sera." J Virol 64(9): 4399-4406.

Steger, G. and H. Pfister (1992). "In vitro expressed HPV 8 E6 protein does not bind p53." Arch Virol 125(1-4): 355-360.

Stehelin, D., H. E. Varmus, J. M. Bishop and P. K. Vogt (1976). "DNA related to the transforming gene(s) of avian sarcoma viruses is present in normal avian DNA." Nature 260(5547): 170-173.

Stenner, M., B. Yosef, C. U. Huebbers, S. F. Preuss, H. P. Dienes, E. J. Speel, M. Odenthal and J. P. Klussmann (2011). "Nuclear translocation of beta-catenin and

decreased expression of epithelial cadherin in human papillomavirus-positive tonsillar cancer: an early event in human papillomavirus-related tumour progression?" Histopathology **58**(7): 1117-1126.

Stöppler, H., M. C. Stöppler, E. Johnson, C. M. Simbulan-Rosenthal, M. E. Smulson, S. Iyer, D. S. Rosenthal and R. Schlegel (1998). "The E7 protein of human papillomavirus type 16 sensitizes primary human keratinocytes to apoptosis." Oncogene **17**(10): 1207-1214.

Strauss, M. J., E. W. Shaw and et al. (1949). "Crystalline virus-like particles from skin papillomas characterized by intranuclear inclusion bodies." Proc Soc Exp Biol Med **72**(1): 46-50.

Stubenrauch, F. and L. A. Laimins (1999). "Human papillomavirus life cycle: active and latent phases." Semin Cancer Biol **9**(6): 379-386.

Stubenrauch, F., J. Malejczyk, P. G. Fuchs and H. Pfister (1992). "Late promoter of human papillomavirus type 8 and its regulation." J Virol **66**(6): 3485-3493.

Sun, S., L. Thorner, M. Lentz, P. MacPherson and M. Botchan (1990). "Identification of a 68-kilodalton nuclear ATP-binding phosphoprotein encoded by bovine papillomavirus type 1." J Virol **64**(10): 5093-5105.

Sun, X., P. Fa, Z. Cui, Y. Xia, L. Sun, Z. Li, A. Tang, Y. Gui and Z. Cai (2014). "The EDA-containing cellular fibronectin induces epithelial-mesenchymal transition in lung cancer cells through integrin alpha9beta1-mediated activation of PI3-K/AKT and Erk1/2." Carcinogenesis **35**(1): 184-191.

Surviladze, Z., R. T. Sterkand and M. A. Ozbun (2015). "Interaction of human papillomavirus type 16 particles with heparan sulfate and syndecan-1 molecules in the keratinocyte extracellular matrix plays an active role in infection." J Gen Virol **96**(8): 2232-2241.

Syrjanen, K. J., S. M. Syrjanen, M. A. Lamberg and R. P. Happonen (1983). "Local immunological reactivity in oral squamous cell lesions of possible HPV (human papillomavirus) origin." Arch Geschwulstforsch **53**(6): 537-546.

Syrjanen, S. and K. Syrjanen (2008). "The history of papillomavirus research." Cent Eur J Public Health **16 Suppl**: S7-13.

Tam, W. L. and R. A. Weinberg (2013). "The epigenetics of epithelial-mesenchymal plasticity in cancer." Nat Med **19**(11): 1438-1449.

Timpl, R., T. Sasaki, G. Kostka and M. L. Chu (2003). "Fibulins: a versatile family of extracellular matrix proteins." Nat Rev Mol Cell Biol **4**(6): 479-489.

Todd, C., S. D. Hewitt, J. Kempenaar, K. Noz, A. J. Thody and M. Ponec (1993). "Co-culture of human melanocytes and keratinocytes in a skin equivalent model: effect of ultraviolet radiation." Arch Dermatol Res **285**(8): 455-459.

Trimmer, C., F. Sotgia, M. P. Lisanti and F. Capozza (2013). "Cav1 inhibits benign skin tumor development in a two-stage carcinogenesis model by suppressing epidermal proliferation." Am J Transl Res **5**(1): 80-91.

Uren, A., S. Fallen, H. Yuan, A. Usubutun, T. Kucukali, R. Schlegel and J. A. Toretsky (2005). "Activation of the canonical Wnt pathway during genital keratinocyte transformation: a model for cervical cancer progression." Cancer Res **65**(14): 6199-6206.

References

Urra, H., V. A. Torres, R. J. Ortiz, L. Lobos, M. I. Diaz, N. Diaz, S. Hartel, L. Leyton and A. F. Quest (2012). "Caveolin-1-enhanced motility and focal adhesion turnover require tyrosine-14 but not accumulation to the rear in metastatic cancer cells." PLoS One **7**(4): e33085.

Ustav, M. and A. Stenlund (1991). "Transient replication of BPV-1 requires two viral polypeptides encoded by the E1 and E2 open reading frames." EMBO J **10**(2): 449-457.

Van Damme, P., P. Bonanni, F. X. Bosch, E. Joura, S. Kruger Kjaer, C. J. Meijer, K. U. Petry, B. Soubeyrand, T. Verstraeten and M. Stanley (2016). "Use of the nonavalent HPV vaccine in individuals previously fully or partially vaccinated with bivalent or quadrivalent HPV vaccines." Vaccine **34**(6): 757-761.

van den Bout, I. and N. Divecha (2009). "PIP5K-driven PtdIns(4,5)P2 synthesis: regulation and cellular functions." J Cell Sci **122**(Pt 21): 3837-3850.

van Roy, F. (2014). "Beyond E-cadherin: roles of other cadherin superfamily members in cancer." Nat Rev Cancer **14**(2): 121-134.

Vasioukhin, V., L. Degenstein, B. Wise and E. Fuchs (1999). "The magical touch: genome targeting in epidermal stem cells induced by tamoxifen application to mouse skin." Proc Natl Acad Sci U S A **96**(15): 8551-8556.

Viarisio, D., K. Mueller-Decker, U. Kloz, B. Aengeneyndt, A. Kopp-Schneider, H. J. Grone, T. Gheit, C. Flechtenmacher, L. Gissmann and M. Tommasino (2011). "E6 and E7 from beta HPV38 cooperate with ultraviolet light in the development of actinic keratosis-like lesions and squamous cell carcinoma in mice." PLoS Pathog **7**(7): e1002125.

Vinzon, S. E. and F. Rösl (2015). "HPV vaccination for prevention of skin cancer." Hum Vaccin Immunother **11**(2): 353-357.

Watt, F. M. (2002). "Role of integrins in regulating epidermal adhesion, growth and differentiation." EMBO J **21**(15): 3919-3926.

Watt, F. M. and H. Fujiwara (2011). "Cell-extracellular matrix interactions in normal and diseased skin." Cold Spring Harb Perspect Biol **3**(4).

Weissenborn, S. J., M. N. De Koning, U. Wieland, W. G. Quint and H. J. Pfister (2009a). "Intrafamilial transmission and family-specific spectra of cutaneous betapapillomaviruses." J Virol **83**(2): 811-816.

Weissenborn, S. J., R. Neale, M. N. de Koning, T. Waterboer, D. Abeni, J. N. Bouwes Bavinck, U. Wieland, H. J. Pfister and E.-H.-U.-C. Group (2009b). "Prevalence and multiplicity of cutaneous beta papilloma viruses in plucked hairs depend on cellular DNA input." J Virol Methods **161**(2): 280-283.

Weissenborn, S. J., I. Nindl, K. Purdie, C. Harwood, C. Proby, J. Breuer, S. Majewski, H. Pfister and U. Wieland (2005). "Human papillomavirus-DNA loads in actinic keratoses exceed those in non-melanoma skin cancers." J Invest Dermatol **125**(1): 93-97.

Westphal, K., B. Akgul, A. Storey and I. Nindl (2009). "Cutaneous human papillomavirus E7 type-specific effects on differentiation and proliferation of organotypic skin cultures." Cell Oncol **31**(3): 213-226.

White, E. A., R. E. Kramer, M. J. Tan, S. D. Hayes, J. W. Harper and P. M. Howley (2012a). "Comprehensive analysis of host cellular interactions with human

papillomavirus E6 proteins identifies new E6 binding partners and reflects viral diversity." J Virol **86**(24): 13174-13186.

White, E. A., M. E. Sowa, M. J. Tan, S. Jeudy, S. D. Hayes, S. Santha, K. Munger, J. W. Harper and P. M. Howley (2012b). "Systematic identification of interactions between host cell proteins and E7 oncoproteins from diverse human papillomaviruses." Proc Natl Acad Sci U S A **109**(5): E260-267.

Wieland, U., A. Kreuter and H. Pfister (2014). "Human papillomavirus and immunosuppression." Curr Probl Dermatol **45**: 154-165.

Willers, I. M., A. Isidoro, A. D. Ortega, P. L. Fernandez and J. M. Cuezva (2010). "Selective inhibition of beta-F1-ATPase mRNA translation in human tumours." Biochem J **426**(3): 319-326.

Wu, Z., X. Li, M. Sunkara, H. Spearman, A. J. Morris and C. Huang (2011). "PIPKIgamma regulates focal adhesion dynamics and colon cancer cell invasion." PLoS One **6**(9): e24775.

Yang, L., I. Mohr, E. Fouts, D. A. Lim, M. Nohaile and M. Botchan (1993). "The E1 protein of bovine papilloma virus 1 is an ATP-dependent DNA helicase." Proc Natl Acad Sci U S A **90**(11): 5086-5090.

You, J., M. R. Schweiger and P. M. Howley (2005). "Inhibition of E2 binding to Brd4 enhances viral genome loss and phenotypic reversion of bovine papillomavirus-transformed cells." J Virol **79**(23): 14956-14961.

Zheng, Z. M. and C. C. Baker (2006). "Papillomavirus genome structure, expression, and post-transcriptional regulation." Front Biosci **11**: 2286-2302.

zur Hausen, H. (1977). "Human papillomaviruses and their possible role in squamous cell carcinomas." Curr Top Microbiol Immunol **78**: 1-30.

zur Hausen, H., W. Meinhof, W. Scheiber and G. W. Bornkamm (1974). "Attempts to detect virus-secific DNA in human tumors. I. Nucleic acid hybridizations with complementary RNA of human wart virus." Int J Cancer **13**(5): 650-656.

Zwerschke, W. and P. Jansen-Durr (2000). "Cell transformation by the E7 oncoprotein of human papillomavirus type 16: interactions with nuclear and cytoplasmic target proteins." Adv Cancer Res **78**: 1-29.

Abstract

High-risk patient groups, such as immunosuppressed organ-transplant recipients and patients with the inherited skin disease Epidermodysplasia verruciformis, exhibit cancerisation of the skin, which are positive for human papillomaviruses (HPV) of the genus beta (e.g. HPV8). Transgenic mouse models, expressing either all HPV8 early proteins (E1, E2/E4, E6, E7) or E2 and E6 individually, develop skin papillomas with varying degrees of dysplasia and squamous cell carcinoma. The specific contribution of the viral E7 protein to tumour formation and the molecular mechanism for HPV8 induced keratinocyte invasion was not known. During this study, a transgenic mouse model expressing the HPV8-E7 oncoprotein in the murine epidermis under the control of the keratin-14 promoter was generated and proved a carcinogenic potential of HPV8-E7 *in vivo*. It could previously be shown that HPV8-E7 induces keratinocyte invasion in organotypic skin cultures (OSCs), which were based on de-epidermalised dermis, whereby invasion could not be triggered in OSCs based on collagen type I. Therefore, it was hypothesised that the composition of the extracellular matrix (ECM) enables HPV8-E7 mediated keratinocyte invasion. We now could show, that the adherens and tight junction proteins β-catenin and zona occludens-1 are strongly upregulated in E7 positive keratinocytes in OSC, in the skin of HPV8-E7 transgenic mice and in betaHPV positive human skin lesions. When cells were grown on a fibronectin matrix, E7-positive keratinocytes acquired an invasive cell phenotype which was accompanied by an epithelial-mesenchymal-transition mediated cadherin switch leading to E-cadherin down-, and N-cadherin up-regulation. In addition, E7-positive keratinocytes displayed enhanced fibronectin expression and secretion and stimulated dermal fibroblasts to express fibronectin. When grown on fibronectin, E7-positive keratinocytes exhibited increased cell surface levels of the integrin α3 chain. Functional blocking of α3 using siRNA confirmed α3 as a critical molecule sufficient to induce E7-mediated invasion. This mechanistic link was further supported by the fact that the invasion-deficient E7-mutant L23A did not target cell surface levels of α3. Furthermore, high α3 levels were coupled with an upregulation of the fibronectin-associated ECM protein Fibulin-2, known to mediate a transformed cell phenotype. Using E7wt and E7-L23A positive cell extracts and Co-IP/mass spectrometric analysis the cellular factors ATP5B, PTRF/cavin-1 and phosphatidylserine could be identified as possibly important for keratinocyte invasion.

These findings highlight the importance of cell-cell and epithelial-ECM interactions required for keratinocyte invasion and provide mechanistic evidence for the role of betaHPV in skin carcinogenesis.

Zusammenfassung

Sowohl Patienten mit der erblichen Hautkrankheit Epidermodysplasia verruciformis, als auch immunsuppremierte Organtransplantatempfänger stellen Patientengruppen dar, die ein erhöhtes Risiko zur Bildung von Hautkrebs vorweisen. Diese Karzinome sind positiv für humane Papillomviren des Genus beta, wie z.B. HPV8. Transgene Mausmodelle, die entweder alle frühen Proteine von HPV8 (E1, E2/E4, E6, E7) oder nur das E2 oder E6 Protein exprimieren, entwickeln Papillome unterschiedlicher Schweregrade und Plattenepithelkarzinome der Haut. Der spezifische Einfluss des viralen E7 Proteins auf die Tumorentwicklung und der molekulare Mechanismus der HPV8 induzierten Keratinozyten-Invasion war bisher nicht bekannt. In dieser Studie wurde ein transgenes Mausmodel generiert, welches das HPV8-E7 Protein unter der Kontrolle des Keratin-14 Promotors exprimiert, womit ein karzinogenes Potential für E7 *in vivo* nachgewiesen werden konnte. *In vitro* konnte bisher gezeigt werden, dass HPV8-E7 positive Keratinozyten nur in organotypischen Hautkulturen invadierten, die auf de-epidermierter Dermis basierten, wohingegen auf Kollagen I basierter Matrix keine Invasion beobachtet werden konnte. Diese Befunde führten zur Hypothese, dass Bestandteile der extrazellulären Matrix die HPV8-E7 induzierte Keratinozyten-Invasion ermöglicht. Wir konnten nun zeigen, dass die Adhesion- und Tight-Junction Proteine β-catenin und Zona Occludens-1 in E7 positiven organotypischen Hautkulturen, sowie in HPV8-E7 transgener Maushaut als auch in betaHPV-positiven humanen Hautläsionen stark hochreguliert sind. Nach der Kultivierung von Keratinozyten auf Fibronektin, entwickelten E7 positive Zellen einen invasiven Zellphänotypus, der mit einer epithelialen-mesenchymalen Transition und einem ‚Cadherin -Switch' verbunden war, was zu einer Runterregulierung von E-Cadherin und einer Hochregulierung von N-Cadherin führt. Außerdem zeigten E7-positive Keratinozyten eine erhöhte Fibronektin-Expression sowie Sekretion und stimulierten die Fibronektin-Expression in dermalen Fibroblasten. Auf einer Fibronektin-Matrix kultivierte E7 positive Keratinozyten wiesen ein erhöhtes Level der Integrin α3 Untereinheit auf der Zelloberfläche auf. Die Runterregulation des Integrin α3 durch siRNA verdeutlichte die entscheidende Rolle von α3 in der E7 induzierten Invasion. Diese mechanistische Verknüpfung wurde durch die Tatsache bekräftigt, dass die Invasions-defiziente E7-L23A Mutante keine veränderte Integrin α3 Menge auf der Zelloberfläche zeigte. Des Weiteren war eine erhöhte Menge von α3 mit der Hochregulierung des Fibronektin-

assoziierten Matrixproteins Fibulin-2 verbunden, was bekannter Weise einen transformierenden Zellphänotypus unterstützt. Mit Hilfe von E7wt und E7-L23A positiven Zellextrakten und Co-IP/massenspektrometrischer Analysen wurden die zellulären Faktoren ATP5B, PTRF/Cavin-1 und Phosphatidylserin als mögliche wichtige Faktoren für die Keratinozyten-Invasion identifiziert.

Zusammenfassend konnte in dieser Studie gezeigt werden, dass sowohl Zell-Zell als auch Zell-Matrix-Interaktionen durch E7 moduliert werden, wodurch die Invasion von Keratinozyten ermöglicht wird. Somit konnten weitere mechanistische Ergebnisse für die Rolle von betaHPV in der Entstehung des Plattenepithelkarzinoms erbracht werden.

Abbreviations

μg	Microgram
μl	Microlitre
aa	Amino acid
AIDS	Acquired Immune Deficiency Syndrome
ATP	Adenosine triphosphate
ATP5B	ATP synthase, H+ transporting, F1-complex, beta-polypeptide
ATR	ATR Serine/Threonine Kinase
BCA	Bicinchoninic acid
BM	Basement membrane
bp	Base pairs
BS	Binding site
BSA	Bovine serum albumin
CER	Complete early region
CKII	Casein kinase II
Co-IP/MS	Co-immunoprecipitation/mass spectrometry
CR	Conserved region
DAPI	4',6-diamidino-2-phenylindole
dH$_2$O	Distilled water
ddH$_2$O	Double-distilled water
DMBA	7,12-dimethylbenzanthracene
DMEM	Dulbecco's modified Eagle medium
DMSO	Dimethyl sulfoxide
DNA	Deoxyribonucleic acid
dATP, dCTP, dGTP dNTP, dTTP	Deoxyadenosine triphosphate, deoxycytidine triphosphate, deoxyguanosine triphosphate, deoxynucleoside triphosphate, deoxythymidine triphosphate
DTT	Dithiothreitol
E1, E2, E4, E5, E6, E7	Early genes 1, 2, 4, 5, 6, 7 of HPV
E6AP	E6 associated protein
EBV	Epstein Barr virus
ECAR	Extracellular consumption rate
ECL	Enhanced chemiluminescence
ECM	Extracellular matrix
EDTA	Ethylene diamine tetraacetic acid
EMT	Epithelial-mesenchymal transition
EtBr	Ethidiumbromide
EtOH	Ethanol

EV	Epidermodysplasia verruciformis
FACS	Fluorescence-activated cell sorting
FAK	Focal adheson kinase
FCCP	Carbonyl-cyanide-p-trifluoromethoxyphenylhydrazone
FCS	Fetal calf serum
g	Gram
g	Relative centrifugal force
HBS	Hepes buffered saline
HBV	Hepatitis B virus
HCV	Hepatitis C virus
he	hemizygous
HE	Haematoxylin and eosin
HEPES	4-(2-hydroxyethyl)-1-piperazineethanesulfonic acid
HIV	Human immunodeficiency virus
HNSCC	Head and neck squamous cell carcinoma
ho	homozygous
HPV	Human Papillomavirus
HSPG	Heparin sulphate proteoglycans
hTERT	Human telomerase reverse transcriptase
HTVL-1	Human T cell lymphotrophic virus, type-1
Hz	Hertz
IARC	International Agency for Research on Cancer
ICC	Immunocytochemistry
IHC	Immunohistochemistry
J	Joule
K10	Keratin10
K14	Keratin14
kb	Kilo base pairs
kD	Kilo Dalton
KSHV	Kaposi's sarcoma herpes virus
L1/L2	Late gene 1/2 of HPV
LANA	Latency-associated nuclear antigen
LB	Luria-Burtani
LCR	Long control region
LMP1	Latent membrane protein 1
LPA	Lysophosphatidic acid
LPC	Lysophosphocholine
LTR	Long terminal repeat
M	Mol l^{-1}
MAGUK	Membrane-associated guanylate kinase homologs
MAML1	Mastermind-like transcriptional co-activator 1

MCPyV	Merkel cell polyomavirus
MT1-MMP	Membrane type1-MMP
min	Minute(s)
ml	Millilitre
mM	Milli mol L-1
MMP	Matrix metalloproteinase
MSM	Men who have sex with men
mRNA	Messenger RNA
NCR	Non-coding region
nM	Nano mol l^{-1}
NMSC	Non-melanoma skin cancer
NS3	Nonstructural *protein* 3
NS4B	Nonstructural protein 4B
NS5A	Nonstructural protein 5A
OCR	Oxygen consumption rate
OD	Optical density
OPSCC	Oropharyngeal squamous cell carcinoma
ORF	Open reading frame
OSC	Organotypic skin culture
OTR	Organ-transplant recipient
PBS	Phosphate buffered saline
PCNA	Proliferating cell nuclear antigen
PCR	Polymerase chain reaction
PC	Phosphatidylcholine
PDZ domain	PSD95/Dlg/ZO-1 motif containing domain
PE	Phosphatidylethanolamine
PHK	Primary human keratinocytes
PI	Phosphatidylinositol
PI(3)P	Phosphatidylinositol (3) phosphate
PI(3,4)P$_2$	Phosphatidylinositol (3,4) biphosphate
PI(4,5)P$_2$	Phosphatidylinositol (4,5) biphosphate
PI(3,4,5)P$_3$	Phosphatidylinositol (3,4,5) triphosphate
PI(4)P	Phosphatidylinositol (4) phosphate
PI(5)P	Phosphatidylinositol (5) phosphate
PMSF	Phenylmethylsulfonyl fluoride
pRB	Retinoblastoma protein
PS	Phosphatidylserine
PTRF	Polymerase I And Transcript Release Factor
PV	Papillomavirus
qRT-PCR	Quantitative real-time polymerase chain reaction
RNA	Ribonucleic acid

RT	Reverse transcriptase
rt	Room temperature
s	Second(s)
SCC	Squamous cell carcinoma
SDS	Sodium dodecyl sulfate
SIP	Sphingosine-1-phosphate
siRNA	Small interferring RNA
Sp1	Specificity protein 1
SV40	Simian virus 40
TBST	Tris buffered saline tween
TCF	T-cell factor
TEMED	Tetra methyl ethylene diamine
TPA	12-O-Tetradecanoylphorbol-13-acetate
U	Units
URR	Upstream regulatory region
UV	Ultraviolet
VLP	Virus-like particle
w/v	Weight per volume
Y2H	Yeast to hybrid
ZO-1	Zona Occludens 1

Acknowledgement

Erklärung

Ich versichere, dass ich die von mir vorgelegte Dissertation selbständig angefertigt, die benutzten Quellen und Hilfsmittel vollständig angegeben und die Stellen der Arbeit − einschließlich Tabellen, Karten und Abbildungen −, die anderen Werken im Wortlaut oder dem Sinn nach entnommen sind, in jedem Einzelfall als Entlehnung kenntlich gemacht habe; dass diese Dissertation noch keiner anderen Fakultät oder Universität zur Prüfung vorgelegen hat; dass sie − abgesehen von unten angegebenen Teilpublikationen − noch nicht veröffentlicht worden ist sowie, dass ich eine solche Veröffentlichung vor Abschluss des Promotionsverfahrens nicht vornehmen werde. Die Bestimmungen der Promotionsordnung sind mir bekannt. Die von mir vorgelegte Dissertation ist von Jun.-Prof. Dr. Baki Akgül und Prof. Dr. Björn Schumacher betreut worden.

Teile der vorliegenden Dissertation sind unter folgenden Titeln veröffentlicht worden:

Heuser, S., Hufbauer, M., Steiger, J., Marshall, J., Sterner-Kock, A., Mauch, C., Zigrino, P. and Akgül, B. (2016) The fibronectin / α3β1 integrin axis serves as molecular basis for keratinocyte invasion induced by βHPV. *Oncogene* [Epub ahead of print]

Heuser, S., Hufbauer, M., Marx, B., Tok, A., Majewski, S., Pfister, H. and Akgül, B. (2016) The levels of epithelial anchor proteins β-catenin and ZO-1 are altered by E7 of Human papillomaviruses 5 and 8. *J Gen Virol.*, 97(2) 463-72

Köln, den 09.05.2016

_____
Sandra Heuser

Curriculum Vitae

Personal Information	Name: Sandra Heuser
	Date of Birth: 08.07.1987
	Place of Birth: Mechernich, Germany
	Nationality: German

Education

Doctoral Thesis

02/2013 – today   Graduate School of Biological Sciences (GSfBS)
University of Cologne, Germany

02/2013 – today   PhD Thesis
University Hospital of Cologne
Institute of Virology
Topic: Mechanism of HPV8-E7 mediated keratinocyte invasion

Master Study Program

09/2010 – 09/2012   Master of Science in Biomedical Sciences
University of Applied Sciences
Bonn-Rhein-Sieg, Rheinbach, Germany

03/2012 – 09/2012   Master Thesis
University Hospital of Cologne
Institute of Virology
Topic: Analysis of the 16E6-mediated inhibition of C/EBPα induced phosphorylation of p300

Bachelor Study Program

09/2007 – 08/2010   Bachelor of Science in Applied Biology
University of Applied Sciences
Bonn-Rhein-Sieg, Rheinbach, Germany

09/2009 – 06/2010   Bachelor of Science 1st class Honours
The Robert Gordon University, Aberdeen, Scotland

02/2010 – 06/2010   Bachelor Thesis
The Robert Gordon University, Aberdeen, Scotland
Topic: Infectious Salmon Anaemia Virus Characterisation and Sequencing of the Viral Non-Coding Ends

08/1998 – 07/2007   A level, Secondary school
Gymnasium Am Turmhof Mechernich, Mechernich, Germany

Publications

Heuser, S., Hufbauer, M., Steiger, J., Marshall, J., Sterner-Kock, A., Mauch, C., Zigrino, P. and Akgül, B. (2016) The fibronectin / α3β1 integrin axis serves as molecular basis for keratinocyte invasion induced by βHPV. *Oncogene* [Epub ahead of print]

Heuser, S., Hufbauer, M., Marx, B., Tok, A., Majewski, S., Pfister, H. and Akgül, B. (2016) The levels of epithelial anchor proteins β-catenin and ZO-1 are altered by E7 of Human papillomaviruses 5 and 8. *J Gen Virol.*, 97(2) 463-72.

	Fourrier, M., **Heuser, S**., Munro, E. and Snow, M. (2011) Characterization and comparison of the full 3' and 5' untranslated genomic regions of diverse isolates of infectious salmon anaemia virus by using a rapid and universal method. *J Virol Methods*, 174, 136-143
Oral Presentation	**Heuser S**., Hufbauer M., Zigrino P., Mauch C., Akgül B. (2014) HPV8-E7 mediated keratinocyte invasion is modulated by extracellular matrix proteins. 7th *International Conference on HPV. Polyomavirus and UV in Skin Cancer*. Novara, Italy.
Award	European Society for Virology Travel Award 7th *International Conference on HPV. Polyomavirus and UV in Skin Cancer*. Novara, Italy